University of California

San Diego

Analysis of an Implantable Lactate Sensor

Mathematical Modeling of Sensor Response

A thesis submitted in partial satisfaction of the requirements for the degree

Master of Science

in

Bioengineering

by

Will (Wei) Wang

Committee in charge:

Robert Lie-Yuan Sah, Chair
Dale A. Baker, Co-Chair
Pao C. Chau
Marcos Intaglietta

2008

The Thesis of Will (Wei) Wang is approved:

Co-Chair

Chair

University of California, San Diego

2008

Table of Contents

NOMENCLATURE

Bi	Biot number
c	concentration
$\bar{c}$	dimensionless concentration
$\bar{c}_o^*$	effective substrate concentration ratio
$\bar{c}_o^*$'	dimensionless bulk oxygen concentration for outer membrane
CAT	catalase
D	diffusion coefficient
h	mass transfer coefficient
i	electrode current
K	Michaelis constant
L	axial length
LOD	lactate oxidase
mM	millimoles/liter
Q	generalized enzyme reaction expression
r	radial coordinate
R'	normalized outer membrane thickness
t	time
V	enzyme reaction expression
$\bar{V}$	dimensionless enzyme reaction expression
V_{max}	maximum reaction velocity per unit volume
z	axial coordinate

Greek letters

α	partition coefficient
γ	solubility
δ	boundary layer thickness
ε	aspect ratio
κ	dimensionless Michaelis constant
λ	diffusion coefficient ratio
λ'	outer membrane diffusion coefficient ratio
ν	stoichiometry coefficient
ξ	dimensionless axial coordinate
ρ	dimensionless radial coordinate
σ	dimensionless enzyme catalytic activity
τ	dimensionless time

Subscripts and Superscripts

B	bulk solution
crit	critical
e	electrode
f	final
i	chemical species index
	initial
inter	interface
L	lactate

lmo	lactate-modulated oxygen
o	oxygen
	outer
out	outer
r	radial
rout	radial, outer
zout	axial, outer
+	in the positive direction
-	in the negative direction

LIST OF FIGURES

LIST OF TABLES

ACKNOWLEDGEMENT

I would like to thank the members of my thesis committee, Dr. Sah, Dr. Intaglietta, and Dr. Chau, for their assistance in the preparation of this thesis. I would also like to thank my advisor, Dr. Dale A. Baker, for his kind encouragement, support and guidance throughout my tenure as a graduate student. I feel very privileged to be part of his laboratory.

I am also grateful for the encouragement and help so generously afforded me by my friends. In particular, I would like to thank Hideru, Ian, Randy, Rakesh and Victoria for their helpful technical assistance and advice.

To my parents, words cannot describe how grateful I am for their sacrifices, faith and understanding throughout my life. Their encouragements have always been my source of strength and will be as I continue moving forward. Finally, I would like to thank my family: my grandparents, uncles, aunts, and cousins for their faith and support throughout my life. To my uncle George, aunt Christine and cousin Jenny - and her family - I am forever indebted for their kindness and support, without which I could not possibly be where I am now.

ABSTRACT OF THE THESIS

Analysis of an Implantable Lactate Sensor:

Mathematical Modeling of Sensor Response

by

Will (Wei) Wang

Master of Science in Bioengineering

University of California, San Diego, 2008

Dale A. Baker, Co-Chair

Robert Lie-Yuan Sah, Chair

Blood lactate concentration has been used as an important diagnostic parameter for assessing patient health conditions for over four decades, yet its measurement is currently time consuming and inconvenient, and its roles in disease development and homeostasis are still poorly understood. While much effort has been focused on developing implantable biosensors to achieve continuous monitoring of lactate concentrations in both blood and tissue, systematic studies of sensor behavior using mathematical modeling techniques have rarely been done. Experimental results complemented with such models would be potentially helpful in understanding the underlying physics behind sensor operation. Therefore, in this thesis we use mathematical models to characterize an enzyme electrode sensor that has shown great

promise as potential implantable device. This thesis will also demonstrate how these theoretical results can be utilized to formulate efficient strategies to improve sensor performance.

Lactate specificity for the enzyme electrode sensor of interest is obtained by immobilizing lactate oxidase which catalyzes the reaction between lactate and oxygen, onto an electrochemical oxygen electrode. Lactate can then be quantitatively detected by measuring the resulting oxygen dependent current. Oxygen and lactate concentration profiles within the sensor were obtained by solving reaction coupled mass conservation equations using a finite element analysis (FEA) software called COMSOL Multiphysics and the currents were calculated from the oxygen flux at the electrode surface. The model is used to predict the roles of geometric, kinetic, and environmental factors on the steady-state and transient responses of these potentially implantable sensors.

CHAPTER I.

Introduction

Lactate concentration is an important parameter in the diagnosis and study of diseases and for continuous monitoring in surgery, sports medicine, and shock/trauma. In a healthy person, the production and utilization of lactate are tightly controlled by lactate homeostasis, which is maintained by the Cori Cycle (Figure 1.1). The balance of lactate is vital to acid-base homeostasis, because the utilization of lactate and regeneration of bicarbonate are required to counter balance the production of hydrogen ion and the loss of bicarbonate. Such delicate lactate balancing system is necessary because our body is only viable within an extremely narrow range of pH (between pH 7.2 to 7.4). When the rate of energy demand by tissues cannot be met by aerobic respiration (or when there is mitochondrial dysfunction), an increase in lactate concentration will occur. This is due to the increased activity of a compensatory metabolic pathway that serves to regenerate NAD^+ needed for glycolysis, thus allowing ATP production to continue. The subsequent production of lactic acid will result when the production of lactate is coupled with the generation of hydrogen ion via the hydrolysis of ATP. Without adequate clearance by the liver and kidney, significant lactic acid accumulation may lead to lactic acidosis. Clinically, this condition is encountered in two settings: type A, disorders in which there is poor tissue oxygenation such as with shock, left ventricular failure, sepsis, hypovolemia, and poisoning with carbon monoxide and cyanide; or type B, disorders caused by certain drugs/toxins or disease states in which poor tissue oxygenation is

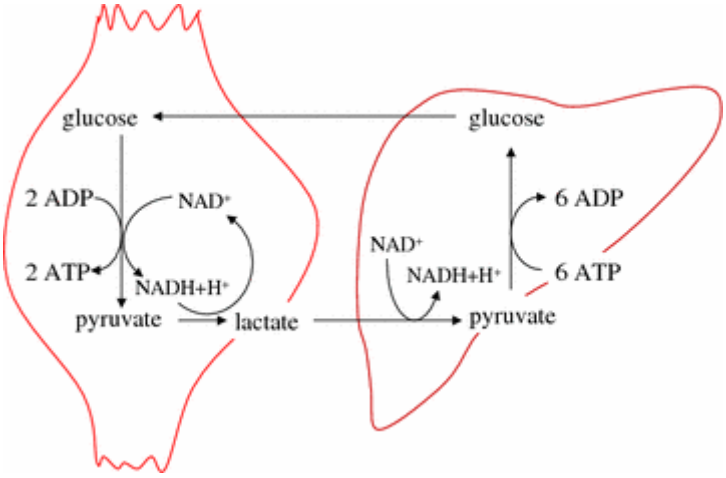

Figure 1.1 Illustration of the Cori cycle. The Cori cycle is responsible for maintaining lactate homeostasis. The pathway to the left represents lactate production in skeletal muscle through glycolysis. The pathway to the right represents lactate clearance in liver through gluconeogenesis.

not a feature (Kreisberg, 1984). Therefore, a patient's blood lactate concentration is an important indicator for the severity of illness and may also be used to improve the diagnoses and treatments of a broad range of diseases.

Due to lactate's physiological significance, there has been a growing need for developing sensors that could continuously monitor its concentrations in the human body. Several of the potential beneficiaries of an implantable lactate sensor would be patients that have chronic heart, kidney or liver problems, because these diseases are often accompanied by lactic acidosis. According to Medicare data and published literature in the year 2000, an estimated of 4.4 million patients were admitted to ICU annually, in which about 25% of these patients had sepsis (which is characterized as a systemic inflammatory and procoagulant response to infection) (Pronovost et al., 2004). When this condition is combined with one or more vital organ dysfunctions, the patient will develop severe sepsis. The mortality rate of sepsis is estimated around 30% to 50%, which corresponds to at least 225,000 deaths annually (Fowler et al., 2003; Angus et al., 2001). Recent studies have shown that early lactate clearance could improve the treatment outcome in severe sepsis and septic shock, which could potentially lead to the decrease in sepsis related mortalities (Nguyen et al., 2004). In addition, clinical observations have also shown that if acidosis persists in patients without any circulatory and respiratory abnormalities (or hypoxemia), and lactatemia of excess lactate has already progressed to the extreme elevations, the recovery of the patient is very unlikely. In such case, any new therapeutic approach which seems reasonable should be implemented (Huckabee, 1961b). Thus, an implantable lactate sensor capable of continuously monitoring tissue or blood lactate concentration could provide physicians

with data in an expedient fashion that would enable appropriate treatments to be utilized in time to save patients' lives.

Because the level of lactic acid changes significantly depending on the individual's health status and physical activities (the blood lactate concentration in the body can change from 1.0-1.3 mmol/L under normal conditions to more than 15 mmol/L during hypoxia or ischemia), the ideal sensor would be required to respond continuously and specifically to lactate over a substantial range of concentrations (Huckabee, 1961a). Additionally, it would also need to function effectively under low-flow conditions, as well as low oxygen concentrations (that often accompany lactate production) and requires only infrequent recalibration, and avoids any unacceptable biocompatibility response (Baker, and Gough, 1995).

Furthermore, an implanted sensor with data logger (Kishiyama, 1999) and telemetry system (Castro, 2002) that continuously monitors blood or tissue lactate concentration and transmits the information to an external receiver would provide information that is not presently available. Such information can be used by physicians and scientists to gain better understanding on disease development and to produce better treatments.

1.1 Previous Work

The lactate sensors that have been previously described by different research groups can be classified into two categories: 1) optical based sensors, and 2) electrochemical or "enzyme electrodes" based sensors. The optical lactate sensors are predominantly enzyme optical fiber based biosensors (optodes), which utilize enzymes

(such as lactate oxidase, lactate dehydrogenase, and lactate mono-oxygenase) to catalyze reactions with a high degree of specificity and detects the products of these reactions directly or via interaction with an indicator (Wolfbeis, 2002; Wu *et al.*, 2005; Marquette and Blum, 2003; Li *et al.*, 2002). Although optical based sensors have gained increased popularity, the majority of the lactate sensors that have demonstrated acceptable bioanalytic capabilities *in vivo* (such as wide detection range and high accuracy) are still based on electrochemical electrodes. Among these, enzyme based amperometric lactate sensors are of the predominant type. These sensors have an immobilized lactate dehydrogenase (Gue *et al.*, 2002; or cytochrome b2, Williams *et al.*, 1970; Kulys *et al.*, 1980; Wang *et al.*, 1994), lactate mono-oxygenase (Makovos *et al.*, 1985), or lactate oxidase (Baker, and Gough, 1995; Meyerhoff *et al.*, 1993; Yang, Atanasov, and Wilkins, 1998; Guiseppi-Elie *et al.*, 2005; Mascini *et al.*, 1985; Ward *et al.*, 2004; Burmeister, Palmer, and Gerhardt, 2005; Petrou, and Jobst, 2003; Bohm *et al.*, 2001; Ritter *et al.*, 2001; Perdomo *et al.*, 2000; Pfeiffer *et al.*, 1997; Revzin *et al.*, 2002; Hu, 1993; Ellmerer *et al.*, 1998; Marzouk *et al.*, 1997) layer on top of the electrode. The products of these reactions are detected directly, via interaction with an electron carrier (Yang and Kissinger, 1995; Ohara, Rajagopaian and Heller, 1994) or another enzyme. In addition to these amperometric lactate biosensors, ion selective lactate sensors have also been described (Kharitonov *et al.*, 2001).

Despite the availability of this vast array of detection elements, the development of an acceptable lactate biosensor for implant application remains a challenge. On the other hand, the suitability of many electrochemical lactate sensors for implant applications has been hindered by their relatively slow dynamic response, but

improvements can be achieved using systematic engineering analysis that combines mathematical modeling and experimentation.

1.2 Enzyme Electrode Principle

Two types of electrochemical lactate biosensors are investigated in this study. These sensors only differ by the types of enzymes immobilized on the oxygen electrode.

The first type of sensor is referred to as the single enzyme (SE) sensor in this thesis, since only the enzyme lactate oxidase is immobilized in the hydrophilic gel covering an electrochemical oxygen electrode. The reaction catalyzed is:

$$L - Lactate + O_2 \xrightarrow{LOD} Pyruvate + H_2O_2$$

$$H_2O_2 + 2H^+ + 2e^- \rightarrow 2H_2O \text{ (Acid solution)}$$

$$H_2O_2 + OOH^- + 2e^- \rightarrow 3OH^- \text{ (Alkaline solution)}$$

Hydrogen peroxide can be reduced in a slightly different fashion depending on its environment (Bockris, and Oldfield, 1954). The rationale for this design is that a more simplistic (only 1 enzyme) system will allow us to make detailed and unambiguous investigation on enzyme degradation with time.

The second type of sensor has two enzymes (lactate oxidase and catalase) co-immobilized in a hydrophilic gel covering an electrochemical oxygen electrode. This is also referred to as the dual enzyme (DE) sensor in this thesis. The reactions catalyzed are:

$$L - Lactate + O_2 \xrightarrow{LOD} Pyruvate + H_2O_2$$

$$H_2O_2 \xrightarrow{CAT} \frac{1}{2}O_2 + H_2O$$

With excess catalase present, the resulting overall reaction is:

$$L - Lactate + \frac{1}{2}O_2 \rightarrow Pyruvate + H_2O$$

Unlike the single enzyme sensors, the reaction catalyzed by catalase in DE sensor regenerates half of the oxygen consumed by LOD. This type of sensor had been used as an implant in the canine right atrium, and was shown to respond specifically to lactate over a broad concentration range with stable response for more than 1 week (Baker, and Gough, 1995).

Since the only difference between these two types of sensors is enzyme membrane composition, both types of sensors share the same hardware components: a lactate electrode, an oxygen reference electrode, and an appropriate means of current subtraction. Each electrode contains three elements: 1) a working electrode, which detects the oxygen dependent current; 2) a reference electrode, which maintains a constant reduction potential difference; and 3) a counter electrode, which maintains stability.

The same sequence of events leading to lactate detection is involved in both types of sensors: 1) lactate and oxygen from the bulk medium diffuse into the enzyme gel and react with enzyme(s), 2) the unconsumed oxygen diffuses to the surface of the oxygen sensor and is electrochemically reduced to generate a lactate-modulated oxygen current, i_{lmo}, 3) another oxygen electrode, the oxygen reference electrode, measures the ambient oxygen concentration and produces an oxygen-dependent current, i_o, and 4) the lactate-dependent current, i_l, is obtained by subtracting i_o from i_{lmo}. With appropriate calibration, this current can be used to correlate with the lactate concentration in the bulk medium.

Due to the complexity of the electrochemical events involved in lactate detection, we would like to first understand the relatively simple system (with just one catalytic

enzyme) before moving to the more complex design. Therefore, this thesis will first present the simulation results for single enzyme sensors before comparing them to those of dual enzyme sensors.

1.3 Thesis Organization

Chapter II highlights the various lactate sensors that are being developed by different research groups and some common performance criteria pertinent to *in vivo* applications. It will show that the enzyme electrode sensor based on oxygen detection holds promising potential as an implantable device for continuous monitoring applications. Chapter III contains the mathematical model for steady-state and transient responses of this enzyme electrode sensor. Chapter IV summarizes this thesis and gives directions for future work.

CHAPTER II.

Background

The term biosensor is defined here as a device that senses a species which is of biological origin, or a species which is an important component in a biological system. The first biosensor was developed through the pioneering work of Leland Clark Jr. less than half century ago (Clark, and Lyons, 1962). Since then there has been enormous interest in developing biosensors that could improve the outcomes of patient care. Over the past 20 years or so, technological advances in the areas of electronics, material science and chemistry have made significant progress in the biosensor industry. Today, biosensors are capable of monitoring clinically important species (e.g. blood-gas measurements such as pH, pO_2, and pCO_2; electrolytes such as Na+, K+ and Ca^{2+}; glucose; and lactate) and have become an indispensable part of the modern health care system. With the exception of those for simple small molecules, the majority of biosensors rely on the specificity of enzymes for detection. The term enzyme electrode, which describes a miniature chemical transducer that functions by combining an electrochemical procedure with immobilized enzyme activity, was first introduced by Updike and Hicks in 1967, who pioneered the first glucose sensor based on this concept (Updike and Hicks, 1967). The simplicity and robustness of the enzyme electrode design allowed it to be widely adapted for sensors that are tailored toward other chemical detections, such as lactate.

Based on their applications, lactate sensors can be classified into three categories (Baker and Gough, 1995). Lactate sensors of the first type are used in bench-top

analyzers and are also the majority type. These sensors are intended for discrete (sample by sample) measurements and dilution (usually by mixing sample with buffer) may be necessary to achieve sensitivity over a useful lactate range and to minimize the effects of interfering substances. The most well known examples of this type are the YSI lactate analyzers, which have been regarded as the industry standard. The second type of lactate sensor is designed to be used as part of an extracorporeal sampling system in which blood is withdrawn from body and diluted prior to lactate measurements. The need for frequent recalibration and slow response also make this type of sensor unsuitable for continuous (non-discrete) monitoring. Although improvements have been made in recent years by several investigators to reduce the sensor response time and to allow for easy recalibration (Yang and Kissinger, 1995; Wu et al., 2005), this type of system nonetheless places restrictions on the movements of patients, and may be unsuitable for patients who have lost a significant amount of blood. The third type of lactate sensor is the implantable sensor, which is usually implanted in blood vessel (intravascular) or under the skin (subcutaneous) and is designed to achieve the ideal of continuous monitoring in specific anatomical locations with no need for sample dilution. Therefore, the continuous implantable sensor is the focus of this thesis.

2.1 Performance Factors/Characteristics

Currently, there are several lactate sensors being developed by various groups. In order to compare the relative performance of these sensors as potential implantable devices, a set of performance characteristics have been introduced over the years by the scientific community. Hence, these common characteristics are described first.

2.1.1. Selectivity and Specificity

Selectivity and specificity are essential for sensors. In short, without adequate selectivity and specificity, the user cannot relate the signal obtained to the target species concentration with any confidence. Specificity for biosensors is gained by employing analyte specific molecular recognition elements, primarily and in particular, enzymes. The byproducts of the enzyme catalyzed reactions (most commonly oxygen or hydrogen peroxide) are the messengers that interact with the electrode surface to give rise to analyte dependent signals. Due to the presence of other biomolecules that possess similar molecular size, surface charge or activity, interference at the electrode surface is likely to occur. Thus selectivity, which is concerned with the problem of interference from endogenous electroactive compounds (such as uric acid, dopamine, and ascorbate) is an important issue that must be addressed when designing an implantable sensor.

One approach to resolve the issue of selectivity was proposed by Gough, which utilizes a polymeric membrane that is only permeable to gas, and a reduction potential at the working electrode (Gough, Lucisano and Tse, 1985). The purpose of the membrane is to exclude all non-gas interferences so that only gases (such as O_2, CO_2, and N_2) are allowed to reach the electrode. A reduction potential which drives the electrochemical reduction of oxygen is used to further increase the selectivity as only oxygen can be reduced at this potential. This approach proved to be highly successful, because it allows the sensor to be selective for only oxygen, thus suitable for bioanalysis (Wilson, and Gifford, 2005). There are also a few alternative approaches to this problem, including: using a permselective membrane so that only oxygen or hydrogen peroxide is allowed to diffuse to the electrode surface, incorporating ascorbate oxidase which produces water

rather than peroxide, or using mediators which wire the enzymatic electron transfer directly to the electrode. These methods are relatively more complicated compared to the one proposed by Gough, and there is no evidence showing that they can achieve a superior level of selectivity. Therefore, the approach of utilizing a reduction potential and polymeric membrane that is only permeable to gas is used in designing sensors for this thesis.

2.1.2. Sensitivity

With any analytical technique, it is important to know the relevant concentration range; over what section of this range – the response is monotonic, and finally, the detection limit. In the case for biosensors, these sensitivity factors are a function of the physical design and the molecular recognition element (e.g. biomolecule activity). The required sensitivity for a particular analyte is determined by the concentration levels found in the environment of interest. For implantable lactate sensors, the narrowest range of detection should be between 0 and 15 mM (Huckabee, 1961a; Weil et al., 1970). There are a number of ways to enhance biosensor sensitivity. For example, platinum black deposition on carbon or platinum (Pt) electrodes has been shown to increase the active surface area, thus increasing sensitivity (Clark et al., 1998; Hoare, 1968). Other approaches include the use of electro-optical chemiluminescent sensors with appropriate molecular recognition elements for its high signal-to-nose ratios; electronic filtering of background noise, changes in aspect ratio and the insertion of diffusion-limiting barriers with permselective polymer membranes to extend the linear range (Wilson, and Gifford, 2005). Most sensors utilize a combination of the above approaches to boost their

sensitivity. However, all of these approaches have their limitations and in most cases, there have to be tradeoffs between sensitivity, range, and response time.

2.1.3. Response Time and Operational Life Time

Traditionally, the standard method of sensor characterization is to record the response to a stepwise increase in substrate concentration and the result is summarized by a single parameter called the response time. Hence, most of the efforts have been to make the response time as short as possible. However, this approach may not be advantageous or even possible in many biosensor applications due to the tradeoffs issue mentioned above (sensitivity, range and time response). For example, by making the membranes as thin as possible, the sensor would have a short response time but low detection range, and short operational lifetime. In light of the new design constraints demanded by continuous biosensors, new criteria must be established. One of the proposed criteria is that the continuous biosensor must be capable of following the maximal anticipated concentration fluctuations within a specified acceptable error, but need not respond faster (Baker, and Gough, 1996). Based on this concept, two new parameters were introduced and proved to be particularly advantageous for continuously operated biosensors. The first parameter is the dynamic delay, which describes the delay, lag, or temporal displacement between physical transients and the sensor responses to those transients. This parameter is dependent on properties of the biosensor and external mass transfer:

$$\delta_D = \frac{K\delta_m^2}{D_m}$$

where K, D_m, δ_m are the proportionality constant, diffusion coefficient and diffusion length, respectively. Dynamic error is the difference between the actual value of the variable at a given moment and the value simultaneously reported by the sensor. Mathematically, this parameter can be described by:

$$\varepsilon_D = R\delta_D$$

where R is the absolute value of the rate of concentration change, given in units of concentration per unit time. In practice, the maximal dynamic error based on the maximal expected rate of concentration change is the upper bound for the difference between the actual and reported concentrations (see Figure 2.1).

Additionally, the sensor's lifetime is equally important for continuous implantable biosensors, because the sensor's response will decline over time (since enzymes decay with time). Other factors that might contribute to this sensor response attenuation and eventual deterioration include material degradation and protein adsorption.

2.1.4. Biocompatibility

It was estimated that perturbations to the host environment by the implanted device could result in 50% loss of sensitivity (Wilson and Gifford, 2005). Although significant advancements were made in biocompatibility research, it is still difficult to

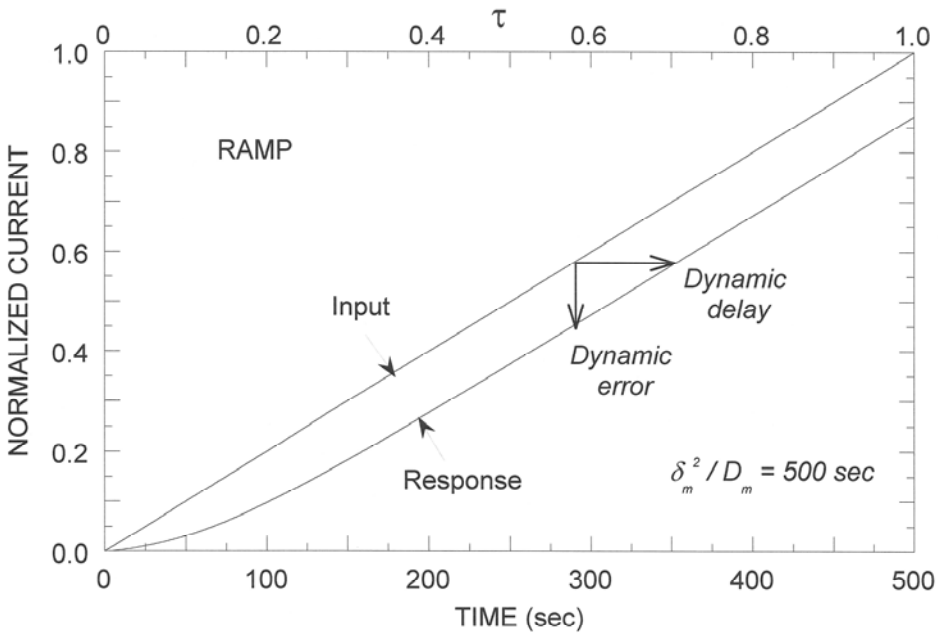

Figure 2.1 Biosensor response to a concentration ramp challenge. Normalized current is plotted as a function of time (Courtesy of Baker and Gough, 1996). Dynamic delay is the temporal displacement between physical transient (input) and the sensor responses to the transient. Dynamic error is the difference between the actual value of the variable at a given moment and the value simultaneously reported by the sensor.

identify the causes of unexpected *in vivo* measurement results. Today, it is widely accepted that biocompatibility means minimal perturbation of the *in vivo* environment and likewise the *in vivo* environment does not adversely affect the sensor performance. In other words, biocompatibility does not mean that an implant is inert. In order to improve the biocompatibility of biosensors, it is important to understand the delicate physiological events following the implantation, namely the inflammatory response to implanted devices: 1) influence of the initial inflammatory events, specifically adsorption of biomolecules; 2) effect the implant has on the local host response that may be coupled to fluctuation in sensor response; 3) biosensor degradation (Goor, 2007; Wilson and Gifford, 2005). Detailed reviews on the mechanisms of sensor failure due to biocompatibility, and methods for characterizing and improving host-implant interactions are given in a series of articles by Reichert (Wisniewski, Moussy and Reichert, 2000; Koschwanez and Reichert, 2007; Polikov, Tresco and Reichert, 2005). The present study does not address biocompatibility issues, because we would like to first model the sensor response independent of these complex factors to gain better understanding of sensor operation. Hence, the main focus of the thesis is on sensitivity (i.e. detection range) and speed of detection (i.e. response time).

2.2. Sensing Principles

Miniaturizing electrochemical devices into catheter designs has been an attractive approach, because almost all instruments used in hospitals to measure blood gases, electrolytes and metabolites in discrete undiluted blood samples employ electrochemical sensors and thus the accuracy of this sensing technology for whole blood

measurements is now well established (Frost and Meyerhoff, 2002). Although optical fiber-based technology offers an alternative approach for chemical sensor design, the development of optical based lactate biosensors for on-line monitoring and implant applications face the challenge of miniaturization (Jaremko and Rorstad, 1998) as well as limited detection range and slow response. Among electrochemical based sensors, those with amperometric mode of detection often have higher accuracy and stability compared to sensors with potentiometric mode of detection (or ion-selective sensors). For these reasons, implantable lactate sensors are based exclusively on amperometric enzyme electrodes. Table 2.1 summarizes the advantages and disadvantages of the three types of sensing techniques. The basic operating principles of amperometric sensor and examples of nascent implantable lactate sensors are presented in the remaining sections of this chapter.

2.2.1. Amperometric Sensors: Amperometric Electrodes

Amperometric sensors utilize the principle that when a species is oxidized or reduced at an electrode, the current produced is directly related to the concentration of that species. Unlike potentiometry, which obtains analytical information from a system at equilibrium (no current passed); in amperometry one can shift the equilibrium and relate the concentration of analyte to the number of electrons transferred across an electrode solution interface that is observed as a current. When the species is oxidized or reduced at the electrode, the current obtained may be limited by either or both of two processes: the kinetics of electron transfer at the electrode or mass transport of the species toward the electrode surface (Turner, Karube and Wilson, 1987).

Table 2.1 Summary of the advantages/disadvantages for the three types of detection methods. The areas of comparisons are pertinent to a continuous implantable lactate biosensor.

Detection Method	Advantage	Disadvantage
Optic	• Small and flexible fiber size • Do not require reference electrode • Do not have electrical interference • Can detect certain analytes in equilibrium • Highly stable with respect to calibration	• Have a limited dynamic range when compared to electrochemical sensors • Difficult to miniaturize the entire sensor • May encounter problems with the long-term stability of the reagents under incident light • Response may be slow because of the time of mass transfer of analytes to the reagent phase • The complex *in vivo* factors that affect optical measurement of lactate is not well understood
Ion-Selective	• Relatively inexpensive • Have wide concentration range • Robust and durable • Rapid measurement and suitable for continuous monitoring of concentration changes • Unaffected by sample color or turbidity	• Relatively low accuracy • Generally require prior sample preparation, such as dilution • Potential drift • Membrane fouling due to the adhesion of organic molecules • Sensitive to environment, such as pH, temperature and pressure
Amperometric	• Long storage time • Highly sensitive • Have analyte-specific surface • Wide detection range and extremely low detection limit; less than pmol/L • Accurate • Do not require prior sample preparation, such as dilution • Proven capability for long term *in vivo* measurements • Unaffected by sample color or turbidity	• Relatively slow in response • Sensitive to environment, such as temperature, pressure and pH • May encounter signal drift and erroneous low readings due to the gradual degradation of the anode material during long term measurements

Most of the electrochemical sensors used in biology and medicine are polarographic sensors. These sensors operate in the region of the current vs. potential curve where the measured current is almost independent of applied potential. This is only possible when the applied potential is high enough so that the concentration of analyte at the surface of the cathode (working electrode) is maintained at zero, but low enough so that no other electrode reactions can occur. The polarized region is usually represented by the plateau portion of the current vs. potential plot and the measured current is completely determined by diffusion:

$$i = nFAf$$

Where i is the current, n is the number of electrons transferred per mole of electrode reaction, F is the faraday constant (96485 coulomb/mole), A is the electrode area and f is the flux of reducible specie to the electrode (i.e. oxygen). If the electrode surface is a disk, the current will be given by:

$$i = 2\pi nFD \int_0^a \left. \frac{\partial C}{\partial z} \right|_{z=0} rdr$$

Where a is the electrode radius and D is the diffusion coefficient of the analyte in the medium (Fatt, 1976).

In practice, it is essential to add background electrolyte into the medium that connects the working and reference electrodes. The background electrolyte acts to shield the large potential difference between the two electrodes from the bulk of solution, so that the potential drop will only occur across a thin layer of solution close to each electrode. This is desirable because it will prevent the migration of electrochemically generated charged species, so that reproducible mass transport can be maintained. In

addition, the presence of electrolyte also strongly reduces the electric resistance in the solution, so that potential drop is prevented. In many applications, however, it is also common to replace this liquid connection with a solid phase hydrophilic material. In this thesis, the electrodes are prepared by first dip-coating them with KCl saturated poly(2-Hydroxyethyl Methacrylate), or pHEMA, and then cover the entire three-electrode unit with a thin layer of silicone rubber. The purpose of using KCl saturated pHEMA is to create salt bridge between the electrodes, and the thin layer of silicone rubber is to allow only oxygen to reach the working electrode.

In addition to the need for background electrolyte, amperometric sensors can also have a third auxiliary electrode in order to be suitable for analytical purposes. This is because: 1) any current flowing from the working electrode flows directly into the reference electrode, which eventually changes the potential of the reference electrode, and 2) there will be an undesirable potential drop between the working and the reference electrodes if a current *i* were allowed to flow between them. The presence of this third auxiliary electrode, which usually takes the form of a graphite rod or platinum mesh/rod, allows the application of a potential to the working electrode with respect to the reference electrode and at the same time forces any current to flow into its terminal (Lucisano, 1987). In order to achieve optimal performance, the third auxiliary electrode (or counter electrode) usually has a larger electrode area than the working electrode (see Figure 2.2).

The sensor's sensitivity and selectivity are mainly obtained through electrode modifications. In particular, the nature of the electrode-electrolyte interface can be

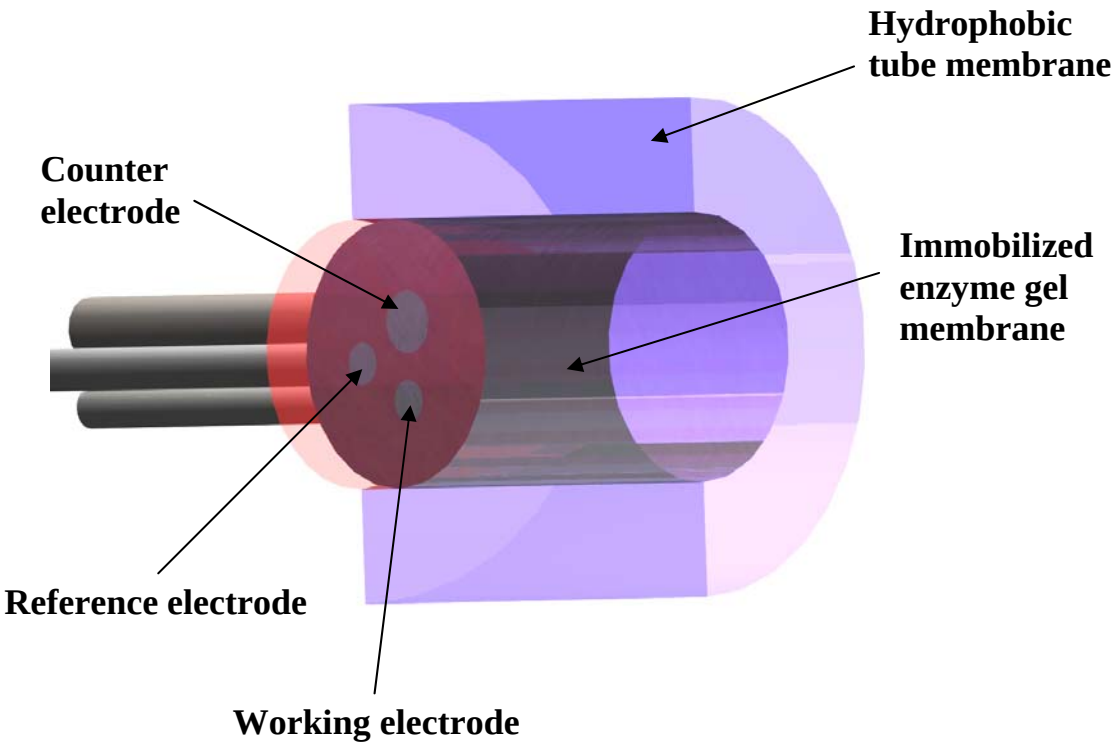

Figure 2.2 The amperometric two-dimensional cylindrical electrochemical sensor. The sensor shown above has three "disk" electrodes, which are located at the bottom of the enzyme gel: a working electrode, for reducing oxygen; a reference electrode, for applying a constant potential to the working electrode; and a counter electrode, for maintaining the sensor's signal stability. The immobilized enzyme membrane fills the region inside the outer hydrophobic tube and on top of the electrodes; it contains the enzymes that catalyze substrate specific reactions. The outer hydrophobic membrane is only permeable to oxygen, and not lactate. Lactate can only diffuse into the sensor from the bulk solution by the open annular end, allowing the two-dimensional sensor to operate at a higher bulk lactate to oxygen ratio (oxygen deficit).

modified to activate/passivate particular reactions or to protect the electrode surface from unwanted reactants. Some of the most important methods used for the modification of electrode surfaces include: covalent attachment by silanization or direct bonding, polymer coatings and modified carbon paste electrodes (Diamond, 1998).

2.2.2. Previous Work

A common feature among lactate biosensors is that they all utilize one or more enzymes as lactate recognition element. The most widely used enzyme of choice is lactate oxidase. Sensors with this type of enzyme are similar to the Clark type glucose sensor and they are commonly referred to as the first generation sensor. When ambient lactate diffuses into the enzyme-immobilized membrane, it reacts with oxygen to produce pyruvate and hydrogen peroxide. This reaction is catalyzed by lactate oxidase that is generally immobilized onto or around the electrode surface. The hydrogen peroxide produced will diffuse to the electrode surface where it is rapidly oxidized by a positive potential (oxidation potential) to produce a lactate dependent electric current:

$$L-lactate + O_2 \xrightarrow{LOD} pyruvate + H_2O_2$$

$$H_2O_2 \rightarrow O_2 + 2H^+ + 2e^-$$

However, in order to oxidize hydrogen peroxide, the electrode must be polarized at +600 mV relative to the reference electrode, which is also high enough to oxidize other molecules that are commonly found in the biological environment, such as ascorbic acid. This problem is usually mitigated by placing a thin layer of permselective membrane between the enzyme layer and the electrode so that only hydrogen peroxide is allowed to diffuse through.

Alternatively, lactate can also be detected through the means of oxygen detection. In this case, the oxygen consumption inside the sensor is proportional to the concentration of lactate and the resultant oxygen dependent current can correlate directly to the lactate concentration. The advantage of oxygen detection is that the oxygen electrode employs a reduction potential, which causes far fewer endogenous chemical interferences. When the electrode is covered by a thin layer of gas permeable-only membrane, all chemical interferents that are endogeneous to blood or tissue fluid can be completely rejected. Because of its simplicity and high selectivity, this is the method of choice for designing lactate sensors in this thesis.

Currently, implantable lactate sensors that are under development require only one calibration before the *in vivo* application and have signal stability over a short period of time in both *in vitro and in vivo* studies as ascertained by a calibration check at post-explant (Hu *et al.*, 1993; Baker and Gough, 1995). Problems associated with these sensors usually involve long term sensor stability, slower dynamic response and biocompatibility.

A number of approaches have been described by different research groups that address these issues. These approaches involve: 1) modifying enzyme immobilization techniques, such as enzyme entrapment in a polymer matrix or hydrogel, direct electrodeposition on the electrode, or covalent attachment (Badea et al., 2003; Mosbach et al., 2001; Padeste et al., 2003), 2) modifying sensor geometry, such as double lumen catheter (Meyerhoff *et al.*, 1993), need-type sensor (Yang et al., 1998), planar biochip sensor (Guiseppi-Elie *et al.*, 2005), microdialysis sampling system incorporated biosensor (Petrou et al., 2003) or wire-based microelectrodes (Ward *et al.*, 2004), 3) modifying the

enzyme gel layer, such as coating with serum albumin to increase biocompatibility, using composite polymer bio-recognition membrane consisting of interference shielding electroactive polypyrrole and biomimetic phosphorylcholine derivatives (Guiseppi-Elie *et al.*, 2005; Gavalas et al., 2006), or coating with polymer to slow down diffusion of L-lactate to shift the linear range, 4) modifying electrode surface, such as coating the electrode with Nafion or electroplymerized poly(1,3-phenylenediamine) to block interferents (Mizutani et al., 2001), coating the electrode with electron transfer mediators and redox polymers to shift the oxidation potential of peroxide (Burmeister et al., 2005; Hirano et al., 2002a; Hirano et al., 2002b), 5) modifying enzymes, such as designing thermostable lactate oxidase (Kaneko et al., 2005), stabilizing enzymes with diethylaminoethyl-dextran (Gavalas, and Chaniotakis, 2000) or PEGylation (Guiseppi-Elie *et al.*, 2005), and 6) using different enzymes, such as immobilized lactate dehydrogenase (Gue *et al.*, 2002; or cytochrome b_2 and cytochrome c oxidoreductase, Williams *et al.*, 1970; Kulys *et al.*, 1980; Wang *et al.*, 1994; Smutok *et al.*, 2005), lactate mono-oxygenase (Makovos *et al.*, 1985), flavocytochrome b_2 (Smutok et al., 2005) or co-immobilization of enzymes to amplify signal (Chaubey et al., 2000).

Table 2.2 lists results from some of the *in vivo* lactate biosensor studies done by different research groups. Although the results from these studies can not be compared directly due to the additional physiological effects present *in vivo*, these examples depict the current state of the art in lactate biosensor research.

Table 2.2 Summary of reports on *in vivo* studies with lactate biosensors.

Sensor Type	Test Conditions	Result and Comment	Reference
Enzyme electrode, thin film, H_2O_2 detection	*In vivo*, (dog, subcutaneous, 7 hours), implant	*In vitro* characterization showed a linear range between 0.5 to 20 mM and the sensitivity drift is below 2% per hour. Correlation between sensor outputs and discrete sample data *in vivo* is 0.9748.	Pfeiffer et al. (1997)
Enzyme electrode, thin-wire, H_2O_2 detection	*In vivo*, (rats, subcutaneous, 3-4 hours), implant	*In vitro* characterization showed a linear range up to 10 mM. Sensors showed tendency for overestimation at high lactate levels.	Ward et al. (2004)
Enzyme electrode, double lumen catheter, H_2O_2 detection	*In vivo*, (human, subcutaneous, right abdominal region, 3-4 hours), microperfusion	A constant flow rate of 1.2 µl min^{-1} was used. The sensor has a linear range up to 25 mM. Variations of lactate concentration and equilibration time between capillary blood and subcutaneous tissue were observed.	Ellmerer et al. (1998)
Enzyme electrode, catheter-type, O_2 detection	*In vivo*, (dog, right atrium, 4 hours), implant	*In vitro* characterization showed a linear range up to 25 mM with response time up to 5 minutes. Sensor signals were in agreement with discrete sample data.	Baker and Gough (1995)
Enzyme electrode, double lumen catheter, H_2O_2 detection	*In vivo*, (human, cubital vein, up to 22 hours), microperfusion	*In vitro* characterization showed a linear range up to 15 mM and a response time of 4 minutes. Flow rates were 43 to 92 µl min^{-1} and the sensor signals were in agreement with discreet sampled data. Thrombus formation at the tip of the catheter was observed in one of the patients.	Meyerhoff et al. (1993)
Enzyme electrode, needle-type, H_2O_2 detection	*In vivo*, (rat, subcutaneous, back of the neck, 2-3 hours), implant	*In vitro* characterization showed a linear range up to 20 mM and a response time of less than 1 minute. Sensor response time to lactate injection is dependent on implant site and may take up to several minutes.	Hu et al. (1993)
Enzyme electrode, needle-type, direct wiring between enzyme and electrode	*In vivo*, (rat, subcutaneous, back of the neck, 24 hours), microperfusion	A constant flow rate of 5 µl min^{-1} was used. The sensor has a linear range up to 5 mM and a response time of 2 minues. Sensor is recalibrated with standard lactate solutions every 2-3 hours.	Yang et al. (1995)

2.2.3. Conclusion

Despite the efforts for improving the overall sensor performance, systematic studies of sensor behavior using mathematical modeling techniques have rarely been done. The focus of this study is therefore to use mathematical models to analyze the sensor behavior and to determine the effects of the various size and mass transport parameters on the transient and steady-state sensor responses. The results from this study can be used to optimize the performance of lactate biosensors more efficiently.

CHAPTER III.

Mathematical Models

3.1. Introduction

Efficient sensor optimization strategy must be derived from a fundamental understanding of sensor behavior, which is based on experimentations and validated models. Thus, this chapter presents a mathematical model that predicts the transient and steady-state responses of a two-dimensional lactate sensor. The model predictions are also investigated and can be compared to experimental data from sensor testing using physiologic conditions. The goals of this study are to: 1) identify the effects of geometric, kinetic and transport parameters on the overall sensor response; 2) predict the response of proposed sensor designs under conditions that mimics the usual physiological environments; and 3) demonstrate how modeling results can be applied to design lactate sensors tailored for specific applications.

3.2. Previous Studies

The transient and steady-state responses of two dimensional glucose sensors, which are similar in design to the sensor of interest in this study, had been predicted and analyzed by investigators at UCSD (Lucisano, and Gough, 1988; Gough, Lucisano, and Tse, 1985; Armour, 1988; Tse, 1984). Several parameters were identified to have profound influence on sensor responses, which suggest that simple adjustments on sensor design may lead to significant performance improvements. However, the results from these studies cannot be used to adequately describe the system of interest in this thesis

due to: 1) most of the transient and steady-state responses had been predicted for sensors with “long” electrodes, which span the entire length of the enzyme membrane, whereas the lactate sensor in this study has a disc electrode at the bottom of the enzyme membrane (Figure 3.1); and 2) the differences in sensor response between single enzyme (lactate oxidase only) and double enzyme (lactate oxidase co-immobilized with catalase) systems had not been investigated. Therefore, it is necessary to characterize the lactate sensor signal response for these cases.

Previous studies employed a numerical solver based on finite difference method (FDM), called alternating direction implicit (ADI) method. In ADI approach, finite difference equations (explicit and implicit) were formulated at alternating time steps. At one time step, one spatial direction has an implicit expression and the other direction has an explicit expression. At the next time step, the expressions of the spatial directions are reversed. The outcome of this approach is a fully implicit method**.** The discretization yielded rectangular grids, which are not uniform in size near the electrode surface. The nonuniform space grid is necessary to ensure the reliability of the results. The overall result after every two time steps is second order accurate.

In this study, a finite element method (FEM) is employed. FEM is an alternative way for solving PDEs and is often the preferred method of choice when the geometry of interest is complex (the quality of the approximation between grid points is not as good in FDM). Although the geometry in this case is not complex, FEM may still yield higher accuracy and smoother convergence due to its better handling of curvatures at the

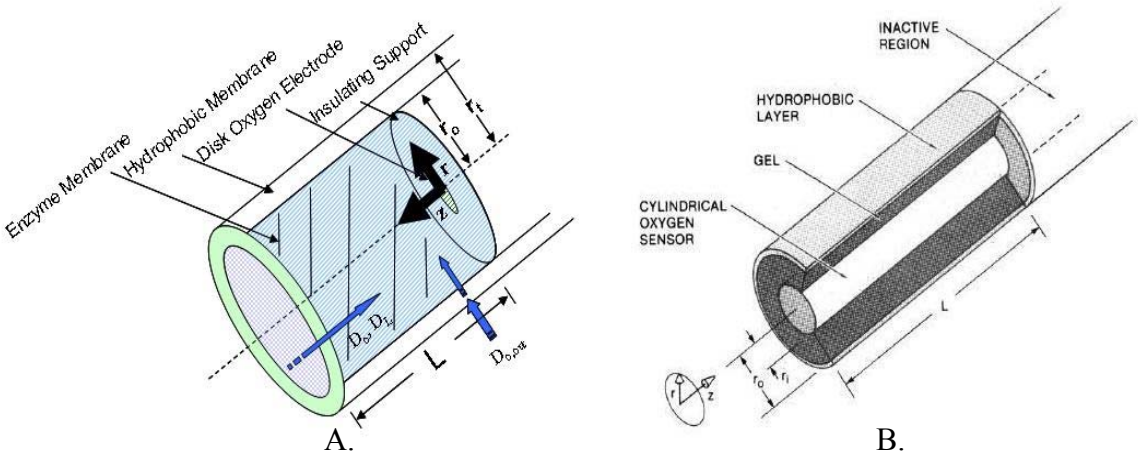

Figure 3.1 Comparison between a sensor having "disk" electrode (A) and "long" electrode (B) (Courtesy of Gough, Lucisano and Tse, 1985). With the "disk" electrode sensor, the electrode is located at the bottom of the enzyme membrane. In contrast, the electrode for "long" sensor spans the entire length of the enzyme membrane. Except for the difference in electrode configuration, the designs for both the "long" and "disk" two-dimensional electrode sensors are otherwise identical.

boundaries. The FEM solver is provided by COMSOL Multiphysics (Comsol, Palo Alto, CA, formerly known as FEMLAB).

3.3. Current Model: System Description

The two dimensional sensor with coordinate system is shown in Figure 3.2. The sensor has a cylindrical enzyme gel with radius r_o, which contains immobilized lactate oxidase (catalase is included later for dual enzyme sensor simulation) and is permeable to both oxygen and lactate. Oxygen and lactate diffusivities and solubility in this layer are denoted as D_o, D_L and γ_o, γ_L, respectively. One end of the enzyme gel is fixed on top of a disc electrode with radius r_e with the remaining surface of that end covered by an insulating material that is impermeable to oxygen and lactate. There is also a thin film of hydrophobic membrane between the enzyme gel and the electrode that only allows the diffusion of oxygen. The other end of the enzyme gel is exposed to the bulk solution. The gel is covered by an outer hydrophobic membrane along the axial direction with a thickness r_t-r_o, where r_t is the total radius of the sensor. The hydrophobic membrane is only permeable to oxygen and has an oxygen diffusion coefficient and solubility $D_{o,\,out}$ and $\gamma_{o,\,out}$, respectively. The sensor is immersed in the bulk medium and has concentration boundary layers with thickness δ_r on the curved radial surface and δ_z on the flat axial end. The bulk oxygen and lactate concentrations beyond the boundary layers are $c_{o,B}$ and $c_{L,B}$, respectively. The oxygen and lactate diffusion coefficients and solubility are $D_{o,\,B}$, $D_{L,\,B}$ and $\gamma_{o,\,B}$, $\gamma_{L,\,B}$, respectively. Table 3.1 lists the material properties just mentioned.

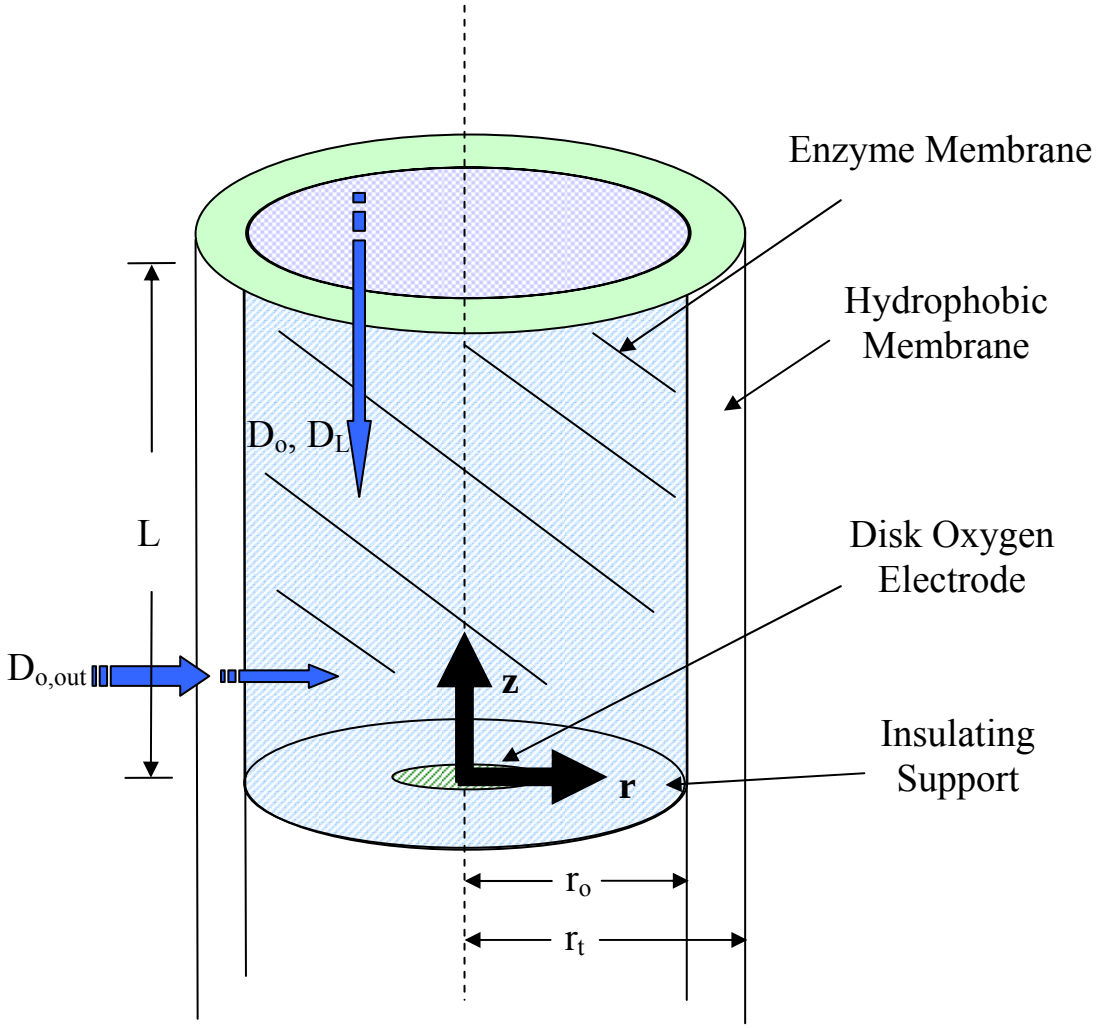

Figure 3.2 Schematic of the 2D disk sensor with coordinate system.

Table 3.1 Properties of system components.

Component	Property				
	Diffusion Coefficient		Substrate Solubility		Effective Thickness
	Oxygen	Lactate	Oxygen	Lactate	
Enzyme Membrane	D_o	D_L	γ_o	γ_L	r_o
Outer Membrane	$D_{o,\,out}$	--	$\gamma_{o,\,out}$	--	$r_t - r_o$
Bulk Medium	$D_{o,\,B}$	$D_{L,\,B}$	$\gamma_{o,\,B}$	$\gamma_{L,\,B}$	δ_r (radial) δ_z (axial)

The mathematical model is based on the consideration of the coupled diffusion reaction of lactate and oxygen within the enzyme gel. The overall enzyme reaction within the gel membrane is:

$$\text{lactate} + \nu O_2 \rightarrow \text{pyruvate} + H_2O \tag{3.1}$$

Where ν is a stoichiometry coefficient based on relative activity of the co-immobilized catalase. In the case of excess catalase, ν equals to one half.

The assumptions used in this analysis are: 1) the hydrophobic membrane between the enzyme gel and the electrode has no effect on oxygen transport, 2) only the steady-state effects of the boundary layers are included in the model due to their relatively short transient phase, 3) all materials are homogeneous and their properties are constant with time, 4) oxygen is instantaneously consumed upon reaching the electrode (the concentration of oxygen is zero at $r = r_e$), and 5) enzyme substrate complex formation is rapid enough to have no contribution to the overall sensor transient times.

3.3.1. Governing Equations

The generalized conservation of mass equation for the system is:

$$\frac{\partial c_i}{\partial t} = D_i \nabla^2 c_i + Q_i \tag{3.2}$$

Where c_i and D_i are the concentration and diffusion coefficient of species i. ∇^2 is the Laplacian operator and Q_i is the rate of reaction for species i. From the above assumptions, the governing equations for oxygen and lactate transport inside the cylindrical sensor membrane can be simplified to:

$$\frac{\partial C_L}{\partial t} - D_L \left\{ \frac{\partial^2 C_L}{\partial r^2} + \frac{1}{r}\frac{\partial C_L}{\partial r} + \frac{\partial^2 C_L}{\partial z^2} \right\} + V(C_L, C_o) = 0 \tag{3.3a}$$

$$\frac{\partial C_o}{\partial t} - D_o \left\{ \frac{\partial^2 C_o}{\partial r^2} + \frac{1}{r}\frac{\partial C_o}{\partial r} + \frac{\partial^2 C_o}{\partial z^2} \right\} + \upsilon V(C_L, C_o) = 0 \tag{3.3b}$$

Where ν is a stoichiometry coefficient and $V(c_L,c_o)$ is the rate of ping-pong reaction expression for lactate oxidase (Lockridge, Massey and Sullivan, 1972) similar to that of the classic glucose oxidase enzyme sensor model (Weibel and Bright, 1971):

$$V(C_L, C_o) = \frac{V_{\max} C_L C_o}{C_L C_o + K_o C_L + K_L C_o} \tag{3.4}$$

Where V_{max} is the maximal reaction velocity per unit volume, K_L and K_o are the Michaelis constants for lactate and oxygen at infinite concentrations of the other substrate, respectively.

The transport of oxygen in the hydrophobic membrane is:

$$\frac{\partial C_o}{\partial t} - D_{o,out} \left\{ \frac{\partial^2 C_o}{\partial r^2} + \frac{1}{r}\frac{\partial C_o}{\partial r} + \frac{\partial^2 C_o}{\partial z^2} \right\} = 0 \tag{3.5}$$

3.3.2. Boundary Conditions

The boundary conditions are summarized in Table 3.2. Along the axial length of the sensor ($0 \le z \le L$), three interfaces can be identified.

1. At the electrode's center (r = 0), no radial diffusion occurs due to symmetry:

$$\frac{\partial C_L}{\partial r} = 0 \qquad \frac{\partial C_o}{\partial r} = 0 \tag{3.6a,b}$$

2. At the interface between enzyme gel and the hydrophobic membrane ($r = r_o$), there is no lactate diffusion but oxygen concentration is continuous:

$$\frac{\partial C_L}{\partial r} = 0 \qquad D_o \frac{\partial C_o}{\partial r}\bigg|_{r=r_o^-} = D_{o,out} \frac{\partial C_o}{\partial r}\bigg|_{r=r_o^+} \tag{3.7a,b}$$

$$C_o = \alpha_{o,\text{inter}} \mathrm{C_o}\big|_{r=r_o^+} \tag{3.7c}$$

3. At the interface between the hydrophobic membrane and the bulk solution ($r = r_t$), convective oxygen transport is taking place:

$$D_{o,out} \frac{\partial C_o}{\partial z} = h_{o,out}\left(C_{o,B} - \frac{C_o}{\alpha_{o,out}} \right) \tag{3.8}$$

Additionally, there are two types of interfaces along the axial end of the sensor (z = L).

1. At the interface between enzyme gel and the bulk medium ($0 \le r \le r_0$), both lactate and oxygen convective transports exist:

$$D_L \frac{\partial C_L}{\partial z} = h_L\left(C_{L,B} - \frac{C_L}{\alpha_L} \right) \tag{3.9a}$$

$$D_o \frac{\partial C_o}{\partial z} = h_o\left(C_{o,B} - \frac{C_o}{\alpha_o} \right) \tag{3.9b}$$

2. At the interface between the hydrophobic membrane and the bulk solution ($r_0 \le r \le r_t$), only oxygen convection transport is present:

$$D_o \frac{\partial C_o}{\partial z} = h_o \left(C_{o,B} - \frac{C_o}{\alpha_{o,out}} \right) \tag{3.10}$$

The electrode end of the sensor (z = 0) also has two interfaces.

1. At the electrode surface ($0 \le r \le r_e$), oxygen concentration and lactate permeability are zero:

$$c_o = 0 \qquad \frac{\partial C_L}{\partial z} = 0 \tag{3.11a,b}$$

2. Outside of the electrode surface ($r_e < r \le r_t$), which is impermeable to lactate and oxygen:

$$\frac{\partial C_L}{\partial z} = 0 \qquad \frac{\partial C_o}{\partial z} = 0 \tag{3.12a,b}$$

3.3.3. Dimensionless Variables

Non-dimensionalization is essential for simplifying experimental parameters and is used in almost all engineering analysis. The new independent variables are:

$$\rho = \frac{r}{r_0} \qquad \xi = \frac{z}{L} \qquad \tau = \frac{D_L t}{L^2} \tag{3.13a,b,c}$$

The new dimensionless concentrations are:

$$\overline{C_L} = \frac{C_L}{\alpha_L C_{L,B}} \qquad \overline{C_o} = \frac{D_o C_o}{\upsilon \alpha_L D_L C_{L,B}} \tag{3.14a,b}$$

Table 3.2 Dimensional boundary conditions.

Lactate	Oxygen	r	z
$\frac{\partial C_L}{\partial r} = 0$	$\frac{\partial C_o}{\partial r} = 0$	r = 0	$0 \le z \le L$
$\frac{\partial C_L}{\partial r} = 0$	$D_o \frac{\partial C_o}{\partial r}\Big\|_{r=r_o^-} = D_{o,out} \frac{\partial C_o}{\partial r}\Big\|_{r=r_o^+}$ $C_o = \alpha_{o,\text{inter}} \mathrm{C_o}\big\|_{r=r_o^+}$	$r = r_o$	
	$D_{o,out} \frac{\partial C_o}{\partial z} = h_{o,out}\left(C_{o,B} - \frac{C_o}{\alpha_{o,out}}\right)$	$r = r_t$	
$D_L \frac{\partial C_L}{\partial z} = h_L\left(C_{L,B} - \frac{C_L}{\alpha_L}\right)$	$D_o \frac{\partial C_o}{\partial z} = h_o\left(C_{o,B} - \frac{C_o}{\alpha_o}\right)$	$0 \le r \le r_0$	$z = L$
	$D_o \frac{\partial C_o}{\partial z} = h_o\left(C_{o,B} - \frac{C_o}{\alpha_{o,out}}\right)$	$r_0 \le r \le r_t$	
$\frac{\partial C_L}{\partial z} = 0$		$0 \le r < r_0$	$z = 0$
	$c_o = 0$	$0 \le r \le r_e$	
	$\frac{\partial C_o}{\partial z} = 0$	$r_e < r \le r_t$	

The size parameters are

$$R' = \frac{r_t - r_0}{r_0} \qquad \varepsilon = \frac{r_0}{L} \tag{3.15a,b}$$

R' normalizes the hydrophobic membrane thickness by that of the enzyme gel. The aspect ratio, ε, is the ratio of enzyme gel radius to the sensor length.

The diffusion coefficient ratio is:

$$\lambda = \frac{D_o}{D_L} \tag{3.16}$$

The dimensionless reaction rate is:

$$\overline{V}\left(\overline{C_L}, \overline{C_o}\right) = \frac{\sigma^2 \overline{C_L}\,\overline{C_o}}{\overline{C_L}\,\overline{C_o} + \kappa_o \overline{C_L} + \kappa_L \overline{C_o}} \tag{3.17}$$

Where the dimensionless Michaelis constants and dimensionless catalytic activity are:

$$\kappa_L = \frac{K_L}{\alpha_L C_{L,B}} \qquad \kappa_o = \frac{K_o D_o}{\upsilon \alpha_L C_{L,B} D_L} \qquad \sigma^2 = \frac{r_0^2}{D_L}\frac{V_{\max}}{K_L} \tag{3.18a,b,c}$$

3.3.4. Dimensionless Governing Equations

Substituting the dimensionless variables into the general equations for oxygen and lactate in the enzyme gel and the hydrophobic membrane yields:

$$\varepsilon^2 \frac{\partial \overline{C_L}}{\partial \tau} - \left\{ \frac{\partial^2 \overline{C_L}}{\partial \rho^2} + \frac{1}{\rho}\frac{\partial \overline{C_L}}{\partial \rho} + \varepsilon^2 \frac{\partial^2 \overline{C_L}}{\partial \xi^2} \right\} + \kappa_L \overline{V}\left(\overline{C_L}, \overline{C_o}\right) = 0 \tag{3.19a}$$

$$\frac{\varepsilon^2}{\lambda}\frac{\partial \overline{C_o}}{\partial \tau} - \left\{ \frac{\partial^2 \overline{C_o}}{\partial \rho^2} + \frac{1}{\rho}\frac{\partial \overline{C_o}}{\partial \rho} + \varepsilon^2 \frac{\partial^2 \overline{C_o}}{\partial \xi^2} \right\} + \kappa_L \overline{V}\left(\overline{C_L}, \overline{C_o}\right) = 0 \tag{3.19b}$$

$$\frac{\varepsilon^2}{\lambda'}\frac{\partial \overline{C_o}}{\partial \tau} - \left\{ \frac{\partial^2 \overline{C_o}}{\partial \rho^2} + \frac{1}{\rho}\frac{\partial \overline{C_o}}{\partial \rho} + \varepsilon^2 \frac{\partial^2 \overline{C_o}}{\partial \xi^2} \right\} = 0 \tag{3.19c}$$

3.3.5. Dimensionless Boundary Conditions

Substituting the dimensionless variables into the dimensional boundary conditions (Table 3.2) yields the non-dimensionalized boundary conditions summarized in Table 3.3.

3.3.6. Method of Solution

The system of coupled, nonlinear partial differential equations is solved with COMSOL Multiphysics software, a nonlinear, finite-element based solver. An automatic meshing function is used for the initial discretization of the domain, with subsequent increase in grid resolution applied manually in regions where high spatial resolution is necessary. This is particularly important near the radial boundary at the domain entry because of the mass transfer boundary layer-type behavior. A typical grid using ~ 30,000 elements causes the convergence of a Galerkin error monitor. Solutions are exported to Matlab for post-processing.

3.3.7. Sensor Dimensions and Parameters

The dimensions of the sensors used in all simulations are listed in Table 3.4. Tubing radius and wall thickness are specified by commercial vendor. Aspect ratios are calculated using equation 3.15b. Table 3.5 summarizes the values of the kinetic and transport parameters used in this model. Unless otherwise mentioned in specific cases, the values listed were used in all simulations in the following discussion. These values were obtained from previous studies of lactate oxidase kinetics (Maeda-Yorita, et al. 1995), collagen based membranes (Gough, Leypoldt, and Armour, 1982), hydrophobic polymers (Crank and Park, 1968), and modeling of the 2D glucose sensor (Gough, Lucisano, and Tse, 1985; Lucisano and Gough, 1988). Since the system described here is

Table 3.3 Dimensionless boundary conditions.

Lactate	Oxygen	r	z
$\frac{\partial \overline{C_L}}{\partial \rho} = 0$	$\frac{\partial \overline{C_o}}{\partial \rho} = 0$	$\rho = 0$	$0 \le \xi \le 1$
$\frac{\partial \overline{C_L}}{\partial \rho} = 0$	$\lambda \frac{\partial \overline{C_o}}{\partial \rho}\Big\|_{\rho=1^-} = \lambda' \frac{\partial \overline{C_o}}{\partial \rho}\Big\|_{\rho=1^+}$ $\overline{C_o} = \alpha_{o,\text{inter}} \overline{C_o}\Big\|_{\rho=1^+}$	$\rho = 1$	
	$\frac{\partial \overline{C_o}}{\partial \rho} = Bi_{o,rout}\left(\overline{C_o'}^{*} - \overline{C_o}\right)$ $\overline{C_o'}^{*} = \frac{C_{o,B} D_o \alpha_{o,out}}{\upsilon \alpha_L D_L C_{L,B}}$	$\rho = \frac{r_t}{r_0}$	
$\frac{\partial \overline{C_L}}{\partial \xi} = Bi_L\left(1 - \overline{C_L}\right)$	$\frac{\partial \overline{C_o}}{\partial \xi} = Bi_o\left(\overline{C_o}^{*} - \overline{C_o}\right)$ $\overline{C_o}^{*} = \frac{\alpha_o D_o C_{o,B}}{\upsilon \alpha_L D_L C_{L,B}}$	$0 \le \rho \le 1$	$\xi = 1$
	$\frac{\partial \overline{C_o}}{\partial \xi} = Bi_{o,zout}\left(\overline{C_o'}^{*} - \overline{C_o}\right)$	$1 \le \rho \le \frac{r_t}{r_0}$	
$\frac{\partial \overline{C_L}}{\partial \xi} = 0$		$0 \le \rho < 1$	$\xi = 0$
	$\overline{C_o} = 0$	$0 \le \rho \le \frac{r_e}{r_0}$	
	$\frac{\partial \overline{C_o}}{\partial \xi} = 0$	$r_e < \rho < \frac{r_t}{r_0}$	

Table 3.4 Dimensions of sensors with varying size.

Index number	r_e cm	r_i cm	r_o cm	r_t cm	L cm	ε
Small size						
I	0.0038	0.0040	0.0254	0.0470	0.0254	1
II	0.0038	0.0040	0.0254	0.0470	0.0508	1/2
III	0.0038	0.0040	0.0254	0.0470	0.0762	1/3
IV	0.0038	0.0040	0.0254	0.0470	0.1016	1/4
Medium size						
V	0.0038	0.0040	0.0318	0.0597	0.0318	1
VI	0.0038	0.0040	0.0318	0.0597	0.0635	1/2
VII	0.0038	0.0040	0.0318	0.0597	0.0953	1/3
VIII	0.0038	0.0040	0.0318	0.0597	0.1270	1/4
Large size						
IX	0.0038	0.0040	0.0381	0.0826	0.0381	1
X	0.0038	0.0040	0.0381	0.0826	0.0762	1/2
XI	0.0038	0.0040	0.0381	0.0826	0.1143	1/3
XII	0.0038	0.0040	0.0381	0.0826	0.1524	1/4

Table 3.5 Parameter values for the model.

Parameter	Value	Description
D_o	$2.0 \cdot 10^{-5} cm^2/s$	Oxygen diffusion coefficient
$D_{o,out}$	$2.0 \cdot 10^{-5} cm^2/s$	Oxygen diffusion coefficient in silicone rubber
$D_{o,B}$	$2.0 \cdot 10^{-5} cm^2/s$	Bulk oxygen diffusion coefficient
D_L	$4.0 \cdot 10^{-6} cm^2/s$	Lactate diffusion coefficient
$D_{L,B}$	$4.0 \cdot 10^{-6} cm^2/s$	Outer lactate diffusion coefficient
α_o	0.80	Oxygen partition coefficient
$\alpha_{o,inter}$	0.16	Oxygen partition coefficient at interface
α_L	0.80	Lactate partition coefficient
σ	0.5 – 12	Dimensionless catalytic activity
K_o	0.001 M	Michaelis constant for oxygen
K_L	0.1 – 0.4M	Michaelis constant for lactate
$C_{o,B}$	0.021 – 0.21 mM	Bulk oxygen concentration
$C_{L,B}$	0 – 20 mM	Bulk lactate concentration
h_o	$4.0 \cdot 10^{-3} cm/s$	Oxygen convective mass transfer coefficient at enzyme gel surface
h_L	$8.0 \cdot 10^{-4} cm/s$	Lactate convective mass transfer coefficient at enzyme gel surface
$h_{oH,z}$	$4.0 \cdot 10^{-3} cm/s$	Oxygen convective mass transfer coefficient at axial hydrophobic membrane surface
$h_{oH,r}$	$3.8 \cdot 10^{-3} cm/s$	Oxygen convective mass transfer coefficient at radial hydrophobic membrane surface
δ_z	0.005 cm	Boundary layer thickness
δ_r	0.005 cm	Boundary layer thickness

similar to the one for glucose sensor, the mass transport parameters for both systems are also expected to be similar.

3.4. Results and Discussion

Simulation results are grouped into three categories. The first category consists of perspective views of calculated lactate and oxygen concentrations in the enzyme gel of the sensor of interest. The second category contains results from simple single parameter changes. These include step changes in either bulk lactate or oxygen concentration and also kinetic parameter changes. The effects of these parameters on sensor response are identified**.** In addition, the effects of overall membrane sizes, aspect ratios and compositions (i.e. with or without catalase co-immobilization) on sensor response will also be presented here. The third category presents the model predictions for complex bulk substrate changes that simulate more physiologic conditions. Sensor design strategy for specific/tailored applications based on the simulation results is discussed in the concluding section.

3.4.1. Perspective Views of Substrate Concentrations

This section presents the lactate and oxygen concentration profiles for the "small sensors" with 1/3 and 1/4 aspect ratios (see Table 3.4) following an increase in bulk lactate concentration step change from 0 to 5 mM. Although only the solutions for the enzyme gel region are shown, lactate and oxygen concentrations through the outer hydrophobic membrane were always calculated. For the sensor with 1/3 aspect ratio, a unit value of τ represents approximately 1500 seconds. For the sensor with 1/4 aspect ratio, a unit value of τ represents approximately 2600 seconds. The increase in

dimensional time reflects the longer diffusion path for the substrates. The perspective views at six discrete times are chosen to illustrate the lactate and oxygen concentration changes in the enzyme gel (Figure 3.3). In each view, the vertical (z) axis represents the substrate concentration (in mM); the right-left (x) axis represents the axial position, and the front-back (y) axis represents the radial position. The front and back borders of each view are the center of the enzyme gel ($r = 0$) and the enzyme gel/outer hydrophobic membrane interface ($r = r_o$), respectively. The left and right borders are the insulating support where the oxygen electrode is embedded ($z = 0$) and the bulk solution ($z = L$), respectively.

At $\tau = 0$, there is no enzymatic reaction and oxygen is only consumed by the oxygen electrode underneath the enzyme membrane. This is the steady-state distribution in the absence of lactate. Oxygen is supplied from both axial and radial directions. This continuous influx of oxygen is sufficient to maintain a uniform oxygen distribution throughout the sensor except in the region near the electrode.

At $\tau > 0$, enzymatic reactions occurred immediately after the bulk lactate concentration step change. This is illustrated by the sudden decrease in oxygen concentration near the axial end of the sensor ($z = L$). The lactate concentration, with time, continues to rise until a steady-state is reached. As time progresses, the oxygen depleted region at the axial end widens and propagates toward the electrode. This "marching" effect is caused by the advancement of lactate in the enzyme gel. The relatively higher oxygen concentration at the right boundary of the figures ($z = L$) is a result of axial oxygen diffusion. Oxygen supplied from the axial direction is consumed almost instantly as it enters the enzyme gel. Non-uniform radial distribution of oxygen,

which is due to radial oxygen diffusion from the outer hydrophobic membrane, is also observed. The enzymatic consumption of oxygen near the insulating support reduces the oxygen available to the lactate electrode, thus causing a lowered current with respect to that measured by an oxygen electrode. Steady-state is reached by $\tau = 0.2$ (approximately 290 seconds).

The oxygen and lactate distributions in the "small size" sensor with a 1/4 aspect ratio is shown in Figure 3.4. The dimensions are specified by series IV in Table 3.4. Other parameters were kept the same. In this case, a unit value of τ represents about 2600 seconds. Comparing Figure 3.4 with Figure 3.3, one significant difference is found: there is a larger region of relatively high oxygen concentration in the enzyme membrane near the electrode. This is due to the increased oxygen supply from the outer hydrophobic membrane that offsets some of the oxygen consumption by the reaction. As a result, relatively more oxygen is retained near the bottom of the enzyme gel where lactate takes the longest time to travel. In addition, because lactate requires a longer time to reach the electrode, the response becomes slower.

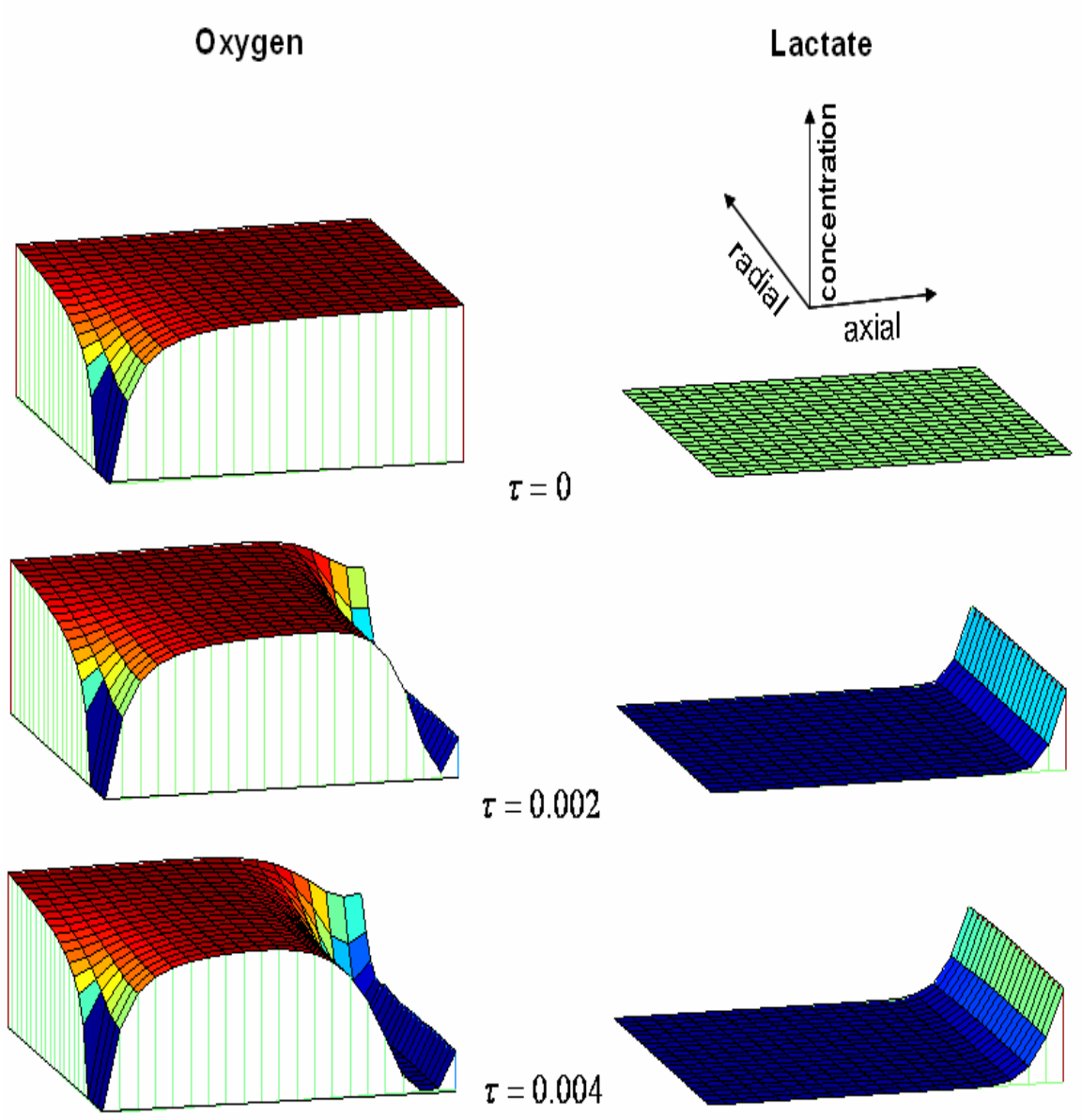

Figure 3.3 Perspective views of calculated oxygen and lactate concentrations in the enzyme gel following a step increase in bulk lactate concentration ($\varepsilon = 1/3$). Bulk oxygen concentration is fixed at 0.053 mM and the bulk lactate concentration is increased from 0 to 5 mM at $\tau = 0$. Sensor dimensions are specified by series III (Table 3.4), $\sigma = 5$, and the values of other parameters are given in table 3.5. In each view, the vertical (z) axis represents the substrate concentration; the right-left (x) axis represents the axial position, and the front-back (y) axis represents the radial position. The front and back borders of each view are the center of the enzyme gel ($r = 0$) and the enzyme gel/outer hydrophobic membrane interface ($r = r_o$), respectively. Similarly, the left and right borders are the insulating support where the oxygen electrode is embedded ($z = 0$) and the bulk solution ($z = L$), respectively.

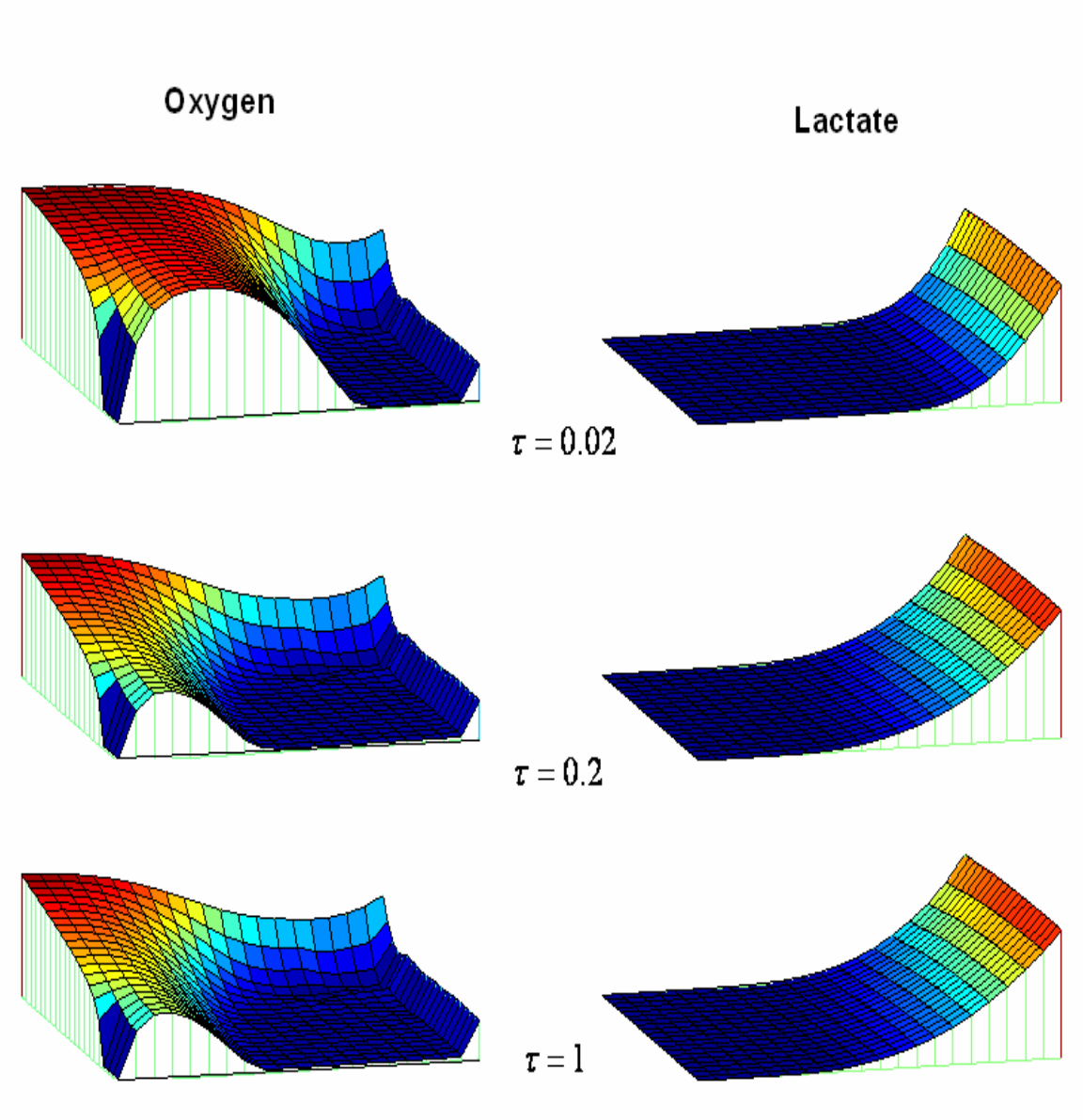

Figure 3.3 continued. Perspective views of calculated oxygen and lactate concentrations in the enzyme gel.

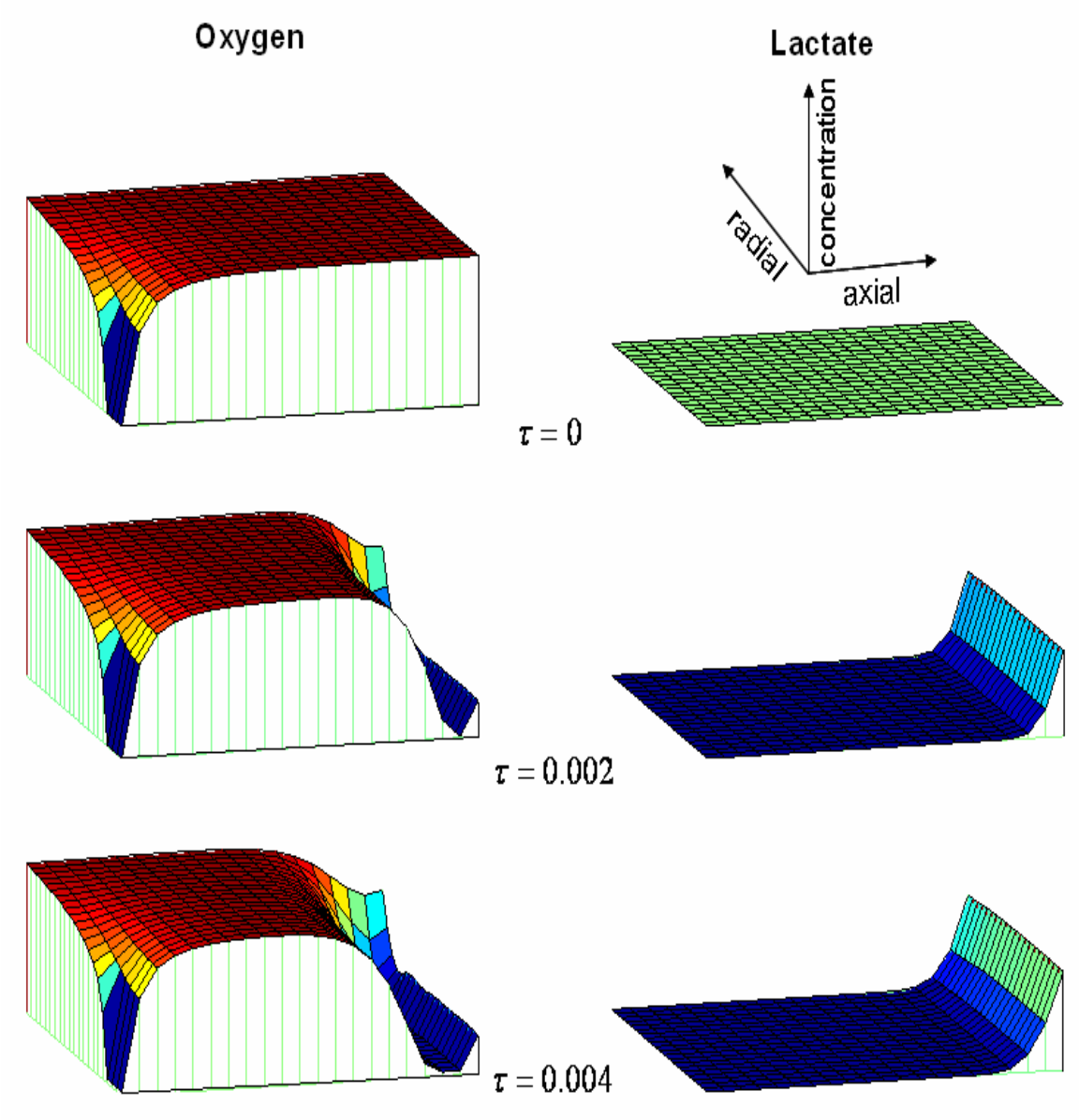

Figure 3.4 Perspective views of calculated oxygen and lactate concentrations in the enzyme gel following a step increase in bulk lactate concentration (ε = 1/4). All parameters are the same as in Figure 3.2 except the length is now equal to 0.1016 cm. (series IV, Table 3.4) τ = 1 represents 2600 seconds.

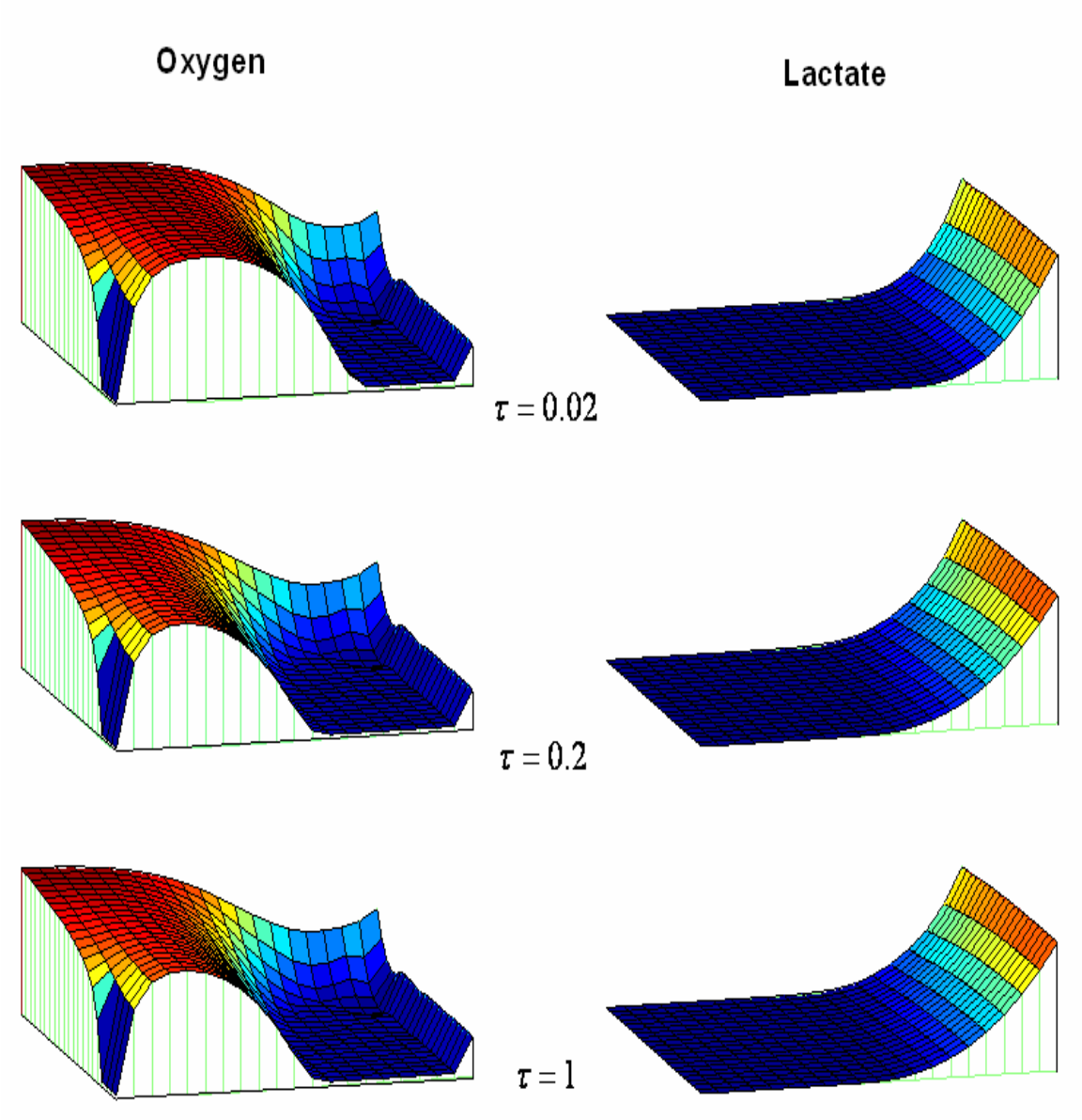

Figure 3.4 continued. Perspective views of calculated oxygen and lactate concentrations in the enzyme gel.

3.4.2. Transient Response to Step Concentration Changes

An important characterization of a sensor is done by investigating the system response to bulk oxygen or lactate concentration step changes when a design parameter (such as aspect ratio or non-dimensional catalytic activity) is varied. While the general equations and boundary conditions contain many dimensionless parameters, some of these provide more design flexibility (i.e. can have a wider range of values) than others. The range of a parameter depends on the physical constraints imposed on the system, as well as application requirements. For example, it is difficult to vary the oxygen and lactate partition coefficients due to the limited number of available biocompatible materials for sensor fabrication. Therefore, the aim of this thesis is to investigate the effects of relatively flexible parameters on sensor response. These parameters include: 1) aspect ratio, 2) bulk lactate concentration, 3) diffusivity ratio, 4) enzyme activity, 5) enzyme coupling, 6) overall sensor size, 7) boundary layer thickness, and 8) electrode configuration. The effect of outer membrane thickness on sensor response will not be presented in this thesis, because another study had shown that higher outer membrane thickness increases the response time, as it increases the radial diffusion path length for oxygen (Lucisano, and Gough, 1988). Experimental data are presented in all figures as discrete points and the model predictions are presented as continuous curves.

3.4.2.1. Bulk Oxygen Step Change With no Reaction: Effect of Aspect Ratio

The transient responses of "small size" sensors (series I to IV, Table 3.4) to a step increase in bulk oxygen concentration demonstrate the effect of sensor's aspect ratio (Figure 3.5). In this simulation, the sensor contains no immobilized enzyme. The current

is normalized by using the expression $(i-i_i)/(i_f-i_i)$ where i_i is the initial current and i_f is the final current, which is also the steady-state current for each sensor. The normalized current is plotted as a function of time. The bulk oxygen step change occurs at t = 0. At t = 0, the oxygen concentration is 0 mM inside the gel and the current is also zero. After the perturbation, the current initially rises from zero at constant rate, eventually slows down as the system is saturated with oxygen and reaches unity asymptotically. As expected, increasing aspect ratio increases the response time, because oxygen requires longer time to reach the electrode due to the additional axial diffusion distance.

3.4.2.2.Bulk Lactate Step Change: Effect of Concentration Level

Figure 3.6 shows the response of a "small size" sensor (series IV, Table 3.4; with lactate oxidase only) to successive step increases in bulk lactate concentration. Normalized electrode current is plotted as a function of time. The normalized current increases monotonically following the increase in lactate concentration. The time of each increase in bulk lactate concentration has been adjusted to t = 0 for better comparison of the responses following each successive step change. There is a clear trend that the time required to reach steady-state increases at higher levels of bulk lactate concentrations. The time to 90% response for the curve at the highest concentration level is about 4 times that of the curve at the lowest concentration.

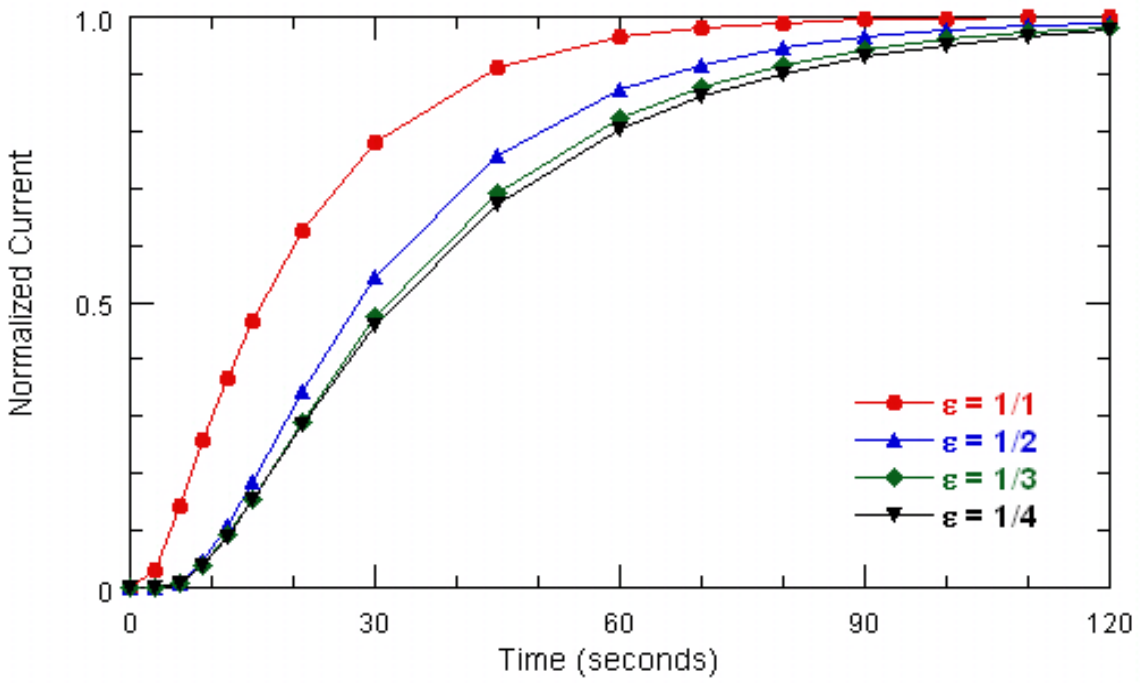

Figure 3.5 Normalized current versus time plot for a step increase in bulk oxygen concentration (0 to 0.053 mM). Increases in sensor length (aspect ratio) are shown to increase the time to reach steady state.

The same trend of strong dependence of response time on bulk lactate concentration level is observed in all sensors considered in this report. The increase in response time at higher concentration is due to the longer effective diffusion path length for lactate. At higher concentrations, there is an increasingly larger oxygen depleted gap near the axial end of the enzyme membrane as shown in Figures 3.3 and 3.4. As a result, lactate must diffuse farther through the gel in order to be fully consumed by the enzymatic reaction. The initial delay of sensor response at higher lactate concentrations is also due to the extended oxygen depleted region in the enzyme gel. Initially (at $C_{L,B} = 0$ mM), the sensor is saturated with oxygen. As lactate diffuses into the enzyme gel, rapid reaction takes place that consumes both substrates, resulting in a decrease in oxygen concentration inside the sensor. The effect of oxygen consumption near the axial end of the enzyme gel propagates rapidly toward the electrode and a change in electrode current is detected within seconds. During the next step increase in bulk lactate concentration, however, the additional lactate must diffuse farther into the enzyme gel in order to encounter higher level of oxygen. As the bulk lactate concentration becomes increasingly higher, the oxygen depleted region becomes larger, thus increasing the effective diffusion path length for the additional lactate.

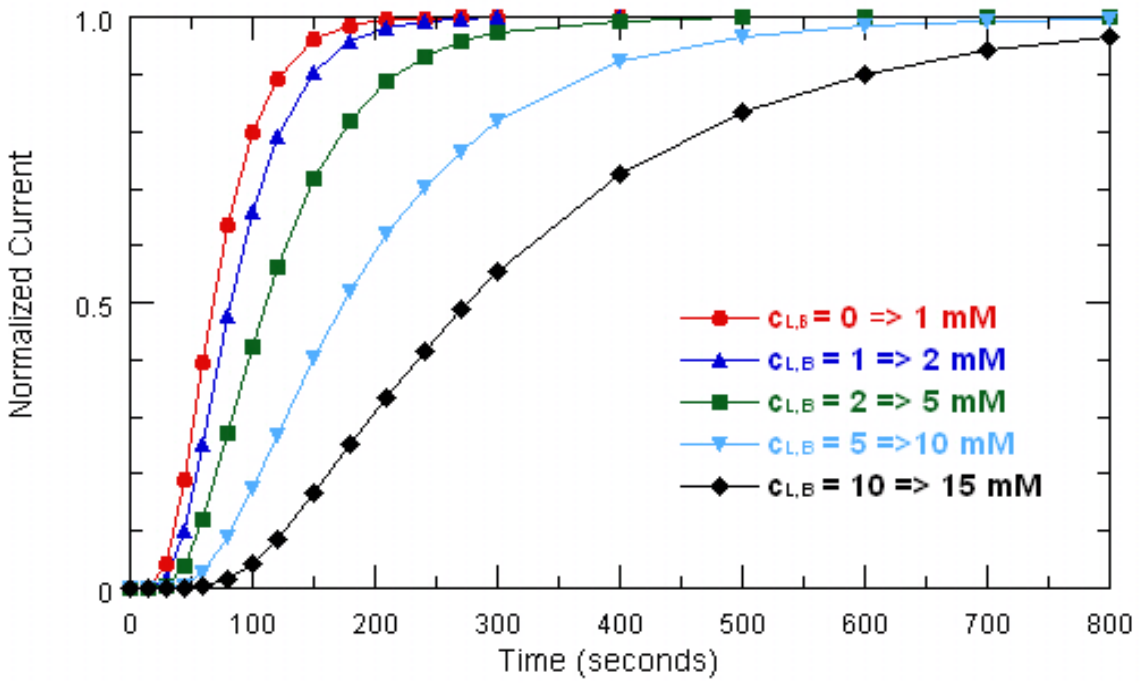

Figure 3.6 Normalized current versus time plot for "small size", ε = 1/4 sensor subjected to successive step increases in bulk lactate concentration. (Series IV, Table 3.4) This sensor contains only one enzyme, lactate oxidase. All increases in bulk lactate concentration occur at t = 0.

3.4.2.3. Bulk Lactate Step Change: Effect of Diffusion Coefficient Ratio

It may be possible to change the ratio of oxygen to lactate diffusion coefficients, λ, by changing the matrix protein from albumin to another biocompatible protein or polymer or by crosslinking/immobilization chemistry. Therefore, the effect of λ on sensor response is investigated here. In this simulation, the bulk lactate concentration is increased from 1 to 2 mM with bulk oxygen concentration fixed at 0.053 mM. The simulations were done by changing the values of λ while keeping the other parameters constant. The normalized electrode current is plotted against dimensionless time τ as shown in Figure 3.7. Increasing λ appears to decrease the response time. This is because as λ increases, the time response of the sensor becomes more limited by the transport of lactate. It is expected that increasing λ above a certain critical value would cause no further decrease in dimensionless time. Furthermore, depending on how λ is varied the trend presented in dimensional time may differ from that shown in Figure 3.7. If D_L is held constant while λ is varied, then the response obtained in dimensional time would be identical to that shown in Figure 3.7. If λ is varied by changing D_L with D_o fixed, then a different dimensional response may result. In this case, the trend may even be reversed: increasing λ increases the dimensional response time (Figure 3.8). This is because decreasing D_L further slows down the transport of lactate, thus increasing the time required to diffuse toward the electrode. In practice, λ cannot be varied over a wide range due to constraints in the choice of membrane materials and chemistry. The range presented here is attainable with most known, suitable sensor biomaterial membranes.

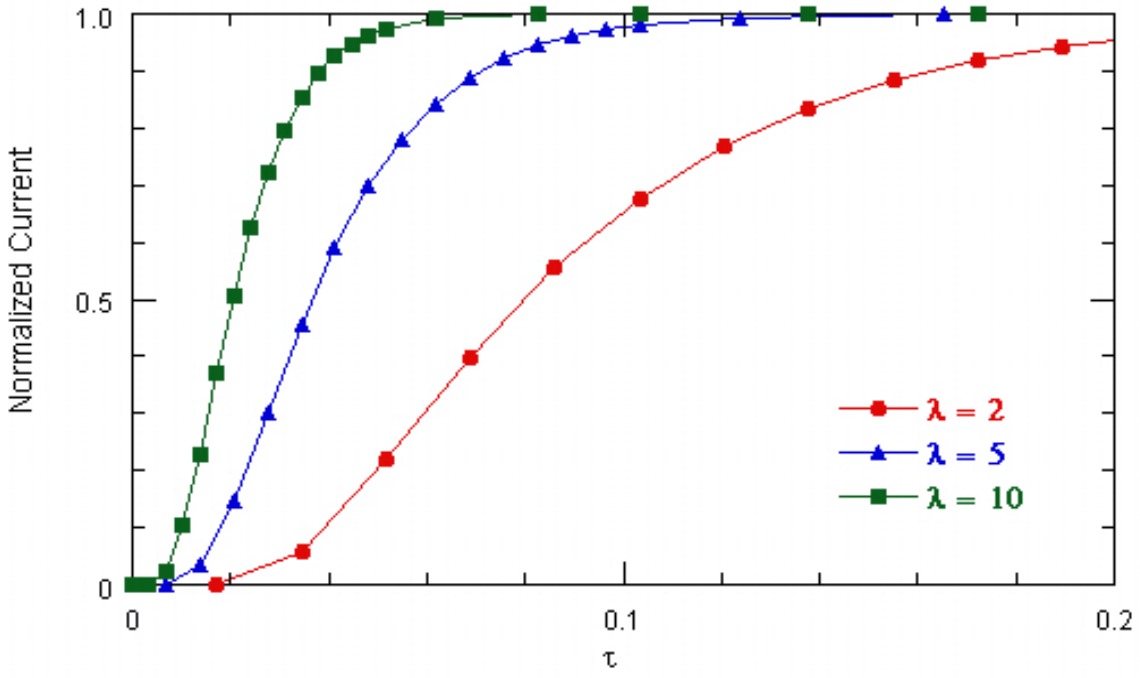

Figure 3.7 Normalized current versus dimensionless time plot for "small size" ε = 1/3 sensor showing the effect of λ during a step increase in bulk lactate concentration at t = 0. (Series III, Table 3.4) The bulk oxygen concentration is fixed at 0.053 mM. Other parameters are given in Table 3.5. Predicted responses show the effects of λ on sensor response.

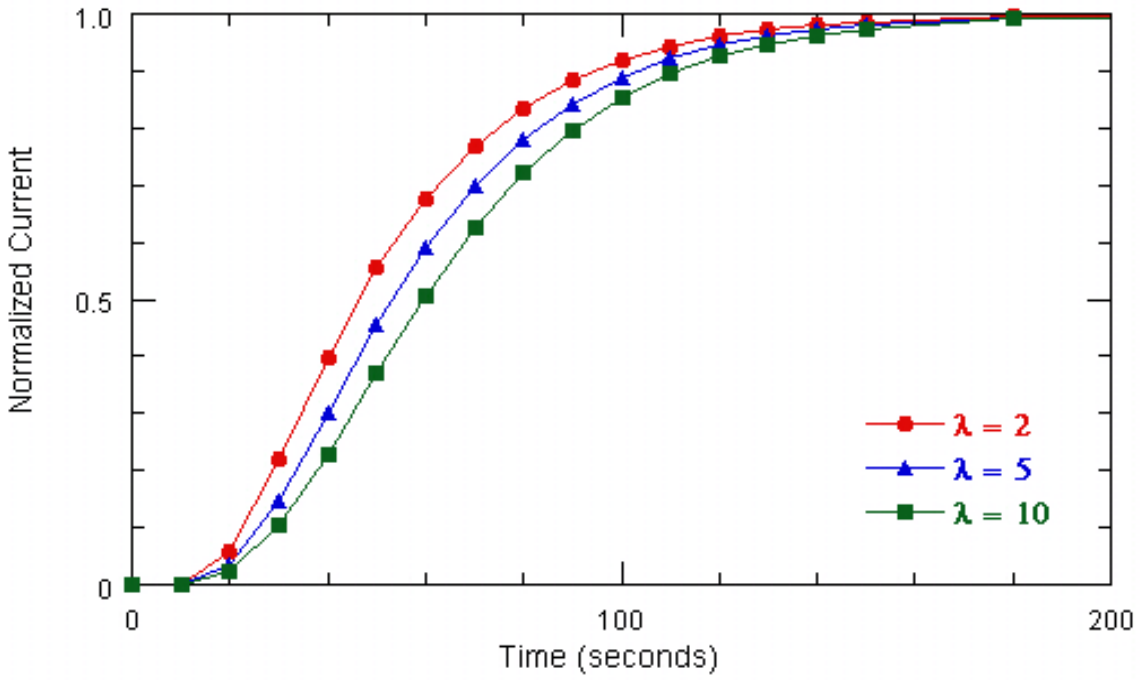

Figure 3.8 Normalized current versus dimensional time plot for "small size" ε = 1/3 sensor showing the effect of λ during a step increase in bulk lactate concentration at t = 0. (Series III, Table 3.4) The bulk oxygen concentration is fixed at 0.053 mM. Other parameters are given in Table 3.5. The value of λ is varied by varying the lactate diffusion coefficient D_L. Predicted responses show the effects of λ on sensor response.

3.4.2.4. Bulk Lactate Step Change: Effect of Enzyme Activity

This section explores the effects of kinetic parameters on sensor response. All sensors modeled in this section contain only lactate oxidase. The effect of dimensionless enzyme activity, σ, on sensor response is presented first in Figure 3.9. Normalized electrode current is plotted as a function of time for a step increase in bulk lactate concentration from 0 to 5 mM at t = 0. As expected, the response time decreases with increasing σ; as the system response shifts from primarily reaction-limited to substrate diffusion-limited. A higher value of σ reflects a higher maximum rate of enzymatic substrate consumption, which results in shorter response time. However, successive increase in σ yields diminishing return. Therefore, improving σ beyond the critical value, σ_{crit}, does not further decrease the response time. This σ_{crit} depends on sensor design and environmental factors, such as bulk analyte concentration (in this case, lactate) and dimensions (Gough et al., 1985; Lucisano, and Gough, 1988; Tse, 1984). The dependence of σ_{crit} on aspect ratio is illustrated in Figures 3.9 and 3.10. Figure 3.10 shows the sensor response with increasing σ under identical conditions as those used in Figure 3.9, but with an aspect ratio of 1/4. The response time for the sensor with ε = 1/4 is relatively longer and more sensitive to changes in the value of σ. In addition, the value of σ_{crit} is increased from 10 to 12 for the sensor with ε = 1/4.

In practice, the value of σ can be changed by varying any of its constituent parameters. These dimensional parameters and σ are related by equation 3.18c:

$$\sigma^2 = \frac{r_0^2}{D_L}\frac{V_{\max}}{K_L}$$

A simplified reaction mechanism for lactate oxidase (LOD) is presented below, along with the corresponding mathematical definitions for V_{max} and K_L:

$$\mathrm{LOD} + \mathrm{Lactate} \underset{k_{-1}}{\overset{k_1}{\rightleftarrows}} \mathrm{LOD} \bullet \mathrm{Lactate} \underset{k_{-2}}{\overset{k_2}{\rightleftarrows}} \mathrm{LOD'} + \mathrm{pyruvate}$$

$$\mathrm{LOD'} + \mathrm{O_2} \underset{k_{-3}}{\overset{k_3}{\rightleftarrows}} \mathrm{LOD'} \bullet \mathrm{O_2} \underset{k_{-4}}{\overset{k_4}{\rightleftarrows}} \mathrm{LOD} + \mathrm{H_2O_2} \tag{3.20}$$

$$V_{max} = \frac{k_2 k_4}{k_2 + k_4}[E_0] = k_{cat}[E_0] \tag{3.21}$$

$$K_L = \frac{(k_{-1} + k_2)k_4}{(k_2 + k_4)k_1} \tag{3.22}$$

The maximum velocity, V_{max}, is seen to be directly related to the turnover number (k_{cat}, or the number of catalytic processes the enzyme can catalyze per unit time) and the initial enzyme concentration, $[E_0]$. Hence, V_{max} is not a fundamental property of an enzyme, since it is dependent on the initial enzyme loading (Cornish-Bowden, 1979). In contrast, the Michaelis-Menten constant, K_L, is an intrinsic rate parameter, which depends only on the rate of the primary collision complex formation (i.e. LOD-lactate complex formation) (Maeda-Yorita, et al., 1995) and the rates of subsequent products formation and substrate dissociation (reverse reaction that separates the complex back to free LOD and lactate) (Lockridge, Massey, and Sullivan, 1972). Therefore, improving K_L requires modifying the enzyme structure and possibly its micro-environments, as these changes are likely to affect the enzyme substrate specificity and catalytic efficiency. Although both parameters depend on the forward rates of products formation, the effects of V_{max} and K_L on sensor response are treated separately to illustrate their relative influence.

The effect of changing V_{max} on sensor response is shown in Figures 3.11 and 3.12. The values of V_{max} are obtained using the above equation for σ^2. The values of σ are the

same as those used in Figures 3.9 and 3.10 and the values for D_L and K_L are given in Table 3.5. The multiplication factors (i.e. 1X, 4X, etc.) are assigned "arbitrarily" to each V_{max} value to demonstrate the relative order of magnitude changes. The effect of changing V_{max} on sensor response is expected to be similar to that of σ^2 when other terms in the equation stay the same. Thus, there is also a $V_{max,crit}$; beyond which point the system is primarily limited by substrate diffusion.

Unlike V_{max}, the effect of K_L on sensor response is quite different due to its nonlinear relationship with the substrate consumption rate, $V(C_L,C_o)$. Figure 3.13 shows that decreasing K_L reduces response time. The physical interpretation of K_L is complicated as it relates to the products of several rate constants. In certain cases, where k_2 is significantly small, K_L can be seen as a relative measure of substrate binding affinity for lactate oxidase and is expressed as:

$$K_L = \frac{k_{-1}}{k_1} \tag{3.23}$$

In this case, a decrease in K_L implies that the system favors the forward reaction (LOD-lactate complex formation), which is part of the lactate catalysis mechanism.

If the value of σ is kept constant while varying the values of K_L and V_{max} by using equation 3.18c, the resulting trend is that higher K_L will decrease the response time, as shown in Figure 3.13. This is because in order to maintain a constant value of σ, there must also be a proportional increase in V_{max} if the value of K_L is increased. Since the new system now has a higher maximum velocity, its transient response time should be reduced. Therefore, there should also be a critical K_L value beyond which no further improvements in response time can be achieved. In addition, the simulation results suggest that improvements in response time through varying K_L and V_{max} while keeping

σ constant are small. For example, the response time for the $\varepsilon = 1/3$ sensor with K_L = 0.4M is only about twice as fast as the same sensor with a K_L value of 0.005M. In other words, increasing the value of K_L by eighty times for this specific case will only reduce the response time by half. In contrast, as Figures 3.9 and 3.10 show, a ten fold increase in σ (from $\sigma = 1$ to $\sigma = 10$) would reduce the response time by roughly four to five times. However, there is still strong incentive for increasing K_L: the steady-state response plot in Figure 3.14 shows that increasing K_L also increases the sensor steady-state detection range. This is due to the fact that LOD can be saturated at lower oxygen concentrations when K_L value is increased; hence, the steady-state oxygen consumption is also reduced.

The above results suggest that it is unlikely to achieve a desired sensor performance through single parameter changes due to the inherent tradeoffs issue. For example, while it is much easier to increase σ by solely adjusting sensor dimensions, the obvious advantage of this approach can be offset by the negative effect of increased substrate diffusion length. On the other hand, there is a diminishing return of improvements for changing V_{max} or K_L. Therefore, a successful sensor optimization strategy will likely involve a combination of parameter changes.

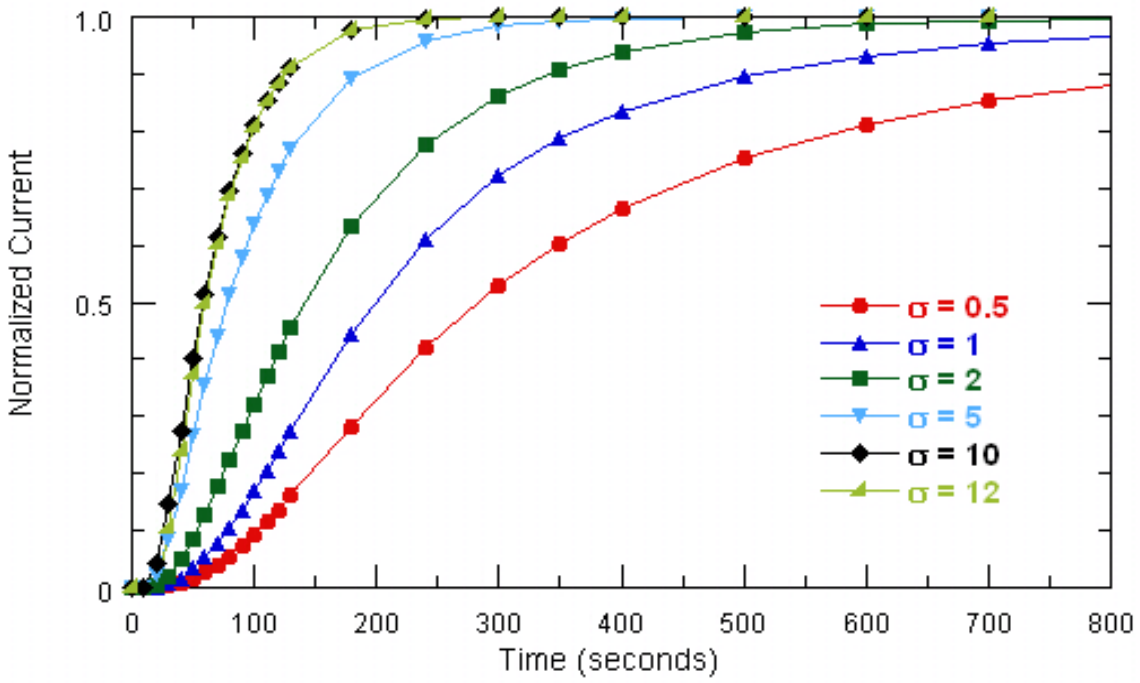

Figure 3.9 Normalized current versus time plot for "small size" ε = 1/3 sensor exposed to a step increase in bulk lactate concentration at t = 0. (Series III, Table 3.4) The bulk oxygen concentration is fixed at 0.053 mM and the lactate changes from 0 to 5 mM. Predicted responses show the effect of changing the nondimensional catalytic activity, σ.

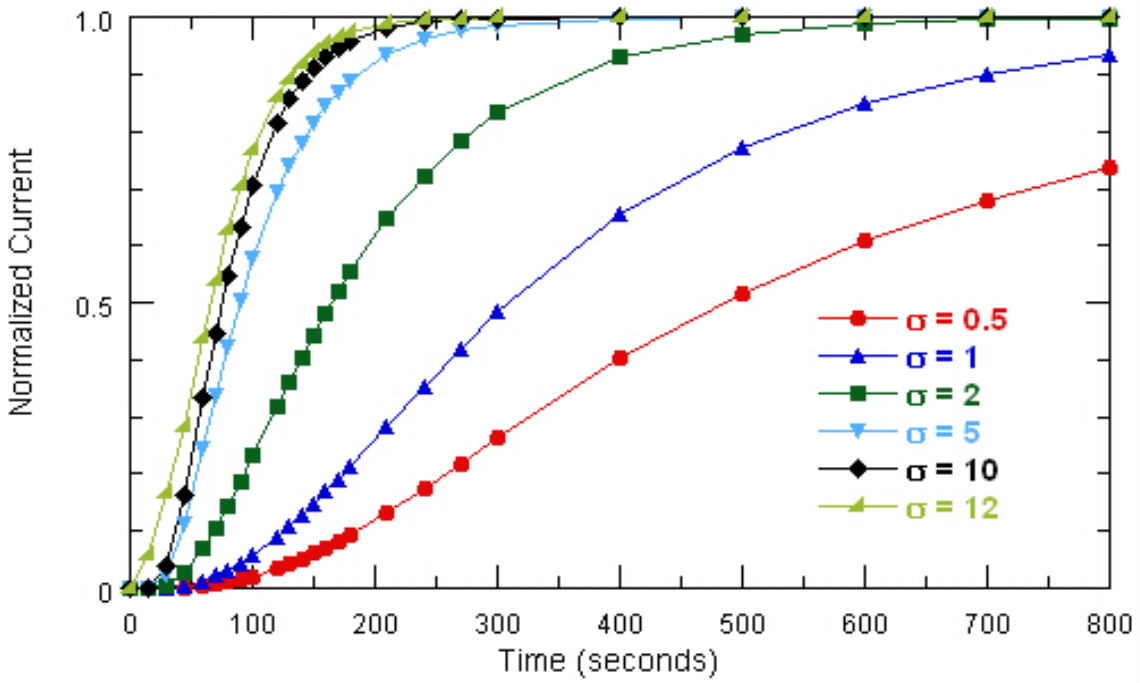

Figure 3.10 Normalized current versus time plot for "small size" ε = 1/4 sensor exposed to a step increase in bulk lactate concentration at t = 0. (Series IV, Table 3.4) The bulk oxygen concentration is fixed at 0.053 mM and the lactate changes from 0 to 5 mM. Predicted responses show the effect of changing the nondimensional catalytic activity, σ.

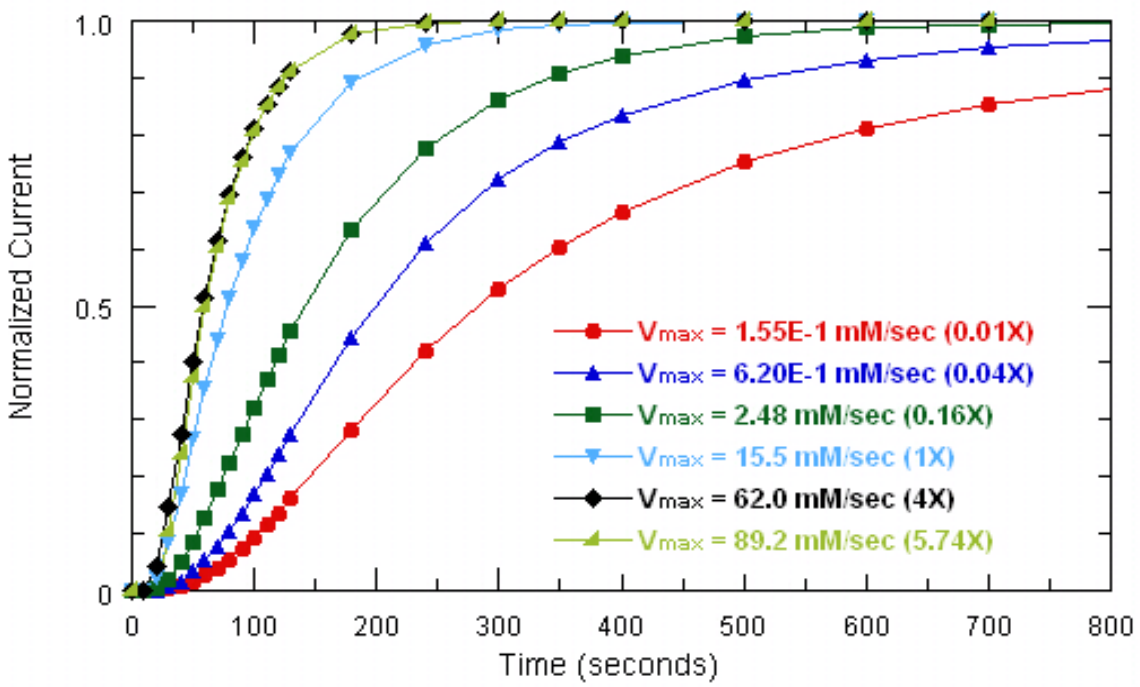

Figure 3.11 Normalized current versus time plot for "small size" ε = 1/3 sensor exposed to a step increase in bulk lactate concentration at t = 0. (Series III, Table 3.4) The bulk oxygen concentration is fixed at 0.053 mM and the lactate changes from 0 to 5 mM. Predicted responses show the effect of changing V_{max}.

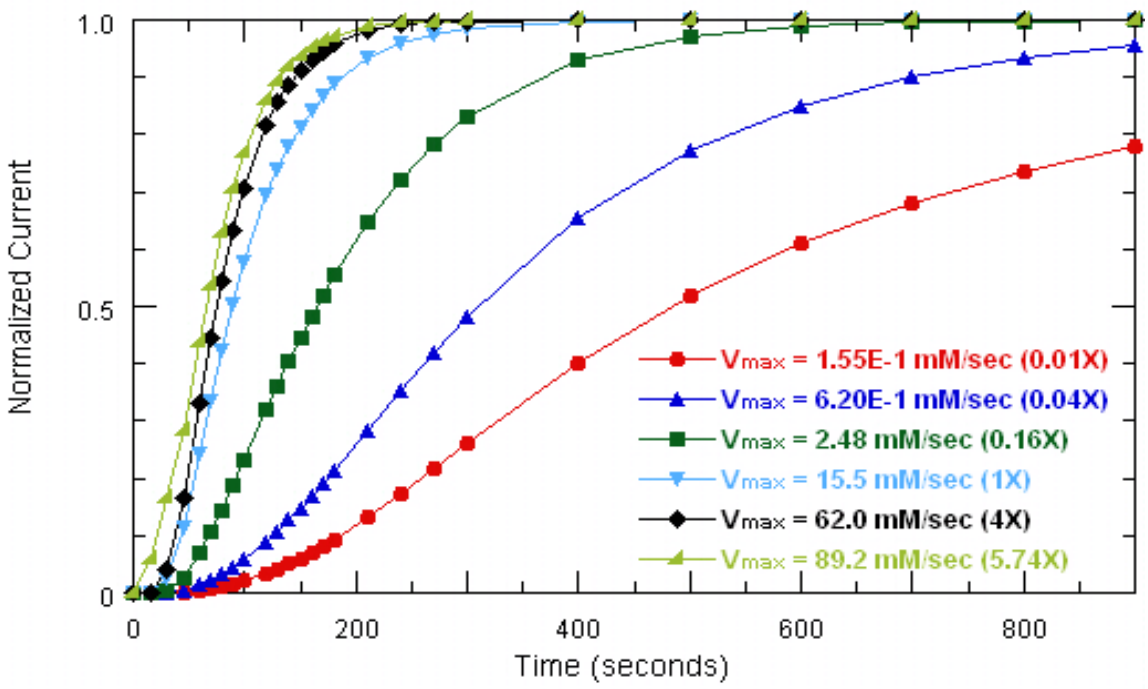

Figure 3.12 Normalized current versus time plot for "small size" ε = 1/4 sensor exposed to a step increase in bulk lactate concentration at t = 0. (Series IV, Table 3.4) The bulk oxygen concentration is fixed at 0.053 mM and the lactate changes from 0 to 5 mM. Predicted responses show the effect of changing V_{max}.

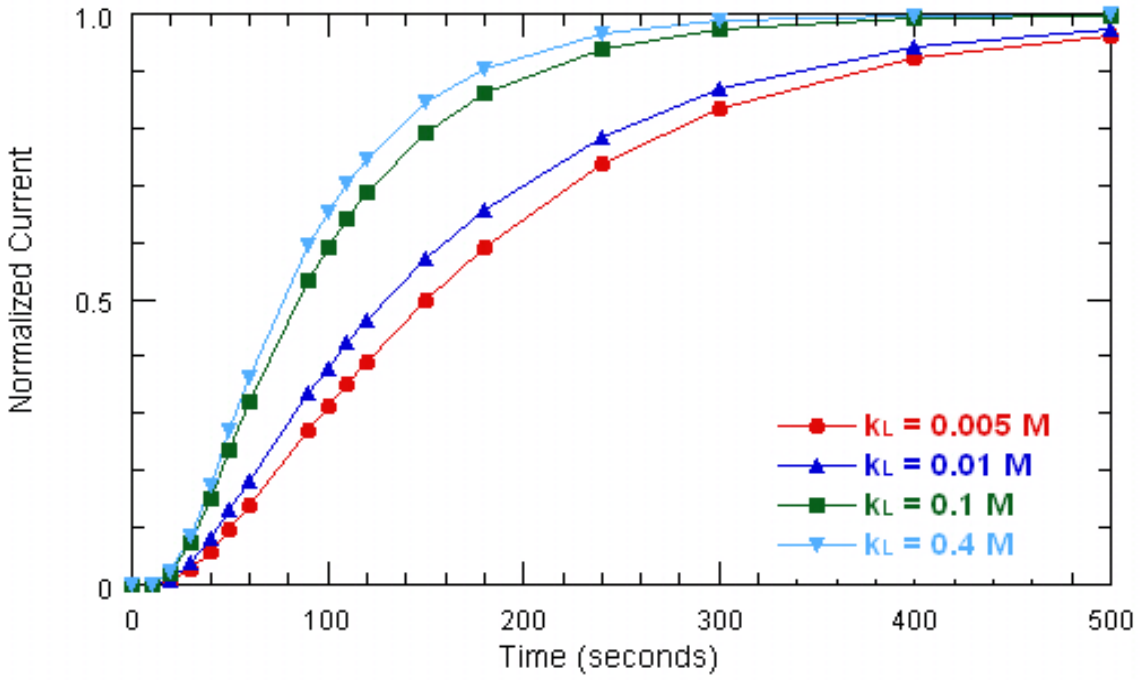

Figure 3.13 Normalized current versus time plot for "small size" ε = 1/3 sensor exposed to a step increase in bulk lactate concentration at t = 0. (Series III, Table 3.4) The bulk oxygen concentration is fixed at 0.053 mM and the lactate changes from 0 to 5 mM. Predicted responses show the effect of changing K_L.

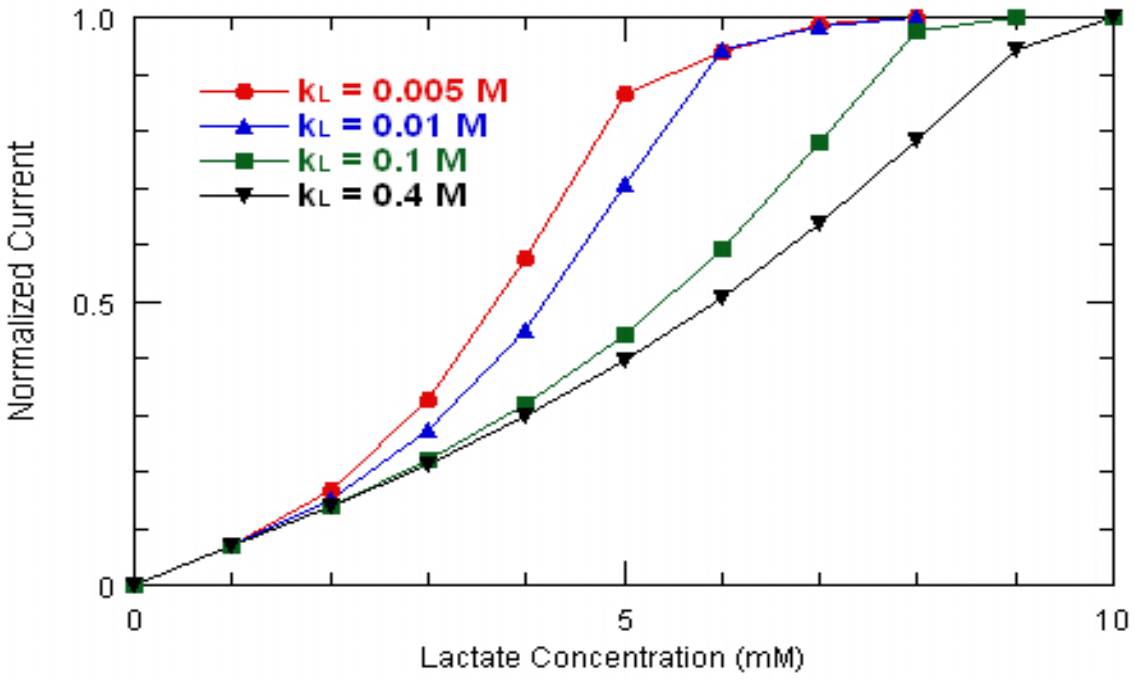

Figure 3.14 Normalized steady-state current versus lactate concentration plot for "small size" ε = 1/3 sensor exposed to step increases in bulk lactate concentration. (Series III, Table 3.4) The bulk oxygen concentration is fixed at 0.053 mM and the values for other parameters are given in table 3.5. Predicted responses show the effect of changing K_L on the sensor steady-state detection range.

3.4.2.5. Step Change in Bulk Lactate Concentration: Effects of Catalase

The sensors modeled so far contain only one enzyme (lactate oxidase or LOD). This single enzyme (SE) system provides a simple view of sensor behavior, which is helpful in studying the effects of various parameters on sensor response. An alternative and perhaps more useful way of designing enzyme membrane for electrochemical lactate sensors involves the co-immobilization of catalase, which rapidly consumes the hydrogen peroxide generated from the LOD catalyzed reaction. It is hypothesized that this dual enzyme (DE) system design would lower levels of hydrogen peroxide within the enzyme membrane and possibly prolonging the life of LOD, thus increasing the operational lifetime of the lactate sensor as well. However, there are no reports that confirm the claim that hydrogen peroxide specifically degrades lactate oxidase. Although hydrogen peroxide's role in LOD inactivation and sensor lifetime is not clear and is beyond the scope of this thesis, sensors with co-immobilized catalase are modeled in order to investigate the advantages/disadvantages in sensor response between the two systems (SE and DE).

Figure 3.15 shows that catalase co-immobilized with LOD increases the sensor's detection range for all aspect ratios. This is expected because catalase is responsible for regenerating half of the oxygen consumed by the LOD catalyzed reaction. Therefore, more oxygen is available to react with higher concentrations of lactate and so the detection range is increased. There is also a clear trend that co-immobilizing catalase decreases the sensor's response time and such improvement becomes more pronounced as the concentration step becomes larger (Figures 3.16 and 3.17). This trend is observed for sensors of all aspect ratios. One possible explanation for this result is that catalase

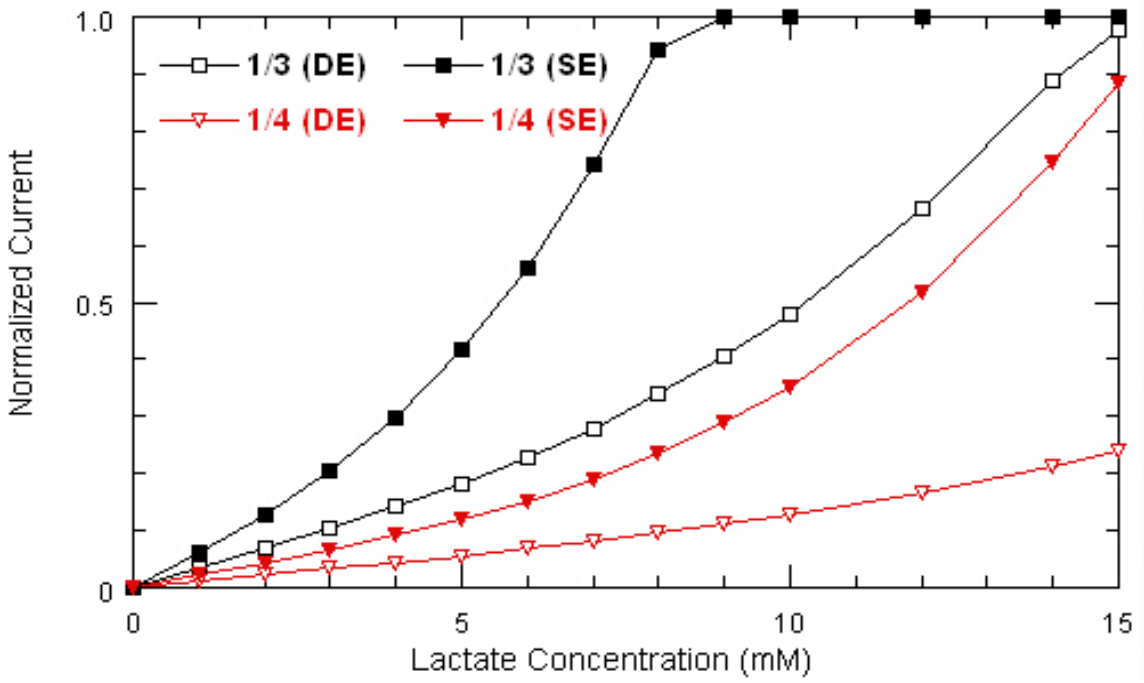

Figure 3.15 Normalized steady state current versus bulk lactate concentration for "medium size" SE (single enzyme) and DE (dual enzyme) sensors. (Series VII and VIII, Table 3.4) The bulk oxygen concentration is fixed at 0.053 mM. Other parameters are given in Table 3.5. Simulated responses demonstrate the increase in detection range from SE to DE.

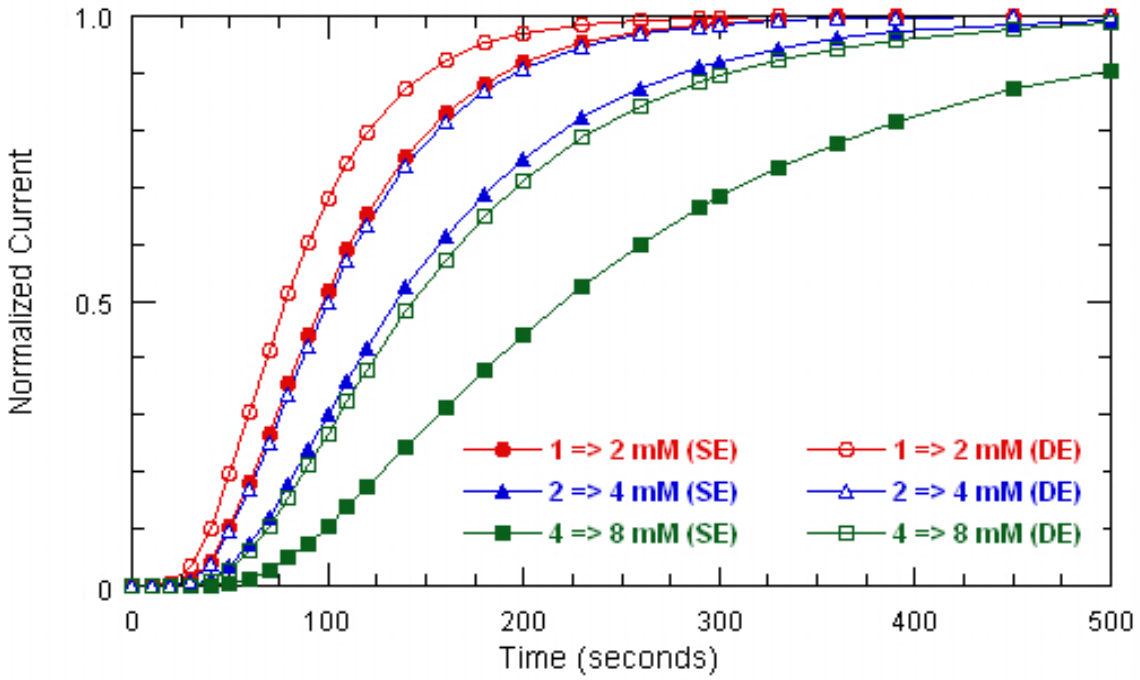

Figure 3.16 Normalized current versus time plot for "medium size" ε = 1/3 sensor exposed to step increases in bulk lactate concentration at t = 0. (Series VII, Table 3.4) The bulk oxygen concentration is fixed at 0.053 mM. Other parameters are given in Table 3.5. SE represents the single enzyme system and DE represents the dual enzyme system, where catalase is co-immobilized with lactate oxidase. Simulated responses show the effects of catalase co-immobilization on sensor transient response.

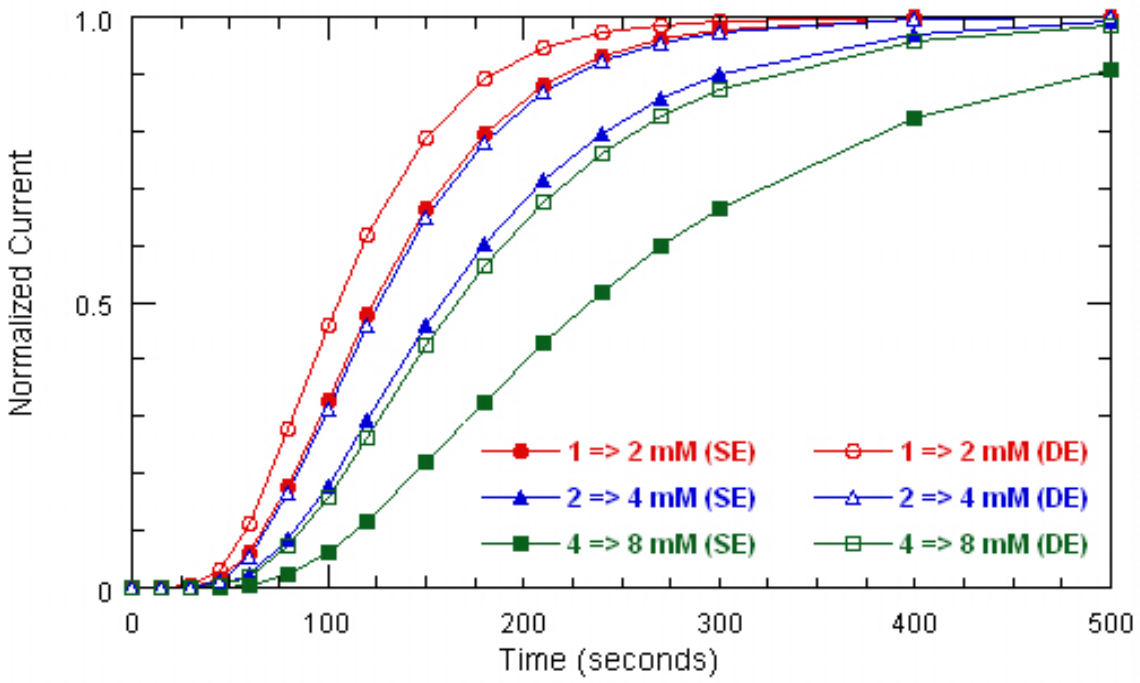

Figure 3.17 Normalized current versus time plot for "medium size" ε = 1/4 sensor exposed to step increases in bulk lactate concentration at t = 0. (Series VIII, Table 3.4) The bulk oxygen concentration is fixed at 0.053 mM. Other parameters are given in Table 3.5. SE represents the single enzyme system and DE represents the dual enzyme system, where catalase is co-immobilized with lactate oxidase. Simulated responses show the effects of catalase co-immobilization on sensor transient response.

helps to reduce the oxygen mass transfer demand inside the enzyme gel by regenerating some of the oxygen lost to the LOD catalyzed reaction, which in turn decreases the effective diffusion distance of lactate and also reduces the oxygen concentration gradient across the interface between the enzyme gel and the outer hydrophobic membrane. This ultimately leads to the reduction of transient response time.

3.4.2.6. Step Change in Bulk Lactate Concentration: Effects of Sensor Size

This section presents the effects of changing sensor's overall size. Figure 3.18 compares the steady-state sensor responses of "small" and "medium" size sensors with LOD co-immobilized with catalase (series I to VIII, Table 3.4). The overall size of a sensor is changed by varying r_o and the corresponding axial length while keeping other parameters constant. The bulk oxygen concentration is fixed at 0.053 mM and other parameter values are given in Table 3.5. Simulation results show that sensors with the same aspect ratio have the same steady-state response. This is expected, because the non-dimensional governing equations and boundary conditions for sensors with the same aspect ratio, regardless of sizes, are identical. The errors, or the difference between normalized currents, at each concentration are all less than 5% and are caused by round-off errors or discrepancies in solver/meshing methods used.

In contrast, the transient responses of four dual enzyme sensors (two "small size" and two "medium size" with aspect ratios 1/3 and 1/4) following step changes in bulk lactate concentration show that the "medium" sensors are slower than "small" sensors (Figures 3.19 and 3.20). In fact, a comparison between the transient responses of "medium size" and "large size" dual enzyme sensors with an aspect ratio of 1/3 shows

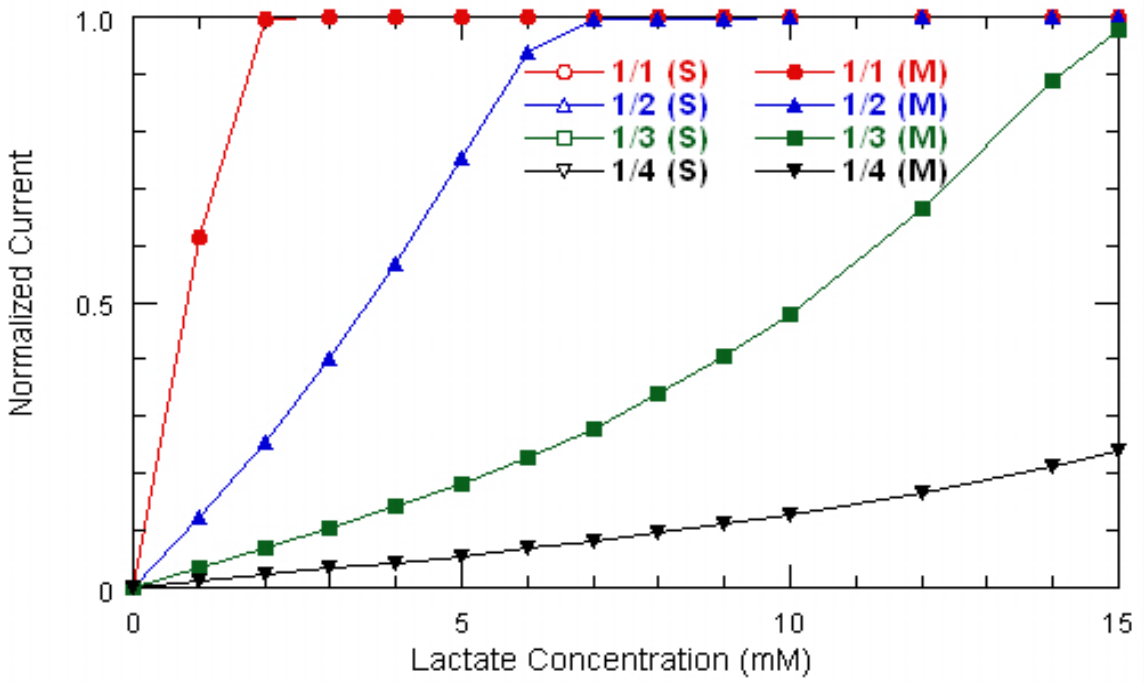

Figure 3.18 Normalized steady-state current versus bulk lactate concentration for "small" (S) and "medium" (M) dual enzyme sensors (series I to VIII, Table 3.4). The bulk oxygen concentration is fixed at 0.053 mM. Other parameters are given in Table 3.5. Predicted responses show the effect of varying sensor size.

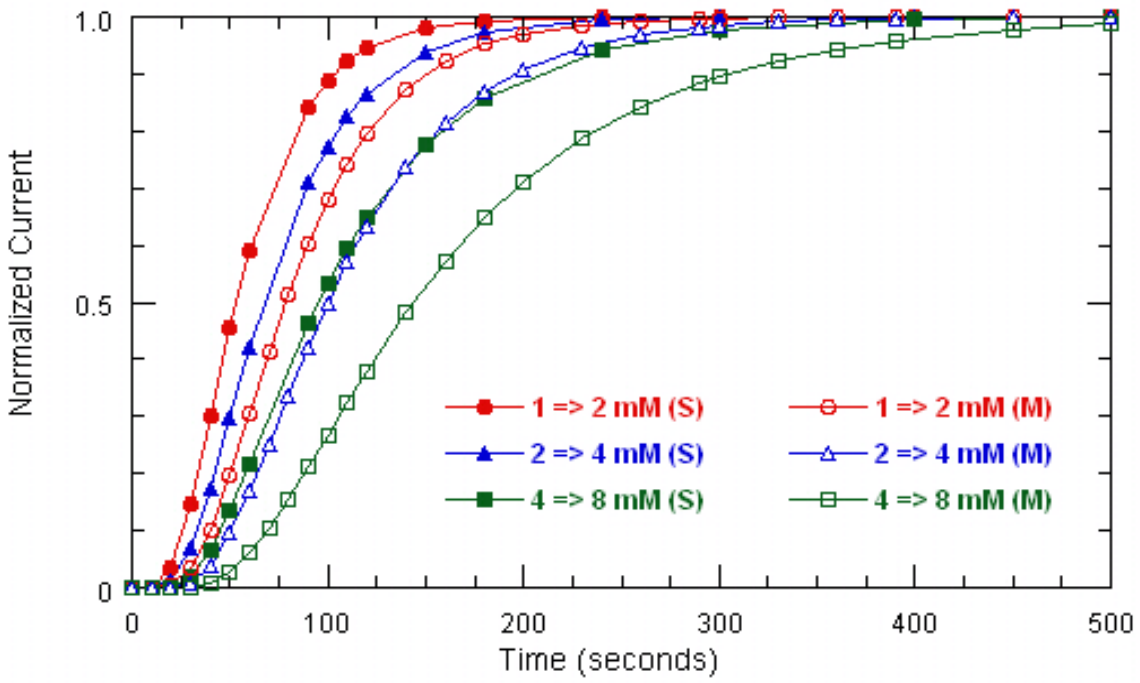

Figure 3.19 Normalized current versus time plot for "small" (S) and "medium" (M) size ε = 1/3 dual enzyme sensors exposed to step increases in bulk lactate concentration at t = 0. (Series III and VII, Table 3.4) The bulk oxygen concentration is fixed at 0.053 mM. Other parameters are given in Table 3.5. Simulated responses show the effects of varying sensor size.

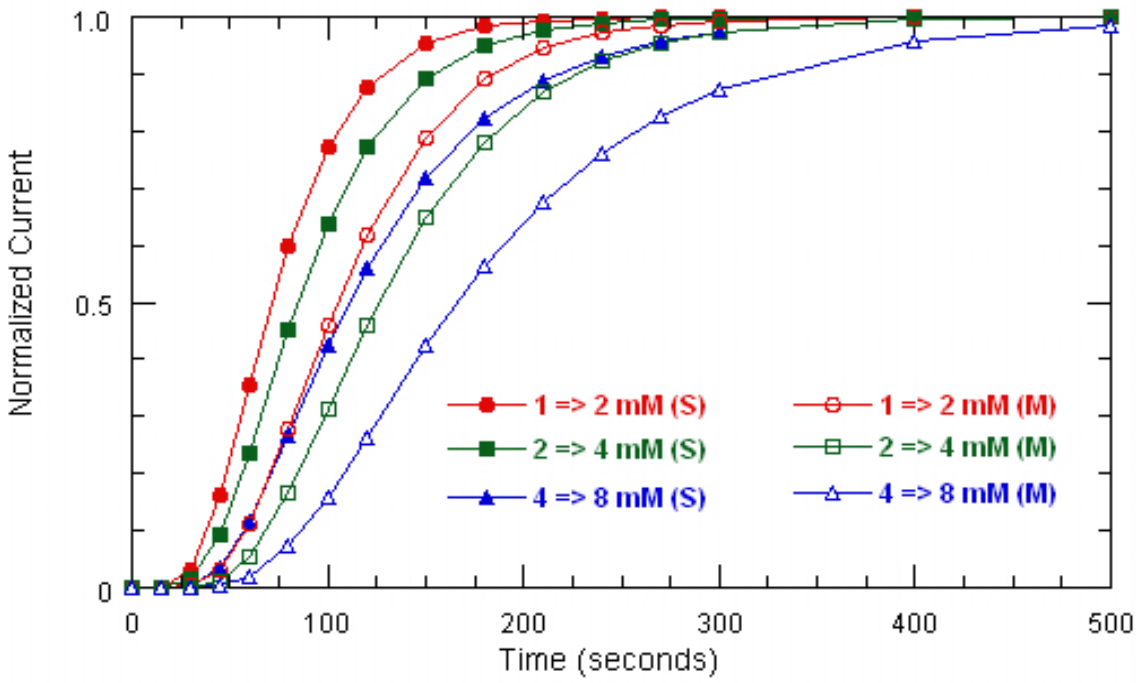

Figure 3.20 Normalized current versus time plot for "small" (S) and "medium" (M) size ε = 1/4 dual enzyme sensors exposed to step increases in bulk lactate concentration at t = 0. (Series IV and VIII, Table 3.4) The bulk oxygen concentration is fixed at 0.053 mM. Other parameters are given in Table 3.5. Simulated responses show the effects of varying sensor size.

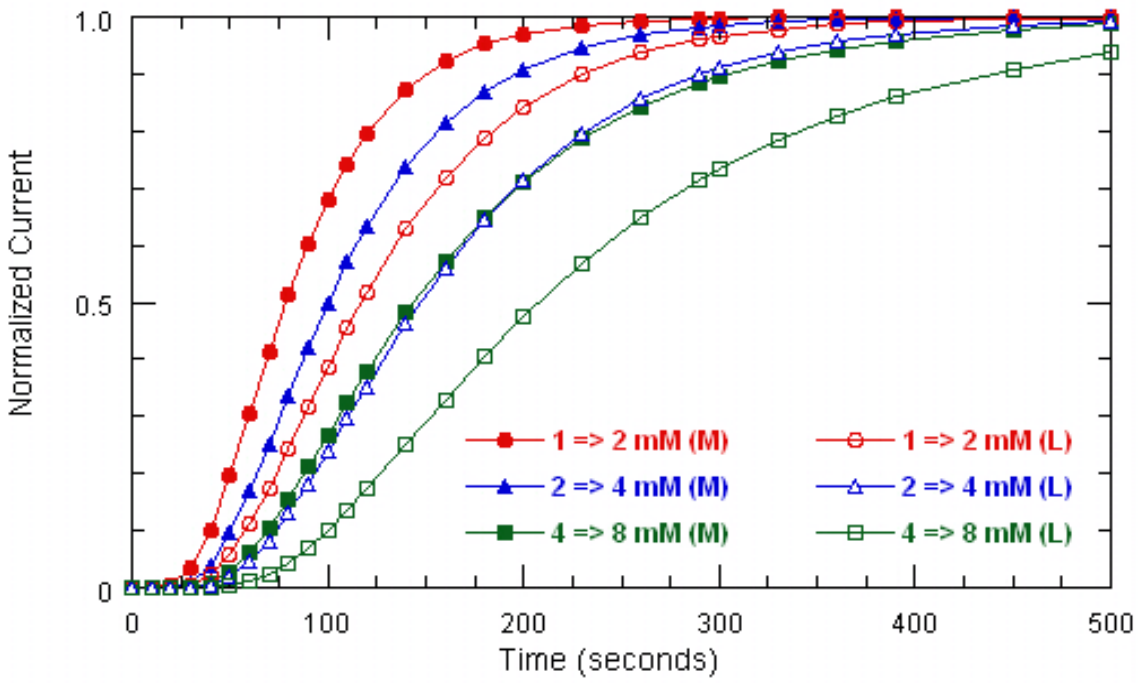

Figure 3.21 Normalized current versus time plot for "medium" (M) and "large" (L) size ε = 1/3 dual enzyme sensors exposed to step increases in bulk lactate concentration at t = 0. (Series VII and XI, Table 3.4) The bulk oxygen concentration is fixed at 0.053 mM. Other parameters are given in Table 3.5. Simulated responses show the effects of varying sensor size.

that longer response time is associated with larger sensor dimensions (Figure 3.21). This general trend is also observed for sensors of all aspect ratios.

The increase in transient response time (from "small" to "large" size) is mainly due to the increased diffusion path length for both oxygen and lactate. In order to keep the same aspect ratio, the larger sized sensors must have longer axial length. Subsequently, the substrates require longer time to reach the disk electrode which is located at the bottom of the enzyme gel. Therefore, there is an incentive to make the sensor as small as possible so that the cost (of enzyme) and response time can be reduced. However, this approach is not without drawbacks. For example, decreasing size also proportionately decreases σ, which is important for ensuring apparent diffusion-limited operation and for prolonging the operational lifetime of the sensor (Conway and Gough, 1987). Furthermore, small sensors are also more sensitive to fluctuations in external mass transfer conditions.

3.4.2.7. Step Change in Bulk Lactate Concentration: Effects of Boundary Layer Thickness

The fluid flow condition surrounding the exterior of an implanted sensor should also be taken into consideration during design analysis, because it influences the external mass transfer resistance of the substrates which ultimately affect the sensor's signal. The effects of fluid flow and its transport properties can be conveniently represented by a single parameter, the Biot number, which is the ratio between diffusive resistance and convective resistance:

$$Bi_i = \frac{h_i L}{D_i \alpha_i} = \frac{L/(D_i \alpha_i)}{1/h_i} \tag{3.24}$$

Where h_i, D_i, and α_i are the mass transfer coefficient, diffusion coefficient, and partition coefficient of the substrate, respectively. L is the characteristic length.

In addition, the mass transfer coefficient is given by:

$$h_i = \frac{D_{i,B}}{\delta} \tag{3.25}$$

Where $D_{i,B}$ is the diffusion coefficient of the substrate in bulk medium and δ is the boundary layer thickness. The Biot number expression then becomes

$$Bi_i = \frac{D_{i,B} L}{D_i \alpha_i \delta} \tag{3.26}$$

Therefore, when the boundary layer thickness, δ, is small, the Biot number is large, which implies that the system is more limited by internal diffusive resistance. Conversely, when δ is large, the system will be more limited by external convective resistance. In practice, increasing fluid flow velocity results in diminishing the value of δ, and decreasing flow leads to larger values of δ. This relationship between fluid flow and boundary layer thickness may have important consequences for sensor design, as different implant locations (for example, subcutaneous versus intravascular) may lead to different responses for the same sensor. The relationship between sensor response and boundary layer thickness is illustrated in Figures 3.22 and 3.23.

Figure 3.22 shows a plot of normalized steady-state current versus bulk lactate concentration for different external flow conditions ranging from relatively fast ($\delta_r = \delta_z = 0.001\text{cm}$) to relatively slow ($\delta_r = \delta_z = 0.01\text{cm}$). The sensor simulated is the "small size" with ε = 1/3, and contains lactate oxidase co-immobilized with excess catalase. The bulk oxygen concentration is fixed at 0.053 mM and other parameters are given in Table 3.5. The results show that decreasing δ has the beneficial effect of

increasing the detection range. This may be due to the fact that the thinner boundary layer, approximating the classic "well-stirred" environment, allows increased oxygen flux into the sensor from both radial and axial directions. As more oxygen is available to react with lactate in the enzyme membrane, the sensor's detection range is increased. Conversely, a higher boundary layer thickness would severely limit the oxygen's access to the sensor; resulting in a much more narrow detection range.

The effect of boundary layer thickness on sensor's transient response is depicted in Figure 3.23. The simulated sensor is the same as the one in Figure 3.22 and all parameters are identical. The results show that lowering δ results in faster sensor response. This is because a thin boundary layer decreases the external diffusion resistance, so that the substrates require less time to reach the sensor. It is expected that as the boundary layer thickness becomes increasingly small (the external medium approaches to a "well-stirred" approximation), the sensor's transient response time will reach a constant value, at which point the system is primarily controlled by internal mass transfer resistance. Conversely, increasing the value of δ will gradually shift the system to become one that is primarily limited by external mass transfer.

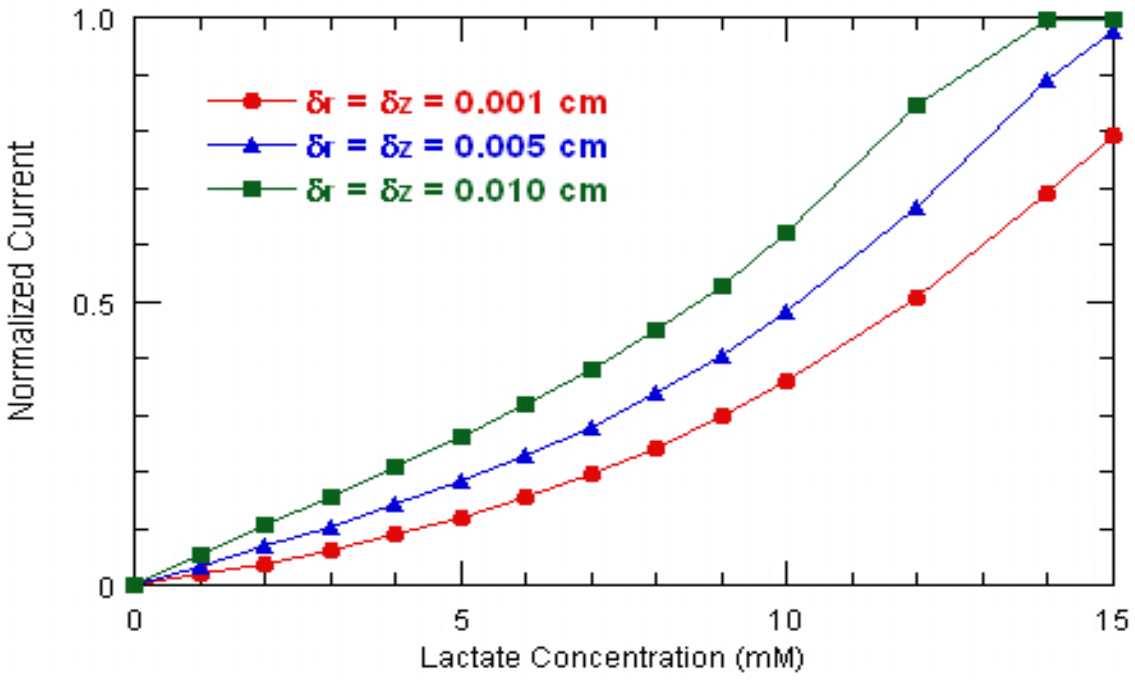

Figure 3.22 Normalized steady-state current versus lactate concentration plot for a sensor subjected to different boundary layer thicknesses. (Series III, Table 3.4) The sensor modeled above is "small size" with ε = 1/3, and contains LOD co-immobilized with catalase. The bulk oxygen concentration is fixed at 0.053 mM. Other parameters are given in Table 3.5. Simulated responses demonstrate the effects of boundary layer thickness (Biot number) on the sensor steady-state detection range.

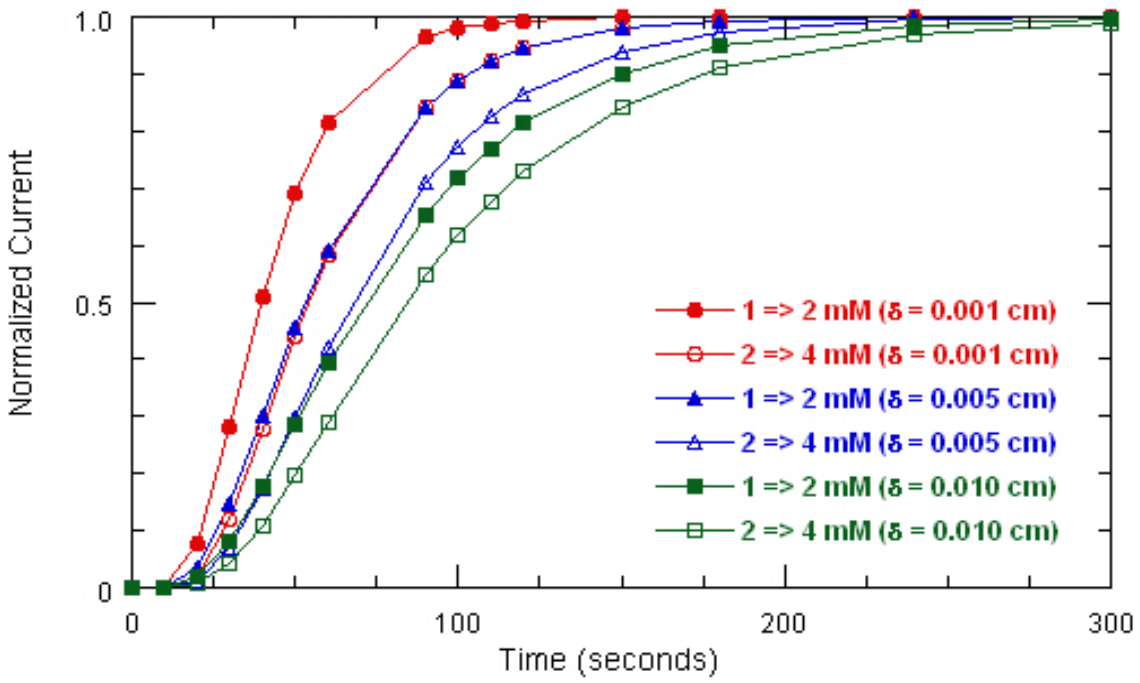

Figure 3.23 Normalized current versus time plot for "small size" sensor (dual enzyme system, $\varepsilon = 1/3$) exposed to step increases in bulk lactate concentration at t = 0. (Series III, Table 3.4) The bulk oxygen concentration is fixed at 0.053 mM. Other parameters are given in Table 3.5. Simulated responses demonstrate the effects of boundary layer thickness (Biot number), where $\delta = \delta_r = \delta_z$ as given above, on the sensor transient response.

3.4.2.8. Step Change in Bulk Lactate Concentration: Effects of Electrode Configuration

This section compares the steady-state and transient responses of "long" electrode sensors with "disk" two-dimensional electrode sensors following step increases in bulk lactate concentration. As illustrated in Figure 3.1, a "long" electrode spans the entire length of the enzyme membrane whereas a "disk" electrode only occupies a small circular area at the bottom of the cylindrical enzyme gel. Aside from the difference in electrode configuration, all other parameters and conditions are identical for both sensors (series III, IV, Table 3.4 and Table 3.5). The simulation results shown in Figures 3.24 ($\varepsilon = 1/3$) and 3.25 ($\varepsilon = 1/4$) suggest that "long" electrode sensors have broader steady-state detection range than "disk" electrode sensors. In addition, these two types of electrode configurations have contrasting steady-state responses: the "long" electrode sensors have a characteristic fast rising "hyperbolic/saturating" calibration curve, whereas the "disk" electrode sensors have a slow rising "polynomial/concave-up" calibration curve.

Beside their distinctive steady-state response patterns, these two electrode configurations also yield different transient responses: the two-dimensional "long" electrode sensors have much faster initial and overall responses compared to their "disk" electrode counterparts. This is seen in Figure 3.26, which shows the transient responses of two single enzyme sensors ($\varepsilon = 1/3$) following step increases in bulk lactate concentration. Both sensors modeled have identical parameters and only differ in their electrode configurations. The observed trend is likely the result of differences in substrate diffusion path length: the "long" electrode extends to the open end of the sensor

(that is, near the bulk solution), therefore lactate is detected as soon as it diffuses into the enzyme gel; in contrast, lactate must diffuse toward the bottom of the enzyme gel before it can be detected near the electrode surface in a "disk" electrode sensor. Since the relatively longer substrate diffusion length appears to be the major cause of response delay for two-dimensional sensors with "disk" electrode, a similar comparison between dual enzyme sensors with different electrode configurations is also expected to yield similar trend as that of Figure 3.26. This is indeed observed in Figure 3.27, which shows the transient responses of two dual enzyme sensors ($\varepsilon = 1/3$) following step increases in bulk lactate concentration. Except for their different electrode configurations, both sensors modeled are otherwise identical. It should also be noted here that all of the dual enzyme sensors in Figure 3.27 have faster transient responses than the single enzyme sensors in Figure 3.26.

The same set of simulations is also performed for sensors with other aspect ratios. For example, Figure 3.28 compares the transient responses of "long" and "disk" two-dimensional electrode single enzyme ($\varepsilon = 1/4$) sensors exposed to step increases in bulk lactate concentration at $t = 0$ and Figure 3.29 compares the transient responses of "long" and "disk" two-dimensional electrode dual enzyme ($\varepsilon = 1/4$) sensors exposed to step increases in bulk lactate concentration at $t = 0$. In both cases, the initial and overall responses of the "long" electrode sensors are always faster than those of the "disk" electrode sensors. It should be noted here again that the dual enzyme sensors simulated in Figure 3.29 have faster transient responses compared to the single enzyme sensors simulated in Figure 3.28 as seen before in previous section on effects of catalase. In addition, the time difference at 90% total response between the "long" and "disk"

electrode sensors also increases with decreasing aspect ratio. This is expected, because the substrate inside the two-dimensional "disk" electrode sensor must diffuse further (i.e. due to longer axial length) in order to reach the electrode surface, while the diffusion distance is unchanged inside the "long" electrode sensor.

Although it may seem desirable to have "long" electrode configuration for all sensors because of the longer steady-state detection range and faster response time, there are situations where a "disk" electrode design is more suitable. The advantages of a "disk" electrode are that it is relatively easy to fabricate and does not occupy any space inside the enzyme gel (so that higher enzyme loading may be achieved). Therefore, in situations where sensors must be made small, such as for subcutaneous implants, the "disk" electrode configuration becomes a superior choice.

3.4.3. Complex Changes in Bulk Substrate Concentration: Sensor Performance

Step changes in single bulk substrate concentration represent simple *in vitro* testing conditions, which can be easily verified experimentally. The results from these studies provide valuable information on the fundamental relationships between the design parameters and sensor responses. The following section presents simulated results for sensors subjected to complex bulk substrate concentration changes that simulate more physiological changes. The condition tested is a ramp increase in bulk lactate concentration. An understanding of the sensor behavior under complex conditions such as this is required for the correct interpretation of the signals from implanted sensors.

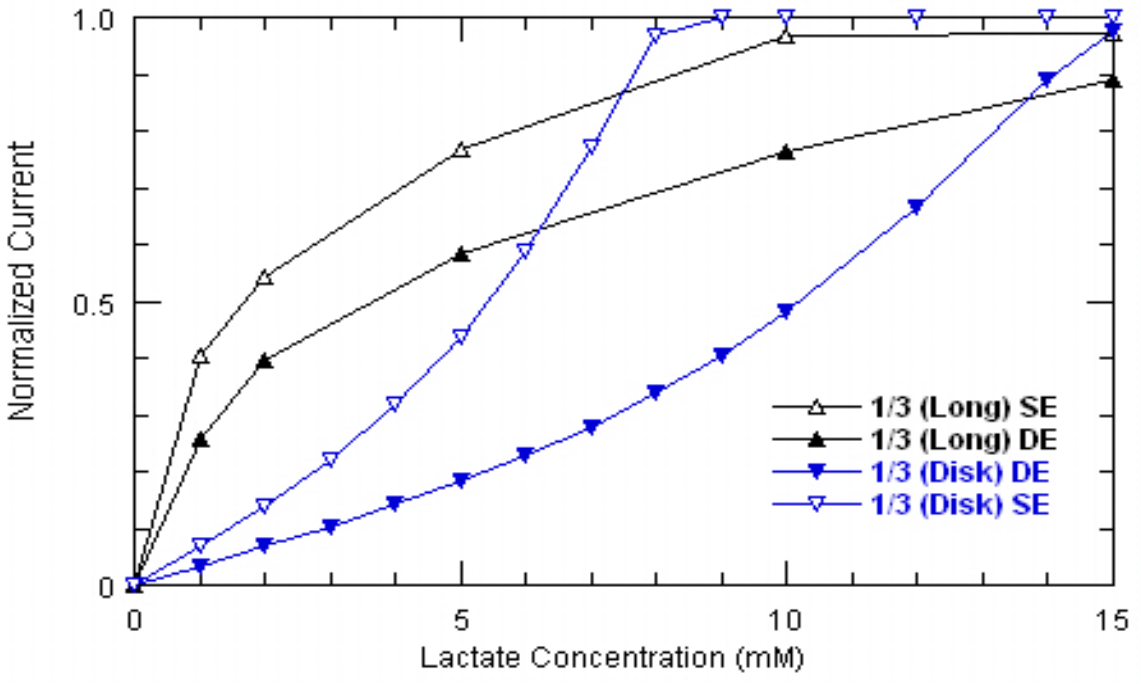

Figure 3.24 Normalized steady-state current versus lactate concentration plot for ε = 1/3 "long" and "disk" two-dimensional electrode sensors. (Series III, Table 3.4) The sensors modeled above are "small size" with ε = 1/3, and contains immobilized LOD with and without catalase (DE and SE, respectively). The bulk oxygen concentration is fixed at 0.053 mM. Other parameters are given in Table 3.5. Simulated responses demonstrate the effects of electrode configuration on the sensor steady-state detection range.

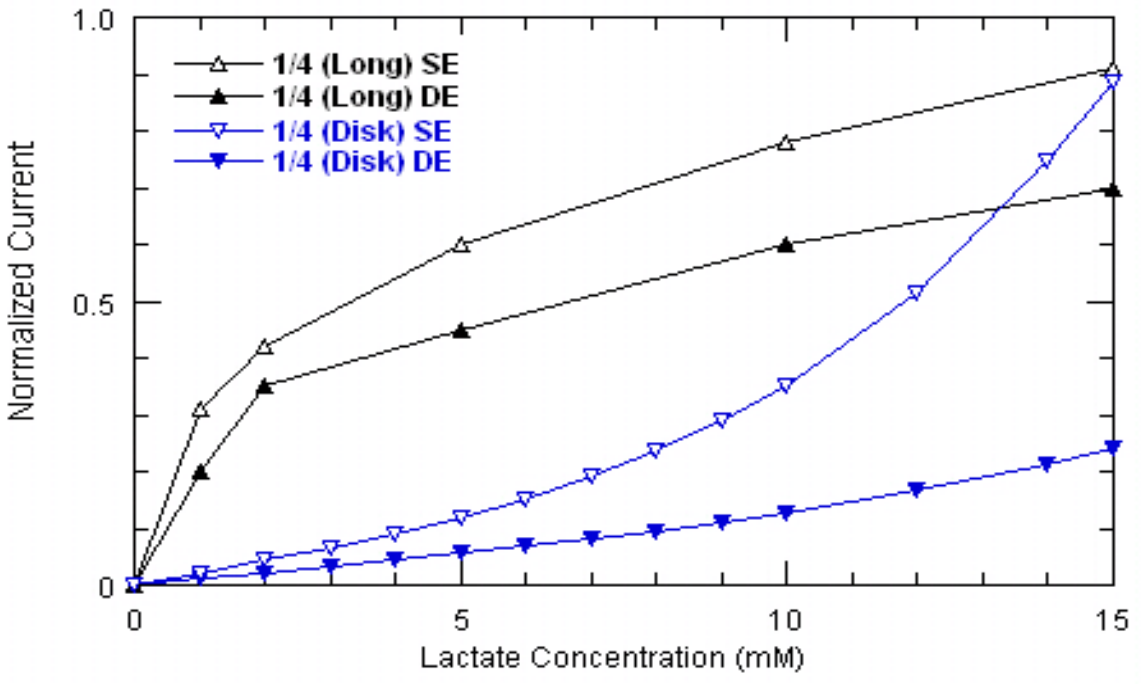

Figure 3.25 Normalized steady-state current versus lactate concentration plot for ε = 1/4 "long" and "disk" two-dimensional electrode sensors. (Series IV, Table 3.4) The sensors modeled above are "small size" with ε = 1/4, and contains immobilized LOD with and without catalase (DE and SE, respectively). The bulk oxygen concentration is fixed at 0.053 mM. Other parameters are given in Table 3.5. Simulated responses demonstrate the effects of electrode configuration on the sensor steady-state detection range.

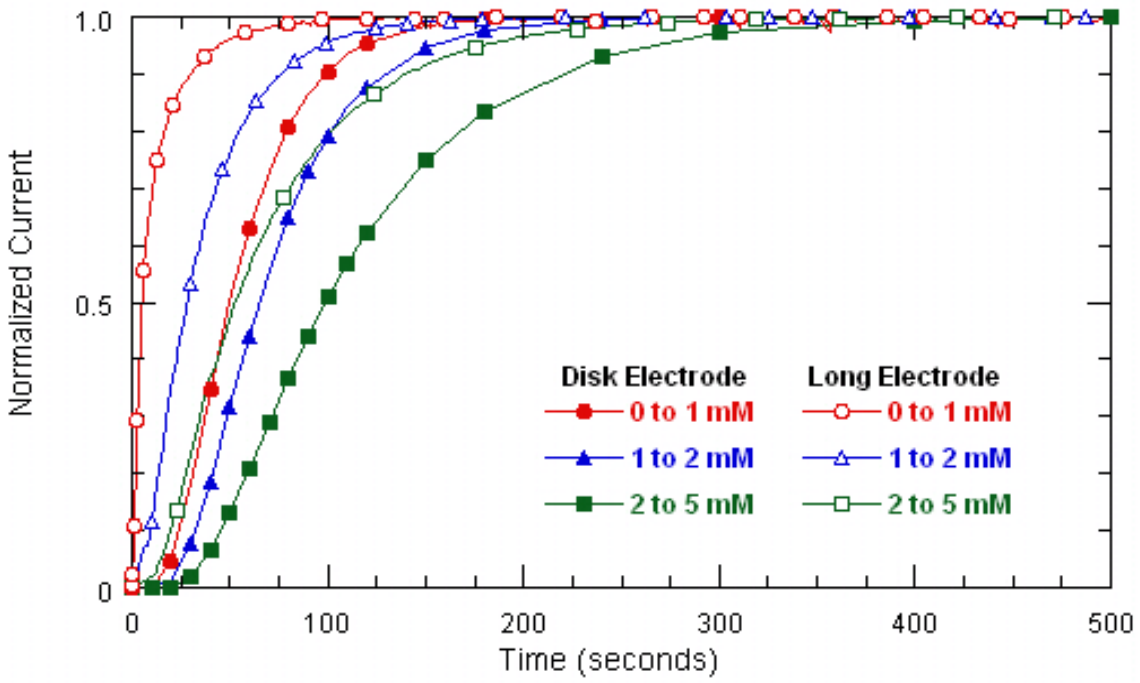

Figure 3.26 Normalized current versus time plot for ε = 1/3 "long" and "disk" electrode sensors (single enzyme) exposed to step increases in bulk lactate concentration at t = 0. (Series III, Table 3.4) The bulk oxygen concentration is fixed at 0.053 mM. Other parameters are given in Table 3.5. Simulated responses demonstrate the effects of electrode configuration on the sensor transient response.

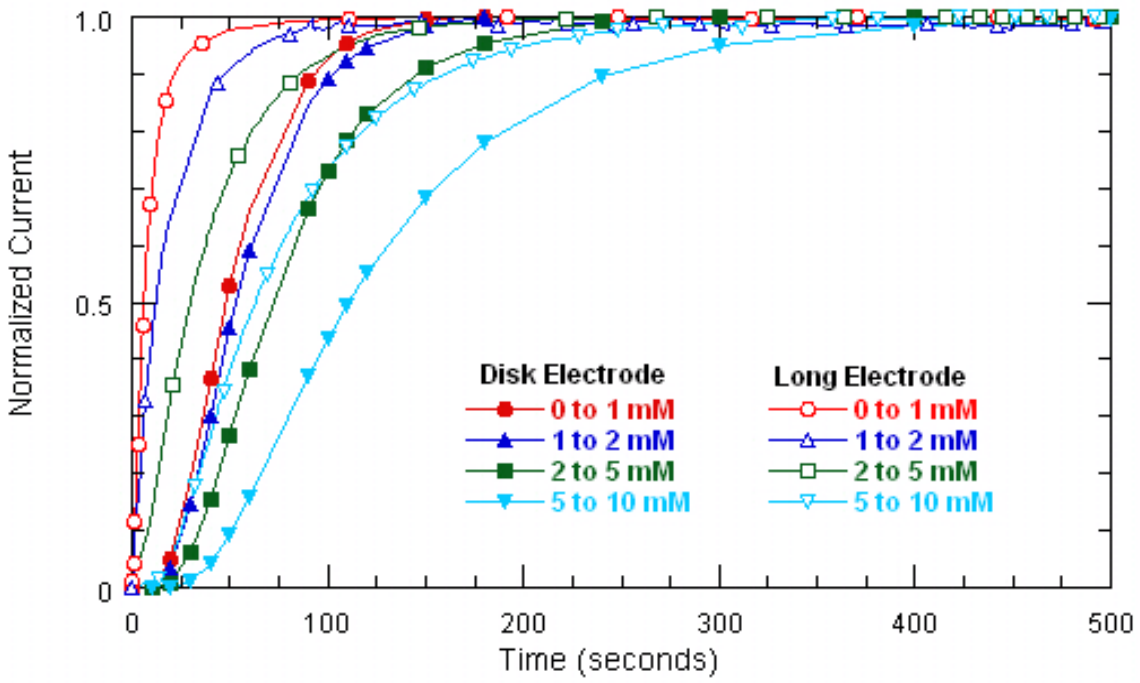

Figure 3.27 Normalized current versus time plot for ε = 1/3 "long" and "disk" electrode sensors (dual enzyme) exposed to step increases in bulk lactate concentration at t = 0. (Series III, Table 3.4) The bulk oxygen concentration is fixed at 0.053 mM. Other parameters are given in Table 3.5. Simulated responses demonstrate the effects of electrode configuration on the sensor transient response.

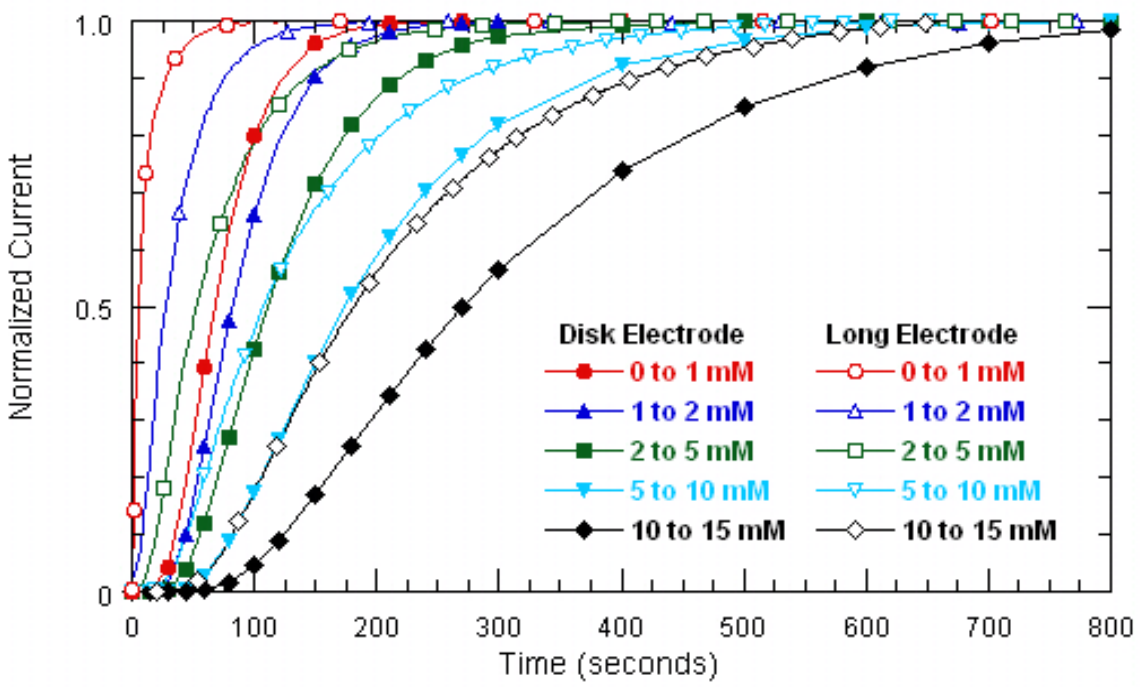

Figure 3.28 Normalized current versus time plot for ε = 1/4 "long" and "disk" electrode sensors (single enzyme) exposed to step increases in bulk lactate concentration at t = 0. (Series IV, Table 3.4) The bulk oxygen concentration is fixed at 0.053 mM. Other parameters are given in Table 3.5. Simulated responses demonstrate the effects of electrode configuration on the sensor transient response.

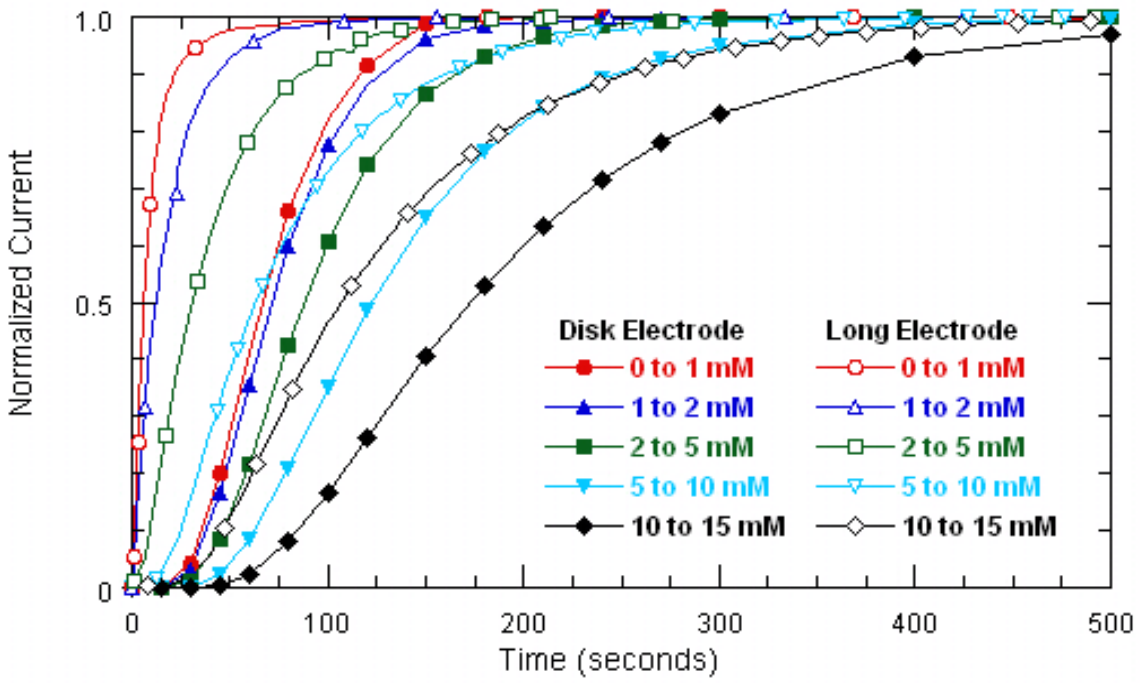

Figure 3.29 Normalized current versus time plot for ε = 1/4 "long" and "disk" electrode sensors (dual enzyme) exposed to step increases in bulk lactate concentration at t = 0. (Series IV, Table 3.4) The bulk oxygen concentration is fixed at 0.053 mM. Other parameters are given in Table 3.5. Simulated responses demonstrate the effects of electrode configuration on the sensor transient response.

3.4.3.1. Ramp Change in Bulk Lactate Concentration: Dynamic Response

Figure 3.30 shows the response of four two-dimensional "disk" electrode sensors of varying aspect ratio to a ramp increase in bulk lactate concentration. The bulk lactate concentration is increased linearly with a ramp rate of 0.006 mM/sec starting at t = 0 and ending at t = 130 sec. This ramp rate is within the same order of magnitude as the maximal physiological in vivo lactate ramp rate observed, which is 1.50 $\frac{\text{mM}}{\text{min}}$ or $0.025\frac{\text{mM}}{\text{sec}}$ (Baker and Gough, 1996). Bulk oxygen concentration is fixed at 0.053 mM. In each case, the normalized current increases monotonically and exhibits a time delay before reaching a slope equivalent to the ramp rate. The smallest sensor exhibits the shortest delay, while the largest sensor lags the changing lactate concentration by about 70 seconds. In terms of relative response speed, this simulation shows the same pattern as that for simple step bulk lactate concentration changes: larger aspect ratio decreases the response time. Similarly, sensors containing lactate oxidase co-immobilized with catalase are also expected to achieve relatively faster response than those without catalase. This trend is shown in Figure 3.31, in which all dual and single enzyme sensors are subjected to a linear ramp increase (ramp = 0.003 mM/s) in bulk lactate concentration starting from $C_{L,B}$ = 1 mM at t = 0 and ending at t = 260 sec. Therefore, design improvements that decrease a sensor's simple step change transient response time are also expected to proportionally reduce its ramp change transient response time. In general, the dynamic lag to a ramp change for these sensors does not follow the trend predicted by the equation

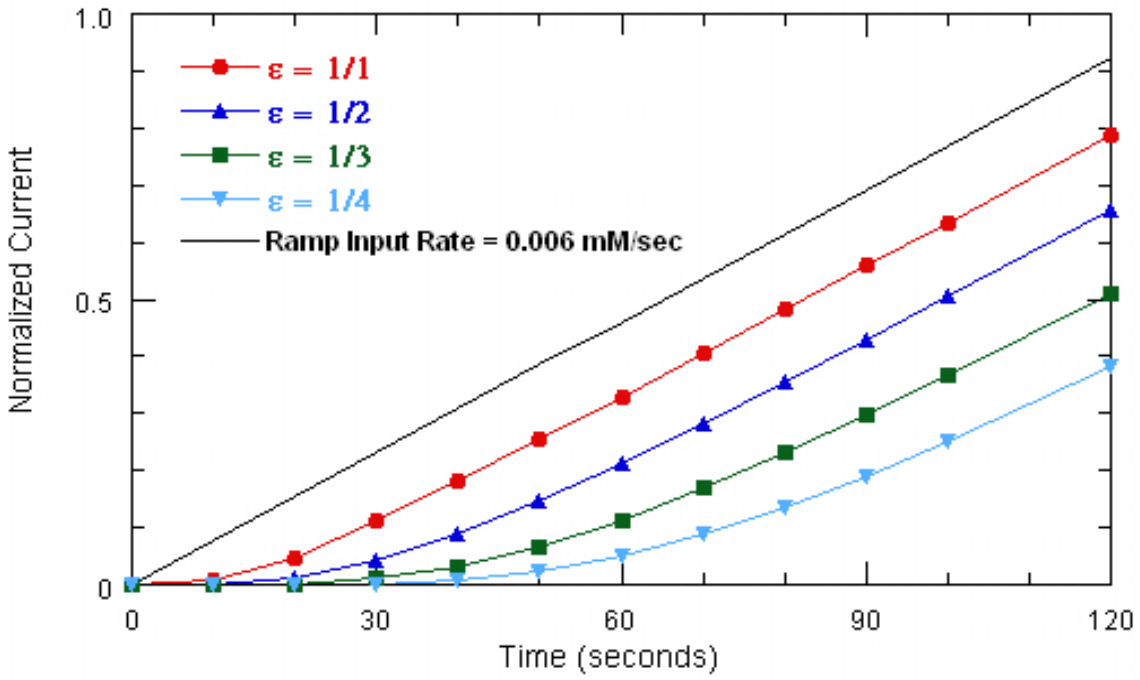

Figure 3.30 Normalized current versus time plot for "small size" sensor (single enzyme system) exposed to a ramp increase in bulk lactate concentration at t = 0. (Series I to IV, Table 3.4) The bulk oxygen concentration is fixed at 0.053 mM. Other parameters are given in Table 3.5. Simulated responses demonstrate the effects of sensor size on dynamic delay (δ_D) and dynamic error (ε_D).

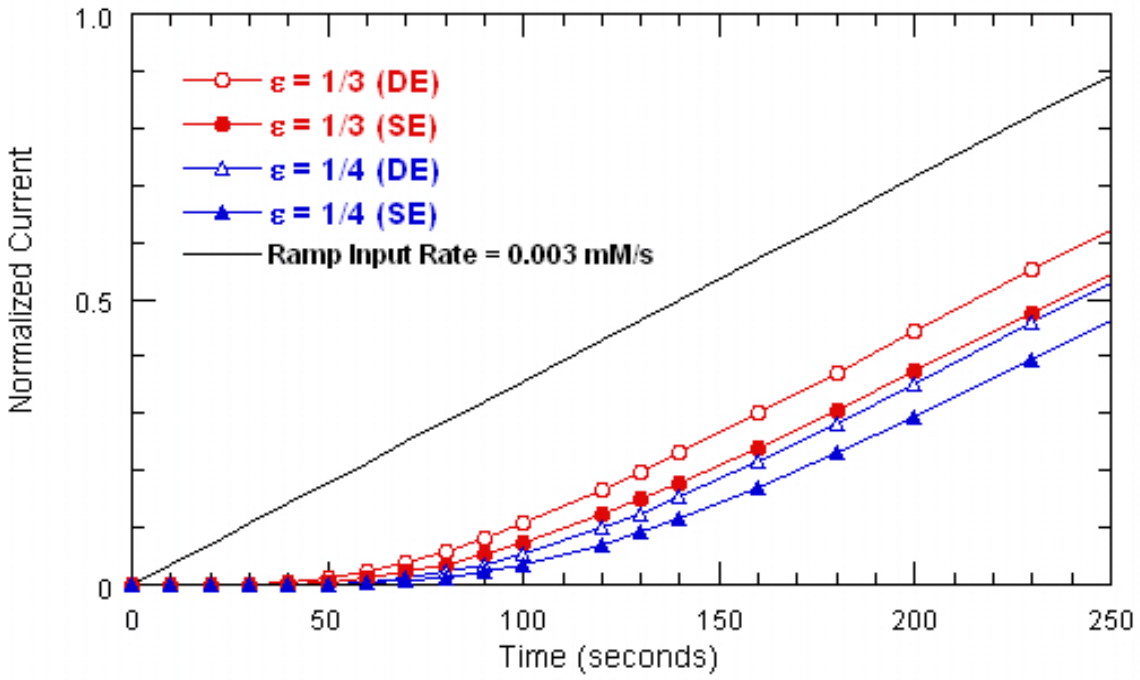

Figure 3.31 Normalized current versus time plot for "medium size" ε = 1/3 and 1/4 sensors showing the effect of catalase co-immobilization during a ramp increase in bulk lactate concentration at t = 0. (Series VII to VIII, Table 3.4) The bulk oxygen concentration is fixed at 0.053 mM. Other parameters are given in Table 3.5. Simulated responses demonstrate the effects of catalase co-immobilization on dynamic delay (δ_D) and dynamic error (ε_D).

$$\delta_D = \frac{K\delta_m^2}{D_m} \tag{3.27}$$

This is due to the fact that the above equation is derived for a linear system, whereas the model considered here is described by non-linear system of equations (Baker and Gough, 1994). Nonetheless, the results still demonstrate the usefulness of these new criteria: optimization for continuous biosensors should focus on decreasing dynamic delay while increasing detection range.

3.5. Conclusions

This thesis has investigated and analyzed eight main aspects of the implantable lactate sensor: the aspect ratio, substrate concentration level, diffusion, enzyme kinetics, sensor size, electrode configuration, boundary layer thickness and enzyme coupling. The central theme involved in almost all of these design factors is the tradeoffs between sensitivity, detection range and time response. Therefore, it is important that the improvement of sensor design should aim to achieve a desirable balance between the advantages and disadvantages of these parameter changes.

The most important characteristics of the sensing environment are the range of lactate concentration that the sensor will be expected to measure and the rate of lactate concentration increase that the sensor will be expected to follow. The specification of the required range of sensitivity alone can immediately narrow the choices of certain design parameters. The maximum allowable aspect ratio for a sensor with a specified range of concentration sensitivity can be determined from steady-state considerations. An implantable lactate sensor should have a minimum lactate detection range of 0 to 15 mM, thus the desired aspect ratio for a sensor with disk electrode should be lower than 1/3. On

the other hand, the lower limit of aspect ratio is determined from transient response considerations.

While the simplest way to shorten the response time is to minimize the size of the sensor (the overall size, not the aspect ratio) or to replace the disk electrode with a long electrode, such approaches may sacrifice other aspects of sensor performance. Most importantly, decreasing size may drastically decrease the nondimensional catalytic activity σ, which is crucial for ensuring diffusion-limited operation and for prolonging the sensor's operational lifetime. In cases where decreasing sensor size is imperative, the desired σ ($\sigma > \sigma_{crit}$) may be maintained by altering V_{max} (such as increasing enzyme loading) and/or K_L (such as modifying the enzyme, LOD, to increase its activity and lifetime under physiologic pH and temperature). However, these strategies may also be financially costly and the improvements that they bring may be limited due to additional physical and environmental constraints. Another potential issue with small sensors is that they may be more susceptible to fluctuations in external mass transfer conditions in certain environments. The advantages for using a long electrode (shorter response time and longer detection range) may also be offset by the disadvantages (difficult to fabricate and lower enzyme loading) when the desired sensor size must be small, such as those for subcutaneous implant applications.

Perhaps the most intriguing result of this thesis is the finding that catalase co-immobilization extends the sensor's detection range while decreases its response time. Therefore, significant sensor improvements can be achieved with almost no additional cost at all (in this case, and with current market trends, catalase costs significantly less than lactate oxidase in terms of units/mg/dollar). Although the finding shows that co-

immobilizing catalase has profound impact on sensor response, further experiments must be carried out to investigate potential limitations of this approach. For example, as the sensor size becomes increasingly small, the addition of excess amount of catalase may dilute the primary enzyme lactate oxidase and result in increased response time. Future investigators may show how ratio between lactate oxidase and catalase can affect the sensor's response. The results from these new studies will provide more design alternatives so that an implantable lactate sensor with wider detection range and faster response time can be developed for continuous monitoring applications.

The above principles can be applied to formulate plausible designs for various applications. For example, an implantable lactate sensor in venous blood of patients may require a lactate detection range of up to 15 mM and a possible maximum acceptable time lag of 300 seconds (5 minutes). Therefore, the sensor should have a maximum aspect ratio of approximately 1/3 (assuming a dual enzyme system) and r_o around 0.0254 cm (assuming $D_L = 4 \cdot 10^{-6} \frac{cm^2}{\sec}$). The minimum enzyme loading required for diffusion limited operation can be calculated by using the desired σ ($\sigma_{crit} = 12$) and the kinetic constants. In addition, a "long" electrode should be used to further shorten the response time. On the other hand, an aspect ratio lower than 1/3 maybe more desirable if the sensor is intended for subcutaneous implantation, because lactate concentration can be higher in certain tissues (such as muscle during exercise) than in blood. Additionally, a "disk" electrode should be used in place of a "long" electrode, so that smaller sensor size can be achieved. The tradeoff here is the increased response time, which can be compensated for by increasing enzyme loading and having smaller overall sensor size. These two potentially practical biomedical implant examples demonstrate that one can

design application specific sensors that are, in principle, guided by a detailed understanding of the sensor behavior with respect to its biotransport and biochemical kinetic parameters.

CHAPTER IV.

CONCLUSION

4.1. Summary

A mathematical model of two-dimensional coupled diffusion reaction system representing an implantable lactate sensor has been developed and solved using a finite element solver called COMSOL Multiphysics. The model predicts the transient sensor response to perturbations in bulk lactate and oxygen concentrations. The modeled sensors have a wide range of dimensions in order to investigate the effects of size and aspect ratio on sensor response. The simulation results show that: 1) decreasing aspect ratio increases lactate detection range but increases response time, 2) increasing bulk lactate concentration increases response time, 3) decreasing diffusion ratio between oxygen and lactate decreases the non-dimensional response time, 4) increasing σ decreases response time, 5) co-immobilizing catalase increases lactate detection range and beneficially decreases response time, 6) decreasing sensor size (while holding the same aspect ratio) decreases response time, 7) decreasing boundary layer thickness decreases response time and increases steady-state detection range, and 8) the "long" electrode sensor has faster response time and higher detection range, but may become undesirable when the required size is significantly small.

4.2. Future Directions

Further experiments will be carried out to fully validate the modeled results presented in this thesis. Once the models are validated, more mathematical bio-mass transport simulations will be carried out to investigate the performance of sensors with aspect ratios having non-unitary numerators (such as 5/12 and 7/24). These results may be useful for fine tuning the sensor design in order to achieve the highest possible detection range while still satisfying the maximum accepted time delay.

Additional experiments should also be carried out to further investigate the potential beneficial effects of co-immobilizing catalase. At minimum, experiments using sensors with excess catalase immobilized with lactate oxidase should be investigated. Experimental data will be obtained to confirm the theoretical results or challenge the model assumptions so that the model can be refined by incorporating more appropriate physico-chemical effects. Future simulations and novel experiments can be used to study the effect of enzyme ratio on sensor response.

Reference

Angus, D.D.; Zwirble, W.T.L.; Lidicker, J.; Clermont, G.; Carcillo J.; Pinsky, M.R., "Epidemiology of Severe Sepsis in the United States: Analysis of Incidence, Outcome, and Associated Costs of Care," *Crit Care Med.* 2001, **29**, 1303-1310.

Armour, J.C., "Implantation of Glucose Sensors," *Ph.D. Thesis*, University of California, San Diego (1988).

Badea, M.; Curulli, A.; Palleschi, G., "Oxidase Enzyme Immobilisation through Electropolymerised Films to Assemble Biosensors for Batch and Flow Injection Analysis," *Biosens. Bioelectron*. 2003, **18**, 689-698.

Baker, D.A.; Gough, D.A., "Comments on the Relationship Between Time Lag and Dynamic Delay in Diffusion – Reaction Systems," *J. Phys. Chem.* 1994, **98**, 13432-13433.

Baker, D.A.; Gough, D.A., "A Continuous, Implantable Lactate Sensor," *Anal. Chem.* 1995, **67**: 1536-1540.

Baker, D.A.; Gough, D.A., "Dynamic Delay and Maximal Dynamic Error in Continuous Biosensors," Anal. Chem. 1996, **68**, 1292-1297.

Bockris, J.O'M.; Oldfield, L.F., "The Oxidation-Reduction Reactions of Hydrogen Peroxide at Inert Metal Electrodes and Mercury Cathodes," *Trans. Faraday Soc.* 1954, **51**, 249-259.

Bohm, S.; Pijanowska, D.; Olthuis, W.; Bergveld, P., "A Flow-Through Amperometric Sensor Based on Dialysis Tubing and Free Enzyme Reactors," *Biosens. Bioelectron*. 2001, **16**, 391-397.

Burmeister, J.J.; Palmer, M.; Gerhardt, G.A., "L-Lactate Measures in Brain Tissue with Ceramic-Based Multisite Microelectrodes," *Biosens. Bioelectron.* 2005, **20**, 1772-1779.

Castro, R., "Development of a Telemetry Instrumentation System for Biosensors," *M.S. Thesis*, University of California, San Diego (2002).

Chaubey, A.; Pande, K.K.; Singh, V.S.; Malhotra, B.D., "Co-Immobilization of Lactate Oxidase and Lactate Dehydrogenase on Conducting Polyaniline Films," *Anal. Chim. Acta* 2000, **407**, 97-103.

Clark Jr., L.C.; Lyons, C., "Electrode Systems for Continuous Monitoring in Cardiovascular Surgery," *Ann. N. Y. Acad. Sci.* 1962, **102**: 29-45.

Clark, R.A.; Zerby, S.E.; Ewing, A.G., "Electrochemistry in Neuronal Microenvironments," *Electronal. Chem.* 1998, **20**, 227-294.

Conway, P.J.; Gough, D.A., "Long-Term *in vitro* Operation of Enzyme Electrode-Based Glucose Sensors," *Sens. Actuat.* 1987, **11**, 305-308.

Cornish-Bowden, A., Fundamentals of Enzyme Kinetics, Butterworth & Co Ltd, England (1979).

Crank, J. and Park, G.S. (eds.), Diffusion in Polymers, Academic Press, London (1968).

Diamond, D., Principles of Chemical and Biological Sensors, John Wiley & Sons, New York (1998).

Ellmerer M.; Schaupp, L.; Trajanoski, Z.; Jobst, G.; Moser, I.; Urban, G.; Skrabal, F.; Wach, P., "Continuous Measurement of Subcutaneous Lactate Concentration During Exercise by Combining Open-Flow Microperfusion and Thin-Film Lactate Sensors," *Biosensors & Bioelectronics* 1998, **13**, 1007-1013.

Fatt, I., Polarographic Oxygen Sensor, CRC Press, Inc., Cleveland, Ohio (1976).

Fowler, R.A.; Hill-Popper, M; Stasinos, J.; Petrou, C.; Sanders, G.D.; Garber, A.M., "Cost-Effectiveness of Recombinant Human Activated Protein C and the Influence of Severity of Illness in the Treatment of Patients with Severe Sepsis," *Journal of Critical Care* 2003, **18** (3): 181-191.

Frost, M.C.; Meyerhoff, M.E., "Implantable Chemical Sensors for Real-Time Clinical Monitoring: Progress and Challenges," *Current Opinion in Chemical Biology* 2002, **6**: 633-641.

Gavalas, V.G.; Chaniotakis, N.A., "Polyelectrolyte Stabilized Oxidase Based Biosensors: Effect of Diethylaminoethyl-Dextran on the Stabilization of Glucose and Lactate Oxidases into Porous Conductive Carbon," *Anal. Chim. Acta* 2000, **404**, 67-73.

Gavalas, V.G.; Berrocal, M.J.; Bachas, L.G., "Enhancing the Blood Compatibility of Ion-Selective Electrode," *Anal. Bioanal. Chem.* 2006, **384**: 65-72.

Goor, J.B., "Oxygen Transfer in the Implant Environment," *Ph.D. Thesis*, University of California, San Diego (2007)

Gough, D.A.; Leypoldt, J.K.; Armour, J.C., "Progress Toward a Potentially Implantable, Enzyme-Based Glucose Sensor," *Diabetes Care* 1982, **5**, 190-198.

Gough, D.A.; Lucisano, J.Y.; Tse, P.H.S., "Two-Dimensional Enzyme Electrode Sensor for Glucose," *Anal. Chem.* 1985, **57**, 2351-2357.

Gue, A.M.; Tap, H.; Gros, P.; Maury, F., "A Miniaturised Silicon Based Enzymatic Biosensor: Towards a Generic Structure and Technology for Multi-Analytes Assays," *Sens. Actuators B* 2002, **82**, 227-232.

Guiseppi-Elie, A.; Brahim, S.; Slaughter, G.; Ward, K.R., "Design of a Subcutaneous Implantable Biochip for Monitoring of Glucose and Lactate," *IEEE Sensors Journa*l 2005, **5**, 345-355.

Hirano, K.; Yamato, H.; Kunimoto, K.; Ohwa, M., "Design of Novel Electron Transfer Mediators Based on Indophenol Derivatives for Lactate Sensor," *Biosens. Bioelectron*. 2002, **17**, 315-322.

Hirano, K.; Yamato, H.; Kunimoto, K.; Ohwa, M., "Novel electron transfer mediators, indoaniline derivatives for amperometric lactate sensor," *Sens. Actuators B* 2002, ***86***, 88-93.

Hoare, J.P., The Electrochemistry of Oxygen, Interscience Publishers, New York (1968).

Hu, Y.; Zhang, Y.; Wilson, G.S., "A Needle-Type Enzyme-Based Lactate Sensor for *in vivo* Monitoring," *Analytica Chimica Acta* 1993, **281**, 503-511.

Huckabee, W.E., "Abnormal Resting Blood Lactate: I. The Significance of Hyperlactatemia in Hospitalized Patients," *Am. J. Med.* 1961, **30**, 833-839.

Huckabee, W.E., "Abnormal Resting Blood Lactate: II. Lactic Acidosis," *Am. J. Med.* 1961, **30**, 840-848.

Jaremko, J.; Rorstad, O., "Advances Toward the Implantable Artificial Pancreas for Treatment of Diabetes," *Diabetes Care* 1998, **21(3)**, 444-450.

Kaneko, H.; Minagawa, H.; Shimada, J., "Rational Design of Thermostable Lactate Oxidase by Analyzing Quaternary Structure and Prevention of Deamidation," *Biotech. Letters* 2005, **27**, 1777-1784.

Kharitonov, A.B.; Zayats, M.; Alfonta, L.; Katz, E.; Willner, I., "A Novel ISFET-Based NAD^+-Dependent Enzyme Sensor for Lactate," *Sens. Actuators B* 2001, **76**, 203-210.

Kishiyama, C., "Development of a Portable Data Logger for Biosensors," M.S. Thesis, University of California, San Diego (1999).

Koschwanez, H.E.; Reichert, W.M., "In Vitro, In Vivo and Post Explanation Testing of Glucose-Detecting Biosensors: Current Methods and Recommendations," *Biomaterials* 2007, **28**, 3687-3703.

Kreisberg, R. A., "Pathogenesis and Management of Lactic Acidosis," *Ann. Rev. Med.* 1984, **35**: 181-193.

Kulys, J.J., Svirmickas, G.J.S., "Reagentless Lactate Sensor Based on Cytochrome b_2," *Analytica Chimica Acta* 1980, **117**, 115-120.

Lockridge, O.; Massey, V.; Sullivan, P.A., "Mechanism of Action of the Flavoenzyme Lactate Oxidase," *Journal of Biological Chemistry* 1972, **247(24)**, 8097-8106.

Li, C.I.; Lin, Y.H.; Shih, C.L.; Tsaur J.P.; Chau, L.K., "Sol-Gel Encapsulation of Lactate Dehydrogenase for Optical Sensing of L-Lactate," *Biosens. Bioelectron*. 2002, **17**, 323-330.

Lucisano, J.Y., "Development of an Implantable Glucose Sensor: Stability of the Oxygen Electrode and Analysis of the Transient Response," *Ph.D. Thesis*, University of California, San Diego (1987).

Lucisano, J.Y.; Gough, D.A., "Transient Response of the Two-Dimensional Glucose Sensor," *Anal. Chem.* 1988, **60**, 1272-1281.

Maeda-Yorita, K.; Aki, K.; Sagai, H.; Misaki, H.; Massey, V., "L-Lactate Oxidase and L-Lactate Monooxygenase: Mechanistic Variations on a Common Structural Theme," Biochimie 1995, **77**, 631-642.

Makovos, E.B., Liu, C.C., "Measurements of Lactate Concentration Using Lactate Oxidase and an Electrochemical Oxygen Sensor," *Biotechnology and Bioengineering* 1985, **27**, 167-170.

Marquette, C.A.; Blum, L.J., "Self-Containing Reactant Biochips for the Electrochemiluminescent Determination of Glucose, Lactate and Choline," *Sens. Actuators B* 2003, **90**, 112-117.

Marzouk, S.A.M.; Cosofret, V.V.; Buck, R.P.; Yang, H.; Cascio, W.E.; Hassan, S.S.M., "Amperometric Monitoring of Lactate Accumulation in Rabbit Ischemic Myocardium," *Talanta* 1997, **44**, 1527-1541.

Mascini, M.; Fortunati, S.; Moscone, D.; Palleschi, G.; Massi-Benedetti, M; Fabletti, P., "An L-Lactate Sensor with Immobilized Enzyme for Use in *in vivo* Studies with an Endocrine Artificial Pancreas," *Clin. Chem.* 1985, **31**, 451-453.

Meyerhoff, C.; Bischof, F.; Mennel, F.J.; Sternberg, F.; Bican, J.; Pfeiffer, E.F., "On Line Continuous Monitoring of Blood Lactate in Men by a Wearable Device Based Upon an Enzymatic Amperometric Lactate Sensor," *Biosensors & Bioelectronics* 1993, **8**, 409-414.

Mizutani, F.; Yabuki, S.; Sawaguchi, T.; Hirata, Y.; Sato, Y.; Iijima, S., "Use of a Siloxane Polymer for the Preparation of Amperometric Sensors: O_2 and NO Sensors and Enzyme Sensors," *Sens. Actuators B* 2001, **76**, 489-493.

Mosbach, M.; Zimmermann, H.; Laurell, T.; Nilsson, J.; Csoregi, E.; Schuhmann, W., "Picodroplet-Deposition of Enzymes on Functionalized Self-Assembled Monolayers as a Basis for Miniaturized Multi-Sensor Structures," *Biosens. Bioelectron*. 2001, **16**, 827-837.

Nguyen, H.B.; Rivers, E.P.; Knoblich, B.P.; Jacobsen, G.; Muzzin, A.; Ressler, J.A.; Tomlanovich, M.C., "Early Lactate Clearance is Associated with Improved Outcome in Severe Sepsis and Septic Shock," *Crit. Care Med.* 2004, **32** (8): 1637-1642.

Ohara, T.J.; Rajagopaian, R.; Heller, A., "Wired Enzyme Electrodes for Amperometric Determination of Glucose or Lactate in the Presence of Interfering Substances," *Anal. Chem.* 1994, **66**, 2451-2457.

Padeste, C.; Steiger, B.; Grubelnik, A.; Tiefenauer, L., "Redox Labelled Avidin for Enzyme Sensor Architectures," *Biosens. Bioelectron*. 2003, **19**, 239-247.

Perdomo, J.; Hinkers, H.; Sundermeier, C.; Seifert, W.; Morell, M.O.; Knoll, M., "Miniaturised Real-Time Monitoring System for L-Lactate and Glucose Using Microfabricated Multi-Enzyme Sensors," *Biosens. Bioelectron*. 2000, **15**, 515-522.

Petrou, P.S.; Moser, I.; Jobst, G., "Microdevice with Integrated Dialysis Probe and Biosensor Array for Continuous Mulit-Analyte Monitoring," *Biosens. Bioelectron*. 2003, **18**, 613-619.

Pfeiffer, D.; Moller, B.; Klimes, N.; Szeponik, J., "Amperometric Lactate Oxidase Catheter for Real-Time Lactate Monitoring Based on Thin Film Technology," *Biosensors & Bioelectronics* 1997, **12**, 539-550.

Polikov, V.S.; Tresco, P.A.; Reichert, W.M., "Response of Brain Tissue to Chronically Implanted Neural Electrodes," *Journal of Neuroscience Methods* 2005, **148**, 1-18.

Pronovost, P.J.; Rinke, M.L.; Emery, K.; Dennison, C.; Blackledge, C.; Berenholtz, S.M., "Interventions to Reduce Mortality among Patients Treated in Intensive Care Units," *Journal of Critical Care* 2004, **19** (3): 158-164.

Revzin, A.F.; Sirkar, K.; Simonian, A.; Pishko, M.V., "Glucose, Lactate, and Pyruvate Biosensor Arrays Based on Redox Polymer/Oxidoreductase Nanocomposite Thin-Films Deposited on Photolithographically Patterned Gold Microelectrodes," *Sens. Actuators B* 2002, **81**, 359-368.

Ritter, C.; Heike, F.; Herbert, K.; Josef, K.F.; Susanne, L.; Christian, N.; Helmut, O.; Gabriele, P.; Bernhard, S.; Marieluise, S.; Wolfgang, S.; Gregor, S., "Multiparameter Miniaturised Sensor Arrays for Multiple Use," *Sens. Actuators B* 2001, **76**, 220-225.

Smutok, O.; Gayda, G.; Gonchar, M.; Schuhmann, W., "A Novel L-Lactate-Selective Biosensor Based on Flavocytochrome b2 From Methylotrophic Yeast Hansenula Polymorpha," *Biosens. Bioelectron.* 2005, **20**, 1285-1290.

Turner, A.P.F.; Karube, I.; Wilson, G.S., Biosensors Fundamentals and Applications, Oxford University Press, Great Britain (1987).

Tse, P.H.S., "Modeling and Inactivation of Immobilized Enzyme Systems," *Ph.D. Thesis*, University of California, San Diego (1984).

Updike, S.J.; Hicks, G.P., "The Enzyme Electrode," *Nature* 1967, **214**, 986-988.

Wang, J.; Chen, Q., "Lactate Biosensor Based on a Lactate Dehydrogenase/Nicotinamide Adenine Dinucleotide Biocomposite," *Electroanalysis* 1994, **6**, 850-854.

Ward, W.K.; House, J.L.; Birck, J.; Anderson, E.M.; Jansen, L.B., "A Wire-Based Dual-Analyte Sensor for Glucose and Lactate: *In Vitro* and *In Vivo* Evaluation," *Diabetes Technology & Therapeutics* 2004, **6**, 389-401.

Weibel, M.K.; Bright, H.J., "The Glucose Oxidase Mechanism," *Journal of Biological Chemistry* 1971, **246(9)**, 2734-2744.

Weil, M.H.; Afifi, A.A., "Experimental and Clinical Studies on Lactate and Pyruvate as Indicators of the Severity of Acute Circulatory Failure (Shock)," *Circulation* 1970, **41**, 989-1001.

Williams, D.L.; Doig Jr., A.R.; Korosi, A., "Electrochemical-Enzymatic Analysis of Blood Glucose and Lactate," *Analytical Chemistry* 1970, **42**, 118-121.

Wilson, G.S.; Gifford, R., "Biosensors for Real-Time in Vivo Measurements," *Biosens. Bioelectron.* 2005, **20**: 2388-2403.

Wisniewski, N.; Moussy, F.; Reichert, W.M., "Characterization of Implantable Biosensor Membrane Biofouling," *Fresenius J. Anal. Chem.* 2000, **366**, 611-621.

Wolfbeis, O.S., "Fiber-Optic Chemical Sensors and Biosensors," *Anal. Chem.* 2002, **74**, 2663-2678.

Wu, M.H.; Cai, H.; Xu, X.; Urban, J.P.G.; Cui, Z.F.; Cui, Z., "A Su-8/PDMS Hybrid Microfluidic Device with Integrated Optical Fibers for Online Monitoring of Lactate," *Biomedical Microdevices* 2005, **7**, 323-329.

Yang, Q.; Atanasov, P.; Wilkins, E., "An Integrated Needle-Type Biosensor for Intravascular Glucose and Lactate Monitoring," *Electroanalysis* 1998, **10**, 752-757.

Yang, L.; Kissinger, P.T.; Ohara, T., "Continuous Monitoring of Subcutaneous Glucose and Lactate Using Microdialysis with On-Line Enzyme Electrodes," *Current Separations* 1995, **14**, 31-35.